DISCOVERY AND CHARACTERIZATION OF NEW BIOSURFACTANT PROTEINS FOR BIOREMEDIATION AND BIOMEDICAL APPLICATIONS

Rossana Pitocchi

Dottorato in Biotecnologie – XXXVI ciclo

Università di Napoli Federico II

Dottorato in Biotecnologie – XXXVI ciclo

Università di Napoli Federico II

DISCOVERY AND CHARACTERIZATION OF NEW BIOSURFACTANT PROTEINS FOR BIOREMEDIATION AND BIOMEDICAL APPLICATIONS

Rossana Pitocchi

Dottorando: Rossana Pitocchi

Relatore: Paola Giardina

Coordinatore: Prof. Marco Moracci

Settore Scientifico Disciplinare BIO/10

A., e per, tutte le giovani brillanti menti
i cui sogni sono stati brutalmente spezzati
in terra palestinese.

INDEX

RIASSUNTO

A. INTRODUZIONE

Molecole che contengono due o più regioni di polarità differente sono note come tensioattivi. Questa definizione, seppur molto semplice, racchiude un vasto insieme di molecole diverse, utili nei più svariati campi di applicazione. La presenza di porzioni idrofobiche/idrofiliche conferisce loro la possibilità di riarrangiarsi strutturalmente all'interfaccia tra fluidi, determinando di conseguenza la capacità di abbassare la tensione superficiale, stabilizzare schiume o emulsioni, formare aggregati (per lo più nella forma di micelle). Sono queste abilità a rendere particolarmente utili i tensioattivi in moltissime industrie come quella tessile, alimentare, farmaceutica, cosmetica, petrolifera, e nei processi di bonifica e risanamento. Essendo prodotti molto richiesti nel mercato globale, hanno ormai raggiunto livelli competitivi di costi e produzione, a discapito però di aspetti negativi che riguardano il loro impatto ambientale e quindi tossicità e biodegradabilità. Un composto è detto biodegradabile quando la sua struttura chimica può essere completamente scomposta da microrganismi. Mentre molti surfattanti chimici non sono facilmente biodegradabili e possono essere tossici, quelli prodotti naturalmente da microrganismi, compresi batteri, lieviti e funghi filamentosi, offrono un'alternativa altamente più ecologica. Questi composti sono noti come biosurfattanti (BS).

La produzione di BS è una delle risposte adattive alle mutevoli e talvolta ostili, condizioni ambientali in cui i microrganismi crescono. Infatti, questi composti possono coadiuvare la pseudo-solubilizzazione di substrati idrofobici. Secondo alcune teorie, essi potrebbero anche essere direttamente coinvolti in processi catabolici, fungendo da riserve energetiche. A seconda poi dell'organismo produttore, possono avere strutture chimiche e efficienze altamente diverse. Uno dei modi più comuni di classificarli è basato sulla loro attività, si distingue infatti tra biosurfattanti e bioemulsionanti (BE). I primi sono prevalentemente efficienti nell'abbassare la tensione superficiale, i secondi invece, nello stabilizzare emulsioni. Questa classificazione è spesso correlata a differenze nei pesi molecolari: BS sono piccole molecole, come zuccheri, acidi grassi, glicolipidi ecc. BE sono generalmente molecole ad alto peso molecolare, come lipopolisaccaridi, proteine ed altri. Tra i microorganismi produttori di tali composti, troviamo i funghi. Grazie alle loro proprietà intrinseche, tali microrganismi sono estremamente interessanti per una vasta gamma di applicazioni. Prima tra tutte, la loro capacità di degradare materiale organico e sostanze polimeriche li rende capaci di crescere in diversi ambienti, talvolta anche estremi, come ad esempio, a bassi pH, pressioni elevate, temperature estreme, ma anche in presenza di composti recalcitranti, come inquinanti o sostanze tossiche. Come strategie per sopravvivere in queste condizioni producono sostanze, quali proteine o

BS. I funghi, rispetto ai batteri, ed in particolare i BS da loro prodotti, sono ancora molto meno studiati rispetto a quelli dai batteri L'ottimizzazione delle condizioni di crescita è uno dei modi più facilmente attuabili per la riduzione dei costi di produzione di BS, usando come substrati, per esempio, materiali di scarto. Non solo la produzione, ma anche protocolli di estrazione e purificazione sono continuamente oggetto di studio e ottimizzazione. Un'altra interessante alternativa è data dalla ingegneria genetica. Un valido esempio a tal proposito è dato dall'industria Henkel (GE) la quale produce BS da ceppi batterici modificati.

Le proteine sono tra le varie classi di BS prodotti da funghi. Tra esse, le più studiate e caratterizzate, sono le idrofobine (HPBs) e le ceratoplatanine (CPs). Le idrofobine sono prodotte da tutti i funghi in diversi steps della loro crescita, adempiendo a diversi scopi. La loro attività principale è quella di diminuire la tensione superficiale per permettere ad esempio, lo sviluppo di spore e corpi fruttiferi. Sono piccole proteine (tra 5 – 20 kDa), che contengono un pattern di otto cisteine altamente conservato. A seconda della posizione di queste cisteine, e ancor di più della stabilità degli aggregati che sono in grado di formare, si possono dividere in due classi. Le idrofobine di classe I formano aggregati estremamente stabili, solubili solo in acidi forti. Gli aggregati formati da quelle di classe II invece, sono solubili in condizioni più blande. Entrambe le classi, comunque, sono caratterizzate da un core strutturale simile, formato da quattro foglietti beta organizzati in "beta barrel". Recentemente un'ulteriore sottodivisione per le idrofobine di classe I è stata suggerita, a seconda se sono prodotte da Ascomiceti o Basidiomiceti, sulla base di differenze nel processo di aggregazione. Nonostante le variazioni strutturali, tutte le proteine di questa famiglia, mostrano nella struttura 3D una separazione tra zone polari e apolari.

Le CPs sono un'altra classe di piccole proteine (sempre tra 5 – 25 kDa), con un pattern conservato di cisteine, originariamente considerate quali membri della famiglia delle HPBs. Studi recenti hanno rivelato in realtà differenze strutturali e di attività. Ad esempio, le CPs mostrano solo quattro cisteine conservate e mancano di grandi zone idrofobiche. Inoltre, i loro aggregati sono nettamente meno stabili. Studi sulla loro attività hanno evidenziato che queste proteine si comportano in alcuni casi da co-fattori di virulenza, in altri casi al contrario, inducono l'espressione dei geni di difesa. Comunque, la loro presenza ubiquitaria tra funghi con diversi stili di vita suggerisce che possano essere coinvolte in altri aspetti del ciclo vitale fungino. La caratteristica peculiare delle CPs è la loro attività non-enzimatica nei confronti della cellulosa, che comporta un indebolimento delle fibre di cellulosa. Studi riguardanti l'attività come tensioattivi invece, sono ancora molto limitati. Solo alcuni autori ne hanno caratterizzato l'abilità di stabilizzare emulsioni, abbassare tensione superficiale o modificare polarità delle superfici. Quello che emerge dal recente lavoro del nostro gruppo di ricerca,

e da questo lavoro di tesi, è però la possibilità che vi siano altre proteine fungine, diverse dalle sopracitate HPBs e CPs, con proprietà di biosurfattanti. Nel presente lavoro di tesi, il focus è principalmente sulle applicazioni in campo biomedico, e del biorisanamento. I biosurfattanti, in particolare quelli fungini, hanno dimostrato ottime proprietà antibatteriche, antiadesive e antitumorali. Possono giocare un ruolo importante anche nello sviluppo di nuovi sistemi di somministrazione dei farmaci, come micro o nano carrier. La natura adesiva dei biosurfattanti risulta preziosa negli impianti biomedici, perché può prevenire l'adesione e la colonizzazione batterica o favorire l'adesione cellulare.

Per quanto riguarda problemi ambientali come le fuoriuscite di petrolio in suolo e acqua, i biosurfattanti sono degli ottimi sostituti dei tensioattivi sintetici, in quanto non si accumulano e non contribuiscono ulteriormente all'inquinamento ambientale. Il meccanismo chiave con il quale agiscono è il potenziamento della biodisponibilità dei contaminanti scarsamente solubili, facilitandone il desorbimento, solubilizzazione e assimilazione da parte dei microorganismi. I biosurfattanti hanno dimostrato efficacia contro vari composti dannosi, inclusi sostanze a base di petrolio, molecole aromatiche e metalli tossici. Il biorisanamento può essere realizzato attraverso tecniche *in situ* o *ex situ*. Per le tecniche in situ, ad esempio, i biosurfattanti offrono il vantaggio di poter essere rilasciati con un impatto ambientale minimo. Nelle metodologie in situ, inoltre, i funghi svolgono un ruolo chiave sia come produttori di metaboliti attivi come surfattanti e enzimi, sia come bio-inoculi. Per bio-inoculi si intendono ceppi specifici resistenti alla presenza di altri microorganismi nel sito contaminato, in grado di interagire con i contaminanti e/o produrre metaboliti per il biorisanamento.

B. NUOVE PROTEINE FUNGINE BIOSURFATTANTI

I funghi sono microorganismi resilienti trovati in vari ambienti ostili, tra cui discariche, aree contaminate dal petrolio sia terrestri che marine. L'ambiente marino, in particolare, con la sua estrema varietà di ambienti, offre una ricca fonte per la scoperta di nuovi composti. Tuttavia, gli ecosistemi marini sono in gran parte inesplorati a causa delle difficoltà nell'isolare e far crescere in laboratorio questi microorganismi. A tal proposito, si è condotto uno studio approfondito sui funghi marini come fonte di biosurfattanti e bioemulsionanti ed in particolare sulle metodologie di screening. Nel presente lavoro, sono state estratte e caratterizzate nuove proteine biosurfattanti prodotte da funghi isolati da alghe o da plastiche rinvenute in discarica. Nel primo caso, una proteina chiamata PAC3, estratta dal ceppo fungino marino *Acremonium sclerotigenum*, ha mostrato caratteristiche strutturali e di auto-assemblaggio molto simili alle proteine idrofobine di classe I. Le caratteristiche di questa proteina sono state analizzate a confronto con quelle di Vmh2, nota

idrofobina di classe I. Entrambe hanno mostrato la capacità di stabilizzare emulsioni in diverse condizioni (concentrazione, pH, etc), di abbassare notevolmente la tensione superficiale e di assemblare spontaneamente in lunghe fibrille amiloidi. Nonostante le similarità funzionali con le idrofobine, la determinazione parziale della sequenza di PAC3 permette di escludere che appartenga alla stessa classe.
Tra i vari ambienti ostili in cui i funghi possono crescere, troviamo anche siti contaminati, come le discariche, poiché, grazie al loro apparato ifale, combinano meccanismi chimici e fisici per colonizzare anche le matrici più complesse, come la plastica, che è oggigiorno motivo di reale preoccupazione. Due ceppi fungini appartenenti al genere *Fusarium* sono stati isolati da substrati plastici prelevati in discariche dalla *Mycoteca Universitatis Taurinensis*, Quando cresciuti in presenza di olio di oliva, il loro brodo di coltura ha la capacità di abbassare la tensione superficiale. Una proteina con ottime proprietà emulsionanti viene secreta in queste condizioni ed è stata identificata e caratterizzata. L'identificazione ha permesso di stabilire che la proteina contiene un dominio ricco in cisteine, tipico dei funghi, noto come CFEM (Common in Fungal Extracellular Membrane). Inoltre, sulla base di modelli strutturali di questa proteina è stato proposto un possibile meccanismo di aggregazione, che gioca un ruolo fondamentale per la stabilizzazione delle emulsioni. Lo studio, dunque, introduce la possibilità di isolare nuove classi proteiche con buone attività tensioattive ed emulsionanti, diverse dalle note idrofobine.

C. APPLICAZIONI

I composti biosurfattanti (BS) hanno significative applicazioni industriali, ma la loro produzione su larga scala rimane una sfida. I BS possono essere utilizzati come coadiuvanti nel trattamento idrolitico dei rifiuti agroindustriali. Infatti, la ceratoplatanina isolata da *Trichoderma harzianum,* e caratterizzata come efficace biosurfattante, è stata utilizzata per pretrattare scarti alimentari (come bucce di mela, o patata) prima della loro idrolisi per l'ottenimento di zuccheri fermentabili, utili ad esempio per la produzione di biocarburanti. Sfruttando la capacità delle Ceratoplatanine di indebolire i legami tra catene di cellulosa, infatti, si è osservato un aumento della conversione di zuccheri a valle dell'idrolisi enzimatica. Questo tipo di trattamento minimizza tempi di incubazione, aumentandone l'efficienza.
Nell'ambito biomedico, la colonizzazione batterica di superfici di interesse, aggravata dai batteri resistenti ai farmaci, è un problema significativo. La funzionalizzazione di tali superfici è una possibile via per risolvere il problema. Un aspetto importante per la funzionalizzazione di superfici è evitare l'uso di sostanze chimiche, reagenti tossici o costosi. È per questo

che l'uso di biosurfattanti, come le idrofobine, è oggetto di studio del presente lavoro di tesi. I layers estremamente stabili formati da queste proteine, possono fungere da punti di ancoraggio per legare molecole di interesse, come enzimi, anticorpi o peptidi. In più, le tecniche di ingegneria genetica apportano il vantaggio di potere fondere queste molecole, fornendo ulteriori vantaggi in termini di facilità e velocità del processo. In particolare, sono state funzionalizzate due superfici, polistirene e cellulosa batterica, con una proteina ingegnerizzata contenente l'idrofobina Vmh2 e un peptide antimicrobico. Quando adesa alla cellulosa batteria, questa proteina, ha dimostrato un buon effetto antibatterico contro i patogeni *Staphyloccoccus. aureus e S. epidermidis.*

In aggiunta, le proprietà dei BS, tra cui la formazione e stabilizzazione di schiume, e la riduzione della tensione superficiale e della viscosità, li rendono adatti per la pulizia di acque e suoli inquinati da petrolio. Sono quindi state effettuate preliminari analisi sulle proteine estratte da *Fusarium solani* per testarne la capacità di rimuovere il petrolio da sabbie contaminate.

D. CONCLUSIONI

I risultati conseguiti nel presente progetto di tesi sono qui di seguito riassunti:

- Una proteina biosurfattante fungina, estratta da *Trichoderma harzianum* precedentemente caratterizzata, è stata utilizzata con successo per il pretrattamento di biomasse ligno-cellulosiche nel processo di idrolisi.
- Due proteine idrofobiche note, una idrofobina di classe I (Vmh2) e una nuova (nominata PAC3) sono state caratterizzate come efficaci biosurfattanti.
- Una nuova proteina è stata isolata ed identificata da due ceppi di *Fusarium solani,* cresciuti su plastica isolata da discariche. La sua caratterizzazione ha mostrato che in forma aggregata la proteina stabilizza emulsioni.
- La cellulosa batterica, purificata da *Komagataeibacter xylinus,* è stata funzionalizzata con una proteina chimerica, che combina Vmh2, idrofobina adesiva di classe I, con un peptide antimicrobico (GKY20), impartendogli proprietà battericida.

SUMMARY

Proteins are intrinsically amphipathic molecules, even if their amphiphilic nature is affected by several factors such as protein folding or post-translational modifications. Hydrophobins and ceratoplatanins are the most studied surface-active proteins to date. They are both small fungal proteins, with high content of cysteines, that fulfill several functions in fungal life cycle.

Hydrophobins are involved in the development of aerial development oh hyphae thanks to their capability to reduce surface tension, while ceratoplatanins can act both as virulence factor and as elicitors, besides possessing the ability to weaken cellulose fibers without enzymatic activity. Fungal biosurfactant proteins are still poorly characterized and exploited as class of biosurfactants. For this reason, one of the purposes of the present PhD project has been the isolation and characterization of new biosurfactant proteins from different fungal strains. The first work was conducted on two *Fusarium solani* strains isolated from a plastic dumpsite, collected by the Mycoteca Universitatis Taurinensins. From these fungi a protein has been extracted and identified as a new unknown protein, containing a cysteine-rich domain. Its characterization revealed that this protein forms aggregates, endowed with excellent emulsifying abilities. Moreover, other two already known hydrophobic proteins, named Vmh2 and PAC3, extracted from *Pleurotus ostreatus* and *Acremonium sclerotigenum* respectively, were herein characterized for the first time in terms of surfactant activities. Although many functional similarities, partial identification of PAC3 excludes that it does belong to the HPBs protein family. In addition, an already known BS protein, in particular the Ceratoplatanin extracted from Trichoderma harzianum, has been exploited for lignocellulosic valorization processes. This protein has proven able to efficiently pre-treat agrifood wastes, increasing the sugar conversion yield achievable after hydrolytic treatment.

Another promising application that has been exploited in my PhD work, has regarded the functionalization of two different materials, to impart antimicrobial and antibiofilm properties. Polystyrene and Bacterial cellulose have been successfully functionalized with an engineered protein that fuses the adhesive protein of Vmh2 and the antimicrobial activity of the peptide GKY20. When adhered on cellulose, this protein has proven a good antimicrobial effect against *Staphyloccoccus*. aureus and *S. epidermidis*.

Results here achieved, indicate that there are other classes of fungal proteins with surfactant abilities; these proteins offer a valid substitute for synthetic surfactants, because of the potential for industrial-scale utilization through genetic engineering.

CHAPTER 1

1. INTRODUCTION

Surfactants are amphiphilic molecules, containing two or more moieties of opposite polarity. This definition actually hides a huge and fascinating world of different molecules which can be entailed to a wide range of possible applications. The presence of both hydrophilic and hydrophobic groups imparts these molecules the ability to re-arrange themselves at fluid interfaces, leading to multiple effects like the decrease of surface tension, formation and stabilization of foam or emulsions (in case of two immiscible liquids), formation of aggregates/nanostructure (mostly in the form of micelles). When the surfactants are fully immersed in water, the structure formed takes on two different names, “micelles” when the concentration of surfactant is low and “surfactant liquid crystals” at very high concentrations of surfactants[1].Those that seem to be just specific phenomena of a certain class of compounds, actually span in a wide range of application fields. The “ambivalent” nature of surfactants makes them valuable in many industries like textile, food-processing, pharmaceuticals, and cosmetics, but also oil and gas industry, refineries, and remediation processes. This can explain why these compounds are highly demanded in the global market and since the early ’30, have been incorporated into various commercial products [2].

The synthetic surfactants that are currently used in the market are usually classified into four different categories, which are anionic, cationic, zwitterionic, and non-ionic surfactants, according to the hydrophilic head group of the molecules, that can affect the different applicability of each compound [3]. As they fit in the global market, they must have accessible and competitive large-scale production costs, something that petroleum-based products possess but with disadvantages such as toxicity, high environmental impact, low biocompatibility and degradability etc.

The two most significant aspects of surfactants affecting the environment are toxicity and biodegradability. Toxicity is the measure of adverse effects caused by surfactants in the soil, whereas biodegradability is the ability of microorganisms to destroy the surfactant [4] A surfactant is said to be biodegradable when its chemical structure is broken down completely by the microbes present in the environment. Most of the chemical surfactants used in soil remediation are not readily biodegradable and can cause a toxic impact on the soil environment. Notably, these surfactants may undergo sorption on the surface of the soil grains and lead to toxic accumulation [5].

1.1 Biosurfactants

When such molecules are produced by microorganisms they are referred to as biosurfactants (BS). Several microorganisms are known for BS production, varying from bacteria, yeasts, and filamentous fungi.

Biosurfactant production is considered one of the numerous adaptations exhibited by microorganisms for metabolizing hydrocarbons. They represent a physiological response to the changing environmental conditions encountered by the cells [6]. Pseudo-solubilization of hydrophobic substrates and motility towards them could underlie this phenomenon [7]. Another explanation for BS production could imply microbial adhesion-release of the cell to surfaces: BS associated with the microbial walls can regulate the properties of the cell surface increasing, for example, the permeability of the membrane [2]. Other authors, moreover, foresee that BS can serve as an energy reserve, since they can enter the catabolic process as a possible source of energy during periods of nutrient limitation [7]. Although a variety of mechanisms and specializations distinguish biosurfactants, they all share a few essential traits. They are part of the process of interaction of microbes with surfaces and substrates, especially when these are of a hydrophobic nature. Depending on the producing organism, they can show different chemical structures, surface properties and efficiency. These molecules are amphiphilic in nature and this property allows their dissolution in both polar and non-polar solvents. BS can be classified following more than one criterion, like chemical composition, microbial origin, mode of action, molecular weight, and other general physico-chemical properties like their charge [8]. However, one of the most acknowledged ways is by their predominant activity, either emulsifying or surface active, whose differentiation is also linked to their molecular weight. It is generally spoken of bioemulsifiers (BE) to refer specifically to high molecular weight molecules that can form and stabilize foams, and BS for low molecular weight compounds that can sensibly reduce surface tension. This classification is widely accepted and used among researchers, since Uzigowe et al. [9] well established that the two terms are not always exchangeable.

BS are generally composed of sugars, aminoacids, fatty acids but also glycolipids (rhamnolipids, sophorolipids, trehalose lipids), and lipopeptides (surfactin, iturin, fengycin). BE usually are complex mixtures of heteropolysaccharides, lipopolysaccharides, lipoproteins, and proteins. Emulsan e.g., one of the most studied BE, can reach a molecular weight of 1000 kDa when produced by *Acinetobacter calcoaceticus* [9].

1.2 Fungal biosurfactants

Fungi constitute a large and diverse kingdom of eukaryotic organisms morphologically classified as yeasts, filamentous fungi, or dimorphic fungi. They are present in diverse environments, both terrestrial and marine, and some have evolved to thrive and proliferate in extreme conditions, e.g. high salinity or hydrostatic pressure, low pH, extreme temperature conditions, and the presence of hydrocarbons. Fungi employ a range of remarkable strategies to counteract

recalcitrant compounds, like pollutants and toxic substances. These strategies include a powerful enzymatic system, but also the production of BS, which enables them to use these recalcitrant compounds (i.e., plastics or other oil-based compounds) as a source of carbon and electrons, providing them with cellular materials and an energy source [10].

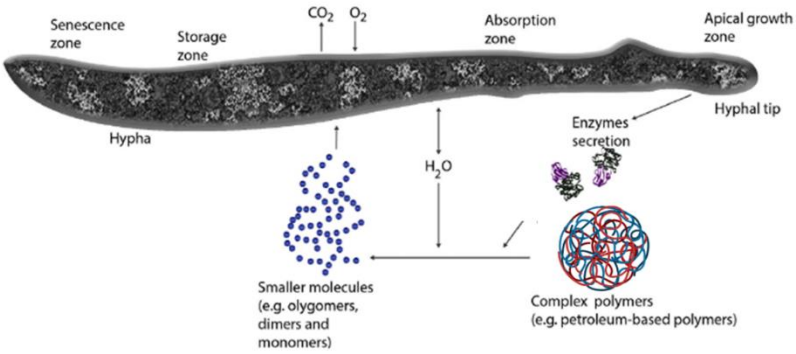

Figure 1. General scheme of biodegradation of complex polymers (e.g., petroleum-based plastics) by a fungal cell (hypha). In general, the hyphal structure can be organized into 4 zones: the apical growth zone, absorption zone, storage zone and senescence zone, each of them with a specific metabolic activity. Image adapted from Sanchez 2020 [10].

Da Silva et al. [2] report a detailed review of the most studied and characterized fungal BS, highlighting that s ophorolipids (SL) and mannosylerythritol (MEL) lipids are the main fungal products investigated so far. Other classes of lipids are Cellobiose and polyol lipids, the latter considered to be exclusive of fungi, differing from other glycolipids for the replacement of the hydrophilic portion by a polyol (typically D-mannitol or D-arabitol) linked to a fatty acid. Another class of BS typical of fungi is that of proteins, in particular Hydrophobins. According to Sanches et al [11], *Aspergillus, Penicillium*, and *Fusarium* are the most studied genera for the production of BS. Unfortunately, fungal BS are still way less exploited when compared to the bacterial ones. Fungal BS, and in particular those from filamentous fungi, represent only 19% out of the total, although they show a wide chemical structural variability [12]. Bacterial strains like *Pseudomonas* and *Bacillus* are the most studied and characterized throughout the scientific literature. The differences between scientific data output on fungal and bacterial BS may lie in the fact that fungal growths are more time-consuming and also growth conditions in the lab still represent quite a challenge. Anyway, the main reason could be linked to the production yields obtained are still lower when compared to those of bacteria [8]. These drawbacks are hard to overcome, but the richness of this class of microorganisms, which reflects an even wider richness of BS compounds, is worthy of further studies.

Additionally, many BS producing bacteria are human pathogens (e.g. *Pseudomonas, Bacillus*) and hence are inadequate for use in food or pharmaceutical industries, while an advantage of using BS producing fungi, and in particular yeasts like *Saccharomyces cerevisiae*, resides in the aspect of most of them of being “generally regarded as safe” [13].
Optimization of growth conditions is one of the most promising ways to reduce production costs, and hence increase applicability of fungal BS. Behind the use of agro-industrial waste and non-conventional substrates (plastics, oil-based compounds), the optimization of bioprocess parameters and downstream processing steps are also constantly being improved to ensure greater yields [2]. A new appealing possibility to increase the production and development of BS is through genetic improvements of strains. Genetic material can be modified e.g. by metabolic engineering, an example is given by the company Evonik, that produces sophorolipids from the genetically modified strain *S. bombicola* through the insertion and deletion of genes that overexpress enzymes involved in the synthesis of those compounds [14]. Other companies like Henkel (GE) or Holiferm (UK), produce SL or MEL via genetically modified bacterial strains; however, no BS produced by filamentous fungi is commercially available to date [11]. Although filamentous fungi can produce BS, the biosynthesis of these compounds, their genetic basis, and the production route are not yet fully understood.

1.2.1 Hydrophobins and Ceratoplatanins

As mentioned above, proteins are a class of fungal BS. Proteins are intrinsically amphipathic molecules, even if their amphiphilic nature is affected by several factors such as protein folding or post-translational modifications. This is particularly true for a class of proteins, named Hydrophobins (HPBs). Usually, all filamentous fungi, both ascomycetes and basidiomycetes, produce HPBs that fulfill several purposes during fungal growth. The importance of these proteins in fungal development processes lies in their ability to self-assemble into stable, amphipathic layers. These layers significantly decrease the interfacial tension, allowing aerial structures to breach the surface and grow into the air. Fruiting bodies or spores are also coated with HPBs layers, which reduces wetting, helps mediate resilience to environmental stresses, and allows the spores to adhere to hydrophobic surfaces [15].

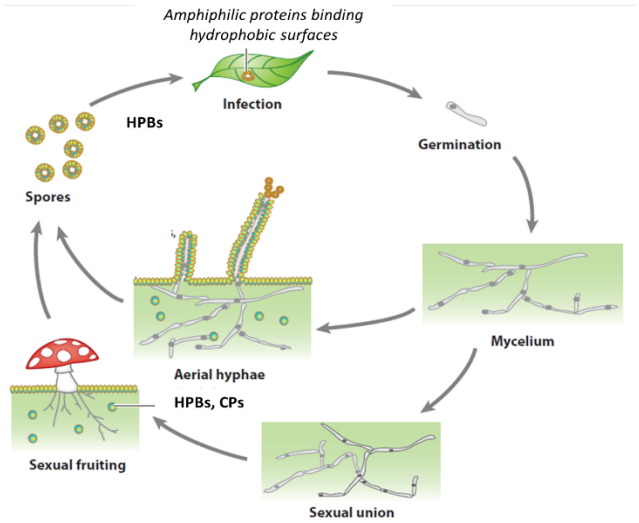

Figure 2. The role of surface-active proteins in fungal growth and development. Most filamentous fungi begin their lives as spores, coated by surface-active proteins, e.g. hydrophobins. Following germination, hyphae are formed and branch into an expanding network that is the mycelium. Because most fungi grow in a moist or liquid environment, aerial structures need to overcome surface tension at the substrate:air interface. Hydrophobins, along with cerato-platanins, are secreted by fungi to control the surface activity and properties of the substrate:air interface, coating aerial structures and conferring water resistance. Image adapted from [15]

HPBs are secreted as monomers, then their polymerization process, called interfacial self-assembly [16], starts when they find an interface between air and water, or a hydrophobic surface. HPBs are small proteins (5 to 20 kDa) with a conserved pattern of eight cysteine residues, that form four disulfide bridges, however, besides this highly conserved pattern, inter-cystein sequences show very low similarities. HPBs are usually classified in two classes mainly based on the solubility properties of their assemblies, but also on the spacing among the Cys residues and the position of hydrophobic residues relative to these Cys [17]. Class I HPBs assemble into insoluble polymeric layers composed of fibrillar structure known as *rodlets*; these layers are extremely stable and can be only solubilized with strong acid treatments. On the other hand, class II HPBs form layers soluble in detergents or alcohol and have a conserved length of the inter-cysteine spaces [18]. Both classes, however, are characterized by the presence of a four-stranded β-barrel core, while the main differences regard the length of the loops and the position of α-helical structures. Class I HPBs have also been recently split into other two sub-classes, depending on whether they are produced by Ascomycetes or Basidiomycetes, class IA and IB, respectively. Differences between the two concern mainly structure and self-assembling processes. Class IB subdivision includes the experimentally confirmed sequences HGFI (*Grifola frondosa*), Vmh2 (*Pleurotus ostreatus*), along with the *S. commune* SC3 and SC16, while Class IA include the

Aspergillus fumigatus RodA [17]. Despite these attempts to group HPBs into classes, high variability was revealed also between proteins produced by the same strain, as SC3 and SC16. SC16 share 56% of the sequence with SC3, from its first to last cysteine, yet it possesses a unique HPBs structure, resembling both class I and II.

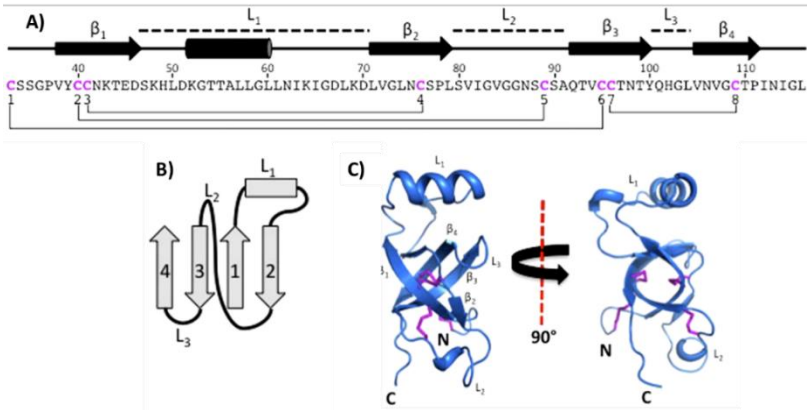

Figure 3.A) The sequence of SC16 from the first cysteine residue to the C-terminus. The secondary structure is indicated for each residue and the locations of the loops, β -sheets and helix of SC16 are indicated. Cysteine residues are coloured fuchsia and disulphide linkages are indicated by a line. B) Schematics of the secondary structure elements of SC16, both β -sheets (1-4) and intervening loops (L_1-L_3) are indicated. C) A ribbon diagram of the lowest-energy SC16 structure. Disulphide bonds are shown in fuchsia and the β -sheets and loops are indicated. Image adapted from [17].

Despite the structural variations across HPBs, they all display a separation of hydrophobic and charged/polar residues on different faces of the protein surface, explaining their high surface activity [19]. Moreover, the nature of the interface or environment that triggers the self-assembly of the Class I hydrophobin influences the structure and properties of the resultant coating [20].

Another class of fungal biosurfactant proteins, poorly studied from this point of view, consists of Ceratoplatanins (CPs), another group of small cysteine-containing proteins. CPs were originally assumed to be HPB-like proteins, while recent studies highlight structural and biological differences among these two classes of proteins. CPs show four conserved cysteines forming two disulfide bridges, and differently from HPBs, they lack a large hydrophobic patch [21]. Similarly to HPBs, they can self-assemble at interfaces, although the layers they form are endowed with a much lower stability. While the self-assembling mechanisms of HFBs have been widely studied, studies on the CPs assembly are still limited, even if it has been confirmed that this process is related to the protein concentration and the interaction with a hydrophobic material [22].

This protein family owes their name to the pathogen fungus *Ceratocystis platani*, from which the protein CP was firstly found and characterized as virulence factor [23]. Indeed, as their biological activity concerns, they are phytotoxic and contribute to full virulence of pathogens, but other protein of this family, can induce expression of defense genes in host and non-host plant tissues. However, the presence and abundant expression of CPs in fungi with all types of lifestyles suggests that the main biological functions are not solely related to fungal–plant interactions but to other, more general aspects of fungal growth, e.g. hyphal growth in submerged mycelium [15,21]. Additionally, according to Silva et al [24], *Trichoderma spp*. can regulate the hydrophobicity of the host or substrate surfaces, making them more hydrophilic to facilitate access to nutrients or plant interactions.
Another interesting feature of these proteins is their structure (a double ψβ-barrel fold with six β-strands and two α-helices) that is homologous to the N-terminal domain of Expansins, which are proteins associated with carbohydrate binding and loosening of the cellulose scaffolds in plant cell walls. Similar to expansins, CPs can weaken cellulose substrate, disrupting its non-covalent bonds without any hydrolytic activity [25]. This action could be useful to efficiently hydrolyze cellulosic substrates; in fact, cellulases must have complete access to the cellulose chains that are tightly packed.

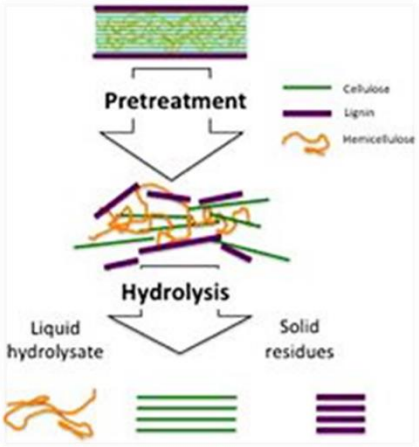

Figure 4. schematic representation of CPs action on lignocellulosic materials.

Although studies about CPs surface properties are still limited, in some cases it has been reported that CPs can increase the polarity of solutions and surfaces e.g. EPL1 from *Tricodherma atroviride* [26]. Other studies, conversely, highlight the surfactant activity that these proteins possess, resembling those of HPBs [27]. In particular, two CPs isolated from marine fungal strains were proven to be effective surfactants, hence stabilizing emulsions and lowering the surface tension of aqueous solutions.

1.2.2 Other classes of BS proteins

HPBs and secondly CPs, are the most studied fungal surface-active proteins. However, results achieved by our research group recently, seem to suggest that there are other classes of fungal proteins with surfactant abilities. In this sense, fungi particularly those grown in hostile environments are a rich and intriguing source of new BS.

A good example is given by the work of Cicatiello et al [28] in which a BS protein secreted by the marine fungal strain *Penicillium chrysogenum,* was identified as a hypothetical protein, annotated as Pc13g06930. Although this protein was extracted according to already set up HPBs extraction protocols, and it also showed similar properties with this class of proteins (e.g. emulsification ability, aggregation in amyloid-like fibrils), identification by a proteomic approach, confirmed that it does not belong to HPBs family.

Fungal surface-active proteins offer a valid yet underexplored substitute for synthetic surfactants. Beyond their intriguing properties, there is the potential for industrial-scale utilization through genetic engineering.

1.3 Applications

Synthetic surfactants able to reduce interfacial tension, increase solubilization of hydrophobic compounds, and stabilize emulsions are highly valuable in so many industrial sectors, that their environmental impact cannot be overlooked any longer. Moreover, one of today's key challenges is to reduce our dependence on fossil fuels (oil, coal, gas) and to move toward using renewable and sustainable sources. As mentioned above, BS represent a valid replacement for such compounds, considering the enormous genetic diversity that microorganisms possess [29]. Application fields for BS are multiple and very diverse, they span from bioremediation to food processes, from pharmaceutical to agricultural practices, and from oil recovery to cosmetic products. The applications of most interest for this work concern bioremediation and biomedical aspects.

BS, and in particular fungal BS, have shown good antibacterial, antiadhesive and also anti-cancer activity. Additionally, they can be used for the development of novel drug delivery systems, such as micro or nano-based drug carriers [30]. Antiadhesive properties arise from their ability to adhere to surfaces, changing their hydrophobicity and hence inhibiting the successive adhesion and colonization of bacteria. This property represents a very potent tool in the field of biomedical implants, often challenged by chronic infections. Activities strictly related to their amphiphilic nature are the capacity to form nano/micro emulsions useful for drug delivery systems and also the antibacterial and antiviral ones [31]. Regions of opposite polarity enable the interaction with the lipid bilayer of the microbial membrane causing disruption, and ultimately death. A similar mechanism is believed to occur also in the case of viruses [32].

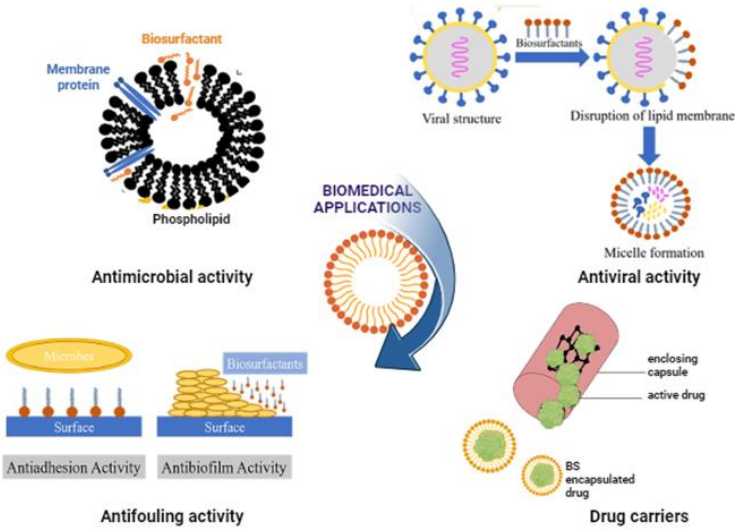

Figure 4. schematic representation of all the possible BS applications in the medical field. image adapted from [30].

BS are particularly suitable to tackle environmental issues, such as oil spills and bioremediations of soil and water, since synthetic chemical surfactants could accumulate and lead to further environmental pollution. The key process of these treatments is to increase the bioavailability of the poorly soluble contaminants. In this sense, BS are very useful for enhancing the desorption and solubilization of hydrocarbons, thereby increasing their bioavailability and facilitating their assimilation by microorganisms, either by enhancing their emulsification or by forming micelles, in which compounds are entrapped [33]. BS have proven to be efficient against multiple kinds of hazardous compounds, not only petroleum-based but also aromatic molecules like styrene, fluoroanthene, benzotriazole [3] and toxic metals (*e.g.* arsenic, lead, mercury) [34]. Bioremediation can be achieved through in situ or *ex-situ* techniques. Compared to their synthetic counterpart, BS can be released *in situ* with minor drawback effects on the environment, having the added advantages of low toxicity and biocompatibility. *In situ* methodologies can be distinguished in those that involve fungal active metabolites as surfactants and enzymes or those in which fungi are used as bioinoculants, also known as the bioaugmentation technique. Bioinoculants are selected strains that resist the presence of other microorganisms in the polluted site and still have the ability to interact with contaminants and/or produce metabolites for remediation [35]. In this way, the autochthonous microflora is enriched by the addition of selected indigenous or genetically modified microbial species to support oil degradation [36].

WORK DESCRIPTION

The main purposes of this PhD project are related to both the identification and characterization of novel BS protein produced by fungi isolated from hostile environments, especially landfill soils. At the same time, the exploitation of already known BS proteins (HPBs and CPs) in biomedical and bioremediation application fields was carried out. More in detail:

- Two fungal strains were studied as BS-producing microorganisms. The isolated surface-active proteins have been characterized as biosurfactants and bioemulsifiers. Their identification revealed the existence of a novel class of BS proteins.
- The Class I HPB Vmh2 was characterized for the first time in terms of emulsifying and surface activity and compared to another unknown small Cys-rich protein, proving their excellent BS properties.
- The BS protein, *ThCP* was tested for its potential application in the valorization of agro-food wastes.
- The engineered variant of Vmh2 with an antimicrobial peptide (GKY20) was used to impart antibiofilm/antibacterial properties to different surfaces of interest in the biomedical field.

In the appendix section, two publications are reported, one regarding studies about BS produced by marine fungal strains, published before this PhD work. The other arises from my collaboration with another research group, about the characterization of collagen-based glue in the art restoration field. Considering my skills in sample preparation and SDS-PAGE analysis, my contribution was related to setting up and optimizing dialysis protocols of glue samples and their visualization by SDS-PAGE.

1. Kronberg, B.; Holmberg, K.; Lindman, B. Types of Surfactants, Their Synthesis, and Applications. In *Surface Chemistry of Surfactants and Polymers*; Wiley, **2014**; 1–47.
2. da Silva, A.F.; Banat, I.M.; Giachini, A.J.; Robl, D. Fungal Biosurfactants, from Nature to Biotechnological Product: Bioprospection, Production and Potential Applications. *Bioprocess Biosyst Eng* **2021**, *44*, 2003–2034.
3. Ng, Y.J.; Lim, H.R.; Khoo, K.S.; Chew, K.W.; Chan, D.J.C.; Bilal, M.; Munawaroh, H.S.H.; Show, P.L. Recent Advances of Biosurfactant for Waste and Pollution Bioremediation: Substitutions of Petroleum-Based Surfactants. *Environ Res* **2022**, *212*, 113126 – 113141
4. Aquino, S.F.; Chernicharo, C.A.L.; Soares, H.; Takemoto, S.Y.; Vazoller, R.F. Methodologies for Determining the Bioavailability and Biodegradability of Sludges. *Environ Technol* **2008**, *29*, 855–862
5. Karthick, A.; Roy, B.; Chattopadhyay, P. A Review on the Application of Chemical Surfactant and Surfactant Foam for Remediation of Petroleum Oil Contaminated Soil. *J Environ Manage* **2019**, *243*, 187–205.
6. Perfumo, A.; Smyth, T.J.P.; Marchant, R.; Banat, I.M. Production and Roles of Biosurfactants and Bioemulsifiers in Accessing Hydrophobic Substrates. In *Handbook of Hydrocarbon and Lipid Microbiology*; Timmis, K.N., Ed.; Springer Berlin Heidelberg: Berlin, Heidelberg, **2010**; 2, 1501–1512
7. Van Hamme, J.D.; Singh, A.; Ward, O.P. Physiological spects. Part 1 in a Series of Papers Devoted to Surfactants in Microbiology and Biotechnology. *Biotechnol Adv* **2006**, *24*, 604–620.
8. Mujumdar, S.; Joshi, P.; Karve, N. Production, Characterization, and Applications of Bioemulsifiers (BE) and Biosurfactants (BS) Produced by Acinetobacter Spp.: A Review. *J Basic Microbiol* **2019**, *59*, 277–287.
9. Uzoigwe, C.; Burgess, J.G.; Ennis, C.J.; Rahman, P.K.S.M. Bioemulsifiers Are Not Biosurfactants and Require Different Screening Approaches. *Front Microbiol* **2015**, *6*, 245 - 251
10. Sánchez, C. Fungal Potential for the Degradation of Petroleum-Based Polymers: An Overview of Macro- and Microplastics Biodegradation. *Biotechnol Adv* **2020**, *40*, 107501 - 107513
11. Sanches, M.A.; Luzeiro, I.G.; Alves Cortez, A.C.; Simplício De Souza, É.; Albuquerque, P.M.; Chopra, H.K.; Braga De Souza, J.V. Production of Biosurfactants by Ascomycetes. *Int J Microbiol* **2021**, *2021*, 1- 11
12. Raaijmakers, J.M.; de Bruijn, I.; Nybroe, O.; Ongena, M. Natural Functions of Lipopeptides from Bacillus and Pseudomonas: More than Surfactants and Antibiotics. *FEMS Microbiol Rev* **2010**, *34*, 1037–1062.
13. Santos, D.K.F.; Rufino, R.D.; Luna, J.M.; Santos, V.A.; Sarubbo, L.A. Biosurfactants: Multifunctional Biomolecules of the 21st Century. *Int J Mol Sci* **2016**, *17*.
14. Steffen, s.; mirja, w.; anja, t. Cells, nucleic acids, enzymes, and use thereof, and methods for the production of sophorolipids PATENT, **2011**.
15. Sunde, M.; Pham, C.L.L.; Kwan, A.H. Molecular Characteristics and Biological Functions of Surface-Active and Surfactant Proteins. **2017**, 86, 585 - 609.
16. Wosten, H.A.B.; De Vocht, M.L. Hydrophobins, the Fungal Coat Unravelled. *Biochim Biophys Acta* **2000**, *1469*, 79–86.
17. Gandier, J.A.; Langelaan, D.N.; Won, A.; O'Donnell, K.; Grondin, J.L.; Spencer, H.L.; Wong, P.; Tillier, E.; Yip, C.; Smith, S.P.; et al. Characterization of a Basidiomycota Hydrophobin Reveals the Structural Basis for a High-Similarity Class i Subdivision. *Sci Rep* **2017**, *7*, 5863 - 5872
18. Cicatiello, P.; Sorrentino, I.; Piscitelli, A.; Giardina, P. Spotligh on Class I Hydrophobins: Their Intriguing Biochemical Properties and Industrial Prospects. In *Grand Challenges In Fungal Biotechnology*; 2020; 333–348.
19. Schor, M.; Reid, J.L.; MacPhee, C.E.; Stanley-Wall, N.R. The Diverse Structures and Functions of Surfactant Proteins. *Trends Biochem Sci* **2016**, *41*, 610–620.
20. Siddiquee, R.; Lo, V.; Johnston, C.L.; Buffier, A.W.; Ball, S.R.; Ciofani, J.L.; Zeng, Y.C.; Mahjoub, M.; Chrzanowski, W.; Rezvani-Baboli, S.; et al. Surface-Induced Hydrophobin Assemblies with Versatile Properties and Distinct Underlying Structures. *Biomacromolecules* **2023**, *24*, 4783–4797
21. Bonazza, K.; Gaderer, R.; Neudl, S.; Przylucka, A.; Allmaier, G.; Druzhinina, I.S.; Grothe, H.; Friedbacher, G.; Seidl-Seiboth, V. The Fungal Cerato-Platanin Protein EPL1 Forms Highly Ordered Layers at Hydrophobic/Hydrophilic Interfaces. *Soft Matter* **2015**, *11*, 1723–1732
22. Martellini, F.; Faoro, F.; Carresi, L.; Pantera, B.; Baccelli, I.; Maffi, D.; Tiribilli, B.; Sbrana, F.; Luti, S.; Comparini, C.; et al. Cerato-Populin and Cerato-Platanin, Two Non-Catalytic Proteins from Phytopathogenic Fungi, Interact with Hydrophobic Inanimate Surfaces and Leaves. *Mol Biotechnol* **2013**, *55*, 27–42
23. Bernardi, R.; Baccelli, I.; Carresi, L.; Comparini, C.; Pazzagli, L.; Scala, A. Cerato-Platanin Elicits Transcription of Defence-Related Genes Earlier than Ceratocystis Platani on Platanus Acerifolia. *For Pathol* **2011**, *41*, 255–261
24. Silva, A.C.; Oshiquiri, L.H.; de Morais Costa de Jesus, L.F.; Maués, D.B.; Silva, R. do N. The Cerato-Platanin EPL2 from Trichoderma Reesei Is Not Directly Involved in Cellulase Formation but in Cell Wall Remodeling. *Microorganisms* **2023**, *11*, 1965 - 1981
25. Baccelli, I. Cerato-Platanin Family Proteins: One Function for Multiple Biological Roles? *Front Plant Sci* **2015**, *5*, 1 - 4
26. Frischmann, A.; Neudl, S.; Gaderer, R.; Bonazza, K.; Zach, S.; Gruber, S.; Spadiut, O.; Friedbacher, G.; Grothe, H.; Seidl-Seiboth, V. Self-Assembly at Air/Water Interfaces and Carbohydrate Binding Properties of the Small Secreted Protein EPL1 from the Fungus Trichoderma Atroviride. *Journal of Biological Chemistry* **2013**, *288*, 4278 - 4287
27. Pitocchi, R.; Cicatiello, P.; Birolo, L.; Piscitelli, A.; Bovio, E.; Cristina Varese, G.; Giardina, P. Cerato-Platanins from Marine Fungi as Effective Protein Biosurfactants and Bioemulsifiers. *Int J Mol Sci* **2020**, *21*, 2913 - 2925
28. Cicatiello, P.; Stanzione, I.; Dardano, P.; De Stefano, L.; Birolo, L.; De Chiaro, A.; Monti, D.M.; Petruk, G.; D'errico, G.; Giardina, P. Characterization of a Surface-Active Protein Extracted from a Marine Strain of Penicillium Chrysogenum. *Int J Mol Sci* **2019**, *20*, 3242 - 3255

29. Nikolova, C.; Gutierrez, T. Biosurfactants and Their Applications in the Oil and Gas Industry: Current State of Knowledge and Future Perspectives. *Front Bioeng Biotechnol* **2021**, *9*, 1 -19
30. Handa, S.; Aggarwal, Y.; Puri, S.; Chatterjee, M. Pharmaceutical Prospects of Biosurfactants Produced from Fungal Species. *J Basic Microbiol* **2022**, *62*, 1307–1318.
31. Guerrini, L.; Alvarez-Puebla, R.A.; Pazos-Perez, N. Surface Modifications of Nanoparticles for Stability in Biological Fluids. *Materials* **2018**, *11*, 1154 - 1182
32. Ceresa, C.; Fracchia, L.; Fedeli, E.; Porta, C.; Banat, I.M. Recent Advances in Biomedical, Therapeutic and Pharmaceutical Applications of Microbial Surfactants. *Pharmaceutics* **2021**, *13*, 466 - 491
33. Chaprão, M.J.; Ferreira, I.N.S.; Correa, P.F.; Rufino, R.D.; Luna, J.M.; Silva, E.J.; Sarubbo, L.A. Application of Bacterial and Yeast Biosurfactants for Enhanced Removal and Biodegradation of Motor Oil from Contaminated Sand. *Electronic Journal of Biotechnology* **2015**, *18*, 471–479
34. da Silva, A.F.; Banat, I.M.; Robl, D.; Giachini, A.J. Fungal Bioproducts for Petroleum Hydrocarbons and Toxic Metals Remediation: Recent Advances and Emerging Technologies. *Bioprocess Biosyst Eng* **2023**, *46*, 393–428
35. Medaura, M.C.; Guivernau, M.; Moreno-Ventas, X.; Prenafeta-Boldú, F.X.; Viñas, M. Bioaugmentation of Native Fungi, an Efficient Strategy for the Bioremediation of an Aged Industrially Polluted Soil With Heavy Hydrocarbons. *Front Microbiol* **2021**, *12*, 1 - 18
36. da Silva, I.G.; da Almeida F.C.; Silva N.M.; Casazza A.A.; Converti A.; Sarubbo L.A. Soil Bioremediation: Overview of Technologies and Trends, *Energies*, **2020,** *13*, 4664 – 4689.

CHAPTER 2

2.1 INTRODUCTION

Fungi are well-known resilient microorganisms, able to inhabit hostile environments such as landfill soils, both terrestrial and marine petroleum-contaminated areas, cold habitats, etc. The marine environment, for example, with its huge diversity of landscape and conditions, represents an abundant source for the discovery of new compounds. Fungal species variety, indeed, is as rich in the terrestrial environment as in the marine ecosystem, although the latter remains mostly unexplored. Culture-independent techniques such as metagenomics, can help for the exploration of otherwise inaccessible microorganisms [1] (See sect. 2.1). As mentioned above, fungi are also often isolated from contaminated sites, like dumpsites, landfills, or highly anthropized areas. Thanks to their hyphal apparatus indeed, they can combine biochemical and physical actions, involving secondary metabolites such as enzymes and BSs, to colonize and survive on different matrices [2,3]. Of particular interest today is the accumulation of plastic waste all around the globe. Plastic materials are remarkably stable over time, however, nature continues to adapt and evolve, and the fungal community can change due to the presence of plastic polymers, as already noticed in the presence of PE [4,5] or even of new generation biodegradable plastics. With this in mind, extraction and characterization of new BS protein from strains isolated from marine sites (see sect. 2.2) and from plastic landfill soils (See sect. 2.3) were herein conducted. A small protein, previously accounted as an HPB, was extracted from the marine fungal strain *Acremonium sclerotigenum*. The protein, named PAC3, showed many structural and self-assembling features in common with class I HPBs [6]. PAC3, indeed, in aqueous solution can spontaneously assemble into amyloid-fibrils, and also showed a high propensity to form lateral assembled, long fibrils when deposited onto a hydrophobic surface. BS extraction from the other fungal strains, isolated from plastic dumpsite, led to the identification of an unknown protein endowed with excellent emulsifying activity. The book chapter in section 2.1 gives a comprehensive introduction to the isolation of new fungal BS proteins, while sections 2.2 and 2.3 point out that there are different classes, besides the already known HPBs, of fungal proteins with surfactant abilities.

1. Gudiña, E.J.; Teixeira, J.A.; Rodrigues, L.R. Biosurfactants Produced by Marine Microorganisms with Therapeutic Applications. Mar Drugs **2016**, 14, 38 - 43
2. Kim, D.Y.; Rhee, Y.H. Biodegradation of Microbial and Synthetic Polyesters by Fungi. Appl Microbiol Biotechnol **2003**, 61, 300–308,
3. Spina, F.; Tummino, M.L.; Poli, A.; Prigione, V.; Ilieva, V.; Cocconcelli, P.; Puglisi, E.; Bracco, P.; Zanetti, M.; Varese, G.C. Low Density Polyethylene Degradation by Filamentous Fungi. Environmental Pollution **2021**, 274, 116548 - 116558
4. Esan, E.O.; Abbey, Lord; Yurgel, S. Exploring the Long-Term Effect of Plastic on Compost Microbiome. PLoS One **2019**, 14, 1 -12
5. Wiedner, K.; Polifka, S. Effects of Microplastic and Microglass Particles on Soil Microbial Community Structure in an Arable Soil (Chernozem). SOIL **2020**, 6, 315–324
6. Cicatiello, P.; Dardano, P.; Pirozzi, M.; Gravagnuolo, A.M.; De Stefano, L.; Giardina, P. Self-Assembly of Two Hydrophobins from Marine Fungi Affected by Interaction with Surfaces. Biotechnol Bioeng **2017**, 114, 2173 - 2184

Marine Fungi as a Source of Biosurfactants and Bioemulsifiers

Rossana Pitocchi, Alessandra Piscitelli, and Paola Giardina

Abstract The state of knowledge of terrestrial and marine fungi is significantly different, and the causes are diverse. However, there is no doubt that marine fungi have a huge potential in providing new compounds with intriguing characteristics. In this respect, biosurfactants and bioemulsifiers are an emerging class of compounds that, thanks to their unique features, can be applied in a wide range of application fields. Up to now, marine fungi are strongly unattended as effective source of these compounds. Herein some examples of screening of marine fungi able to produce biosurfactants and the characterization of their surface-active compounds are reported.

Keywords Surface tension · Emulsion · Surface active proteins · Screening methods

1 Introduction

The richness of fungal species is generally associated with that of terrestrial fungi. Indeed, marine fungi considerably contribute to the global fungal diversity and recently, marine environment is proving to be an inexhaustible source of new microorganisms producing many useful compounds thanks to their peculiar metabolism. The physical and chemical factors unique to the marine environment, which can mainly influence marine fungi are high salinity and hydrostatic pressure, low temperature, oligotrophic nutrient conditions. Because of these unique physic-chemical properties, marine fungi are endowed with unusual physiological adaptative systems that can be widely exploited in biotechnology.

There is a significant gap between the state of knowledge of terrestrial and marine fungi, and the causes are diverse. One could be the relative difficulty of sampling of marine fungi compared to terrestrial, or problems encountered in growing marine fungi in laboratory conditions, or the lower achievable yield of certain secondary

R. Pitocchi · A. Piscitelli · P. Giardina (✉)
Department of Chemical Sciences, University Federico II, Naples, Italy
e-mail: giardina@unina.it

S. K. Deshmukh et al. (eds.), *Fungal Biopolymers and Biocomposites*,
https://doi.org/10.1007/978-981-19-1000-5_15

metabolites compared with that of bacteria. However, according to Amend et al. (2019), the first challenge of marine mycology is in defining which fungi are truly "marine."

Pang et al. (2016) defined marine fungus as "any fungus that is recovered repeatedly from marine habitats and is able to grow and sporulate on substrates in marine environments or forms symbiotic relationships with other marine organisms or is shown to adapt and evolve at the genetic level and be metabolically active in marine environments".

According to Raghukumar (2008), marine fungi can be classified as obligate and facultative. The first are fungi that grow and sporulate only in sea water and their spores germinate in sea water. On the other hand, facultative fungi have undergone physiological adaptations from other environments to the marine one where they can grow and sporulate.

Marine fungi have been isolated in a huge range of conditions, for example associated with other organisms (plant, algae, sponges) (Kiran et al. 2009), in deep-see sub-surfaces (Rédou et al. 2015), or even associated with dwelling macrofauna and zooplankton (Raghukumar et al. 2010). In addition, fungi can be isolated in oil-contaminated costal area and/or sediments (Bovio et al. 2017; Maamar et al. 2020). Indeed, they can survive even in extreme environmental conditions, in those habitats that appear challenging for life, since they can promptly adapt to changing environments and tolerate several types of pollutants. This peculiar ability is well exhibited in both terrestrial and marine environments, however, literature about bioactive compounds produced by marine fungi is still poor compared with that of terrestrial fungi.

In marine environment the hydrocarbon-degrading capability is widespread. One possible adaptive system to enhance bioavailability and gain access to hydrophobic compounds could be the production of biosurfactants (BS), substances with surface-active properties (Kaczorek et al. 2018). Due to their amphiphilic structure, they can lower interfacial tension and facilitate solubilisation of hydrophobic substances in water. Indeed they can migrate to hydrophobic:hydrophilic interfaces thanks to their amphiphilic nature, aligning their hydrophobic region facing the hydrophobic side and their hydrophilic region facing the polar side of the interface. This alignment balances the interfacial forces and reduces the surface tension (Sunde et al. 2017). The capability to produce BS is most widespread among the hydrocarbon-degrading microbial communities (Perfumo et al. 2010).

Chemical structures of BS produced by different microorganisms are extremely diverse. Hydrophobic and hydrophilic components establish their amphiphilic character, with the hydrophobic part usually composed by fatty acids, or fatty alcohols with variable chain lengths. The hydrophilic components can be small hydroxyl, carboxyl or phosphate groups, or carbohydrate (mono-, oligo-, or polysaccharides) or (poly-)peptide moieties.

According to different studies (Uzoigwe et al. 2015; McClements et al. 2017; Tao et al. 2019), high molecular weight BS, such as hetero/lipopolysaccharides, proteins and lipoproteins are named bioemulsifiers (BE) since they efficiently emulsify immiscible liquids even at low concentrations and are less effective at reducing

surface tension (Kubicki et al. 2019). Nevertheless, it can be reasonably assumed that one kind of activity does not preclude the other. The low molecular weight microbial products generally referred as BS, are composed of sugars, amino acids, fatty acids. These compounds are mostly known to decrease interfacial tension between two or more immiscible liquids, thus possessing a low critical micelle concentration (CMC), however they can also form stable emulsions. BS are mainly anionic and ionic compounds; cationic BS are rare and, in most cases, toxic.

Thanks to their amphiphilic nature, BS can form and stabilize foam, act as detergent and lubricant, solubilize hydrocarbons (Kaczorek et al. 2018). Consequently, they are valuable in a great variety of application fields such as medical, pharmaceuticals, food and beverages, cosmetics, agriculture, detergent, textiles, and petrochemical production. They represent a promising alternative with respect to their synthetic counterparts due to their eco-friendly nature, and temperatures, pH, and salinity resistance. Nevertheless, BS global market is comparatively low, mainly because of poor productivity from microorganisms and expensive downstream processes. To overcome these drawbacks genetic modification and growth condition optimization of microorganisms can be carried out, for example using agricultural wastes as carbon source (Bhardwaj et al. 2013; Fenibo et al. 2019).

BS indeed are considered as "*green molecules*" because of their wide applications in soil bioremediation (Mujumdar et al. 2019). The use of surfactant solution in remediation processes is assessed; different synthetic surfactants had been used for treatment of contaminated soil and/or water. Mechanisms are diverse and depend on the nature of surfactant, and characteristics of soil and/or water. In general, it has been seen that surfactants can increase petroleum, and hydrocarbons solubilisation thus helping its removal from soil and water.

Recently, promising technologies for remediation of petroleum contaminated soil have been developed based on surfactant solution and surfactant foam flushing processes (Karthick et al. 2019). The two main problems of synthetic surfactants are their high toxicity and low biodegradability. Toxicity is the measure of adverse effects caused by surfactants in the soil, whereas biodegradability is the ability of microorganisms present in the environment to completely degrade the surfactant (Aquino et al. 2008). Another serious problem concerning with synthetic surfactants lies in the fact that they can easily accumulate in soil, this accumulation could cause modification in soil characteristics. For example, soil hydrophobicity can change, thus inhibiting the normal fluid retention in the soil and leading to the death of microorganisms (Karthick et al. 2019).

Among marine-BS producing microorganisms, bacteria are widely studied and even exploited in some application fields, for example they had been used in bioremediation processes (Harayama et al. 1999), while the study of marine fungi has been neglected for many years. Among the different genera of bacteria, the best studied and characterized for their BS/BE producing activity are *Acinetobacter spp, Bacillus* and *Pseudomonas* (Satpute et al. 2010; Waghmode et al. 2020). For instance, an extensive and comprehensive collection of BS and BE produced by several *Acinetobacter* strains, is given by Mujumdar et al. (2019).

Only recently the extremely various group of marine fungi has been considered as an excellent source of natural products. Actually, numerous secondary metabolites from marine fungi have been characterized, showing pharmaceutically/medical relevant bioactivities. Among these natural products, BS deserve attention for the unique growing conditions of their producing microorganisms (Gudiña et al. 2016).

BS also display anti-biofilm and anti-adhesive activities, and anticancer activities which are particularly relevant for medical applications. The antiadhesive ability makes them able to decrease adhesion and colonization by pathogens, as well as to remove pre-formed biofilms. Antimicrobial activity of surfactants is well known, but literature mainly concerns about terrestrial microorganisms or synthetic surfactants (Satpute et al. 2010; Coelho et al. 2020). Several studies conducted by Das et al. (2008) show that BS produced by a marine bacterium belonging to Bacillus genera, *Bacillus circulans,* possesses both good surface tension reduction with low CMC and antimicrobial activity. They isolated and identified a BS compound as lipopeptide, trough Thin layer chromatography (TLC) and Fourier-transform infrared spectroscopy (FTIR) experiment. This compound share most of the IR spectrum pattern with a known BS, surfactin. It was found to inhibit growth of some Multi Drug Resistant bacteria (like *Klebsiella pneumoniae* and other two MDR strains of *E. coli*), beside several gram positive and negative bacteria. They also investigate on substrate dependence production, doubling the yield production and antimicrobial activity in the presence of glycerol or starch when compared to glucose (Das et al. 2008).

Mukherjee et al. (2009) moreover, isolated a lipopeptide from another *Bacillus (Bacillus licheniformis* BAS509) able to inhibit most of the tested bacterial (both Gram positive and negative) and fungal strains (*Aspergillus niger*, *Aspergillus flavus* and *Candida albicans*). The antimicrobial action against bacterial strains were checked by agar well diffusion test.

As far as the anticancer activity, many of the drugs involved in chemotherapy are cytotoxic, non-specific and are extracted from natural sources such as plants. The latter represent a big disadvantage because of the high processes' costs and relative low production. The advantages of using microbial surfactant lie for example, in the possibility of genetically engineering microbes, that allows to increase production yield. Furthermore, they exhibit high efficacy, low toxicity, and easy biodegradability, which are relevant features in any anti-cancer agent (Gudiña et al. 2016). As mentioned before, in the search of novel compounds with medical applications, BS from marine fungi are considerably less exploited respect to the bacterial derived ones.

Acute respiratory distress syndrome (ARDS) is a progressive syndrome which result in inefficient oxygen transfer across alveolar membranes into the blood (Matthay et al. 2019). Covid-19 can often cause ARDS, with the resulting lack of oxygen to organs. One of the causes of this alveolar fluid build-up, is surfactant dysfunction which has negative consequences on the emulsification of liquid from this particular region. Future studies will be aimed at using BS as a novel treatment for ARDS, through solubilizing the alveolar substrate (Smith et al. 2020).

2 Methods of Screening and Characterization of Surfactants

2.1 Drop Collapse Test

Drop collapse test is a very rapid, non-expensive and reliable experiment to perform in order to establish if the sample is surface active. In addition, it requires small volumes of sample and no specialized equipment (Bodour and Miller-Maier 1998). The test consists in depositing a sample drop onto a hydrophobic surface and measuring its collapsing area. When in contact with a hydrophobic surface, in fact, BS solution collapses, spreading more extensively than water over it.

Although this test is manly qualitative, Bodour and Miller (1998) proposed an alternative protocol that allows quantification of BS, too. Plotting drop diameter as a function of surfactant concentration, they obtained a calibration curve with a good range of linearity. This curve can be used to determine surfactant concentration of unknown samples.

2.2 Oil Displacement Test

This test is based on the characteristic of surfactants to decrease interfacial tension between different phases, and it is a semi-quantitative method to detect surfactant presence. When oil is added to the surface of a petri dish filled with distilled water and then a drop of surfactant solution is spotted on the surface, oil is displaced, and a clear halo expands (Luepongpattana et al. 2017b). The more the surfactant concentration is, the bigger the oil-displacement area is (Fig. 1). Similarly, to the drop collapse test, this test is very rapid to perform, does not require big volume of sample and does not implies particular equipment. As disadvantage indeed, a big quantity of wastes is produced.

2.3 2,6-Dichlorophenol Indophenol (DCPIP) Colorimetric Assay

The DCPIP based colorimetric assay is not specific to detect the presence of BS, but it is often used as screening method for their production, since it measures the utilization/degradation of hydrocarbons by microorganisms, that is normally related to BS production (Obi et al. 2016).

DCPIP is blue when oxidized and colourless when reduced, being a pH dependant redox indicator. If it is incorporated in a microbial culture during hydrocarbon oxidation, electrons are transferred to DCPIP rather than to O_2, nitrate and sulphate, as usual. Therefore, degradation of hydrocarbons is visualized by monitoring loss of

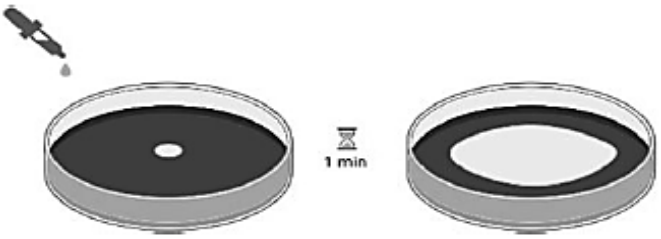

Fig. 1 schematic representation of oil displacement test performed in a petri dish

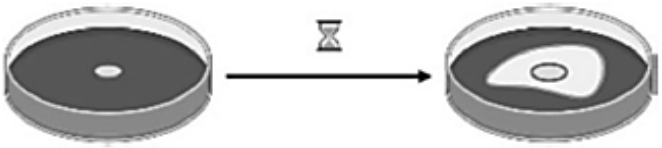

Fig. 2 Schematic representation of the DCPIP discolorization method performed in agar-based culture

colour spectrophotometrically (Hanson et al. 1993; Varjani and Upasani 2013). This test can be performed in agar-based culture, in the presence of hydrocarbons, showing a discoloration halo around fungal hyphae (Fig. 2).

2.4 Emulsification Activity

Ability of surfactants to stabilize emulsions between immiscible phases is commonly reported in terms of Emulsification Index, labelled E_{24}. The experiment is easy to perform and give a rapid and reliable answer. It consists in mixing surfactant solution with a non-polar solvent (kerosene or a 65:35 mix of decane:toluene) and homogenising them to form an emulsion (Fig. 3). Then, the emulsification index is calculated as:

$$E_{24} = \frac{\text{emulsion layer height}}{\text{total volume height}} \times 100$$

To have more detailed information about emulsion nature, thus establishing if it is oil-in-water emulsion or rather water-in-oil, it is possible to analyse emulsions through, for example, confocal microscopy technique. Specific dyes to stain oil and/or surfactant molecules can be used to better visualize emulsions structure (Blesic et al. 2017).

An intriguing feature of this experiment is the possibility to explore emulsification activity varying several parameters besides concentration, such as pH, salinity, temperature, etc. This is important because it allows to understand whether a compound is suitable for a certain application field or not. As an example, for marine bioremediation purpose, a BS must retain its emulsification ability even at high salt concentration or high pressure.

Fig. 3 schematic representation of surfactant-emulsion formation in the presence of an immiscible phase

Table 1 surface tension value of different absolute solvents. (Abe 2019)

Compound	γ (mN/m)
Water	72.75
Glycerin	63.4
Toluene	28.5
Ethanol	22.8
n-hexane	18.4
Olive oil	32.9

2.5 Surface Tension Measurement

Surface tension, indicated as γ, is a force to shrink the surface and has the dimension of force per unit length (mN/m) (Abe 2019). Surface tension measurement is the most accurate technique to detect the presence of surfactant compounds and the most widespread methods are the Du Nouy ring and the Wilhelmy plate. Experimentally these methods are very similar: a platinum ring in the case of Du Nouy method, and a platinum or glass plate for the other, are immersed into the testing liquid to form a liquid–solid–air interface. Then the force necessary to rise the ring and/or the plate is measured by the tensiometer.

This measurement requires a well specialized equipment, big volumes of sample (at least 10 ml) and it is more time-consuming measure. As a pro indeed, it gives no false positive and it allows to calculate Critical Micelle Concentration, that is a very important parameter when characterizing BS. In Table 1 some examples of γ value of absolute solvent are reported.

3 Screening of Marine Fungal Strains Biosurfactant Producers

A limited number of examples about BS producing strain screening, on fungal communities inhabiting in hostile environments, can be found in literature. Indeed, in most of these studies, these BS were only partially characterized, and their

activities analysed using the crude extracts, while only few examples of isolation, identification and characterization of BS compounds from marine fungi are present. Here are briefly reported example of screening on BS producing marine fungal strains, in which the afore described methods are used. In addition, some examples of identification and purification of the BS compounds are reported too.

The *Mycotheca Universitatis Taurinensis* (MUT) represents one of the most important banks of fungal biodiversity in Italy. The purposes of the MUT are the acquisition, identification, preservation and distribution of macro and micromycetes. In particular, it deals with fungal strains isolated from sites of interest, such as landfill, marine chronically contaminated sites etc.

At this regard, in the work of Bovio et al. (2017), 67 taxa were isolated from water samples and sediments, from a contaminated site in the Mediterranean Sea, along the coastal zone of Sicily. For many of the identified species it is the first time of their discovery in seawater and sediments. All isolated fungi were tested primarily for their capabilities to grow on crude Arabian Light oil as sole carbon source, in agar-based culture. Percentage of stimulation was estimated comparing mycelium growth in the presence and absence of crude oil. A percentage stimulation greater than 20% was considered as significant. All the isolated fungi were able to grow on crude oil, although only 24% showed a good percentage of stimulation. Fungi were classified according to their features and by molecular analysis. The most represented genera among the water collected samples were *Penicillium, Aspergillus* and *Trichoderma*. Four strains (*Aspergillus terreus*, *Trichoderma harzianum*, *Penicillium citreonigrum*, Lulworthaiales sp.) were then selected and their capability to degrade oil in liquid cultures was assessed using a modified protocol of the DCPIP colorimetric assay (Varjani and Upasani 2017). Three main parameters were valued: changing from blue to colourless of the culture medium, fungal biomass growth and disappearance of crude oil. Petroleum hydrocarbons degradation by the same fungi was analysed using GC-FID analysis, and two of them, *A. terreus* and *P. citreonigrum*, showed the highest potential for bioremediation.

Another good example of screening on marine fungi BS producing strains, in which simple and fast techniques are involved, is offered by the work of Maamar et al. (2020). Eighty-four filamentous were fungi collected from the port of Oran, Algeria, a chronically contaminated site, and identified through PCR analysis. BS production was proved testing ability of fungi to grow on Arabian Light oil in different concentration and use it as the sole carbon source. Twelve among the fungi selected gave positive results, showing a good growth rate in the presence of 1% and 5% crude oil. No one was able to growth in the presence of 0.1% crude oil. These 12 fungi belong mainly to *Aspergillus* and *Penicillum* genera. Further analysis on the 12 BS producing fungi were performed using different techniques, such as crude oil degradation assay using the decolorization method with DCPIP, oil-drop collapse test and oil-displacement test. Just five among the strains previously selected are the most promising BS producers and all of them belong to *Penicillum* genus.

A very similar investigation on marine fungi as producers of BS was conducted by Luepongpattana et al. (2017b). Sixteen strains were isolated from the coastal

areas of Koh Si Chang (Thailand) and identified. Screening for BS production was performed on the cell-free supernatant of each strain using the oil-displacement test and the Du Nouy method. Among them, the one identified as *Aureobasidium pullulans* (YTP6-14) gave the best results in both the experiments, reaching a surface tension value of 38.4 mN/m. Optimization of growth parameters condition of this strain was then performed.

4 Protein Biosurfactants Produced by Marine Fungi

Proteins are intrinsically partially amphipathic, being composed of amino acids with charged, polar, and nonpolar side chains. However, the amphipilic character of a protein is affected by several factors, such as its fold, conformational stability, flexibility and posttranslational modifications. Surface-active proteins achieve their function through different forms, ranging from peptides to large proteins, from monomers to large assemblies, and from highly ordered structures to disordered regions. Some of them can also undergo major conformational changes.

An array of surface-active proteins expressed during the life cycle of fungi, helps their growth in liquid, semiliquid, and moist substrates, as well as into the air and onto solid surfaces or interfaces.

Hydrophobins (HPB) are probably the most surface-active proteins known and the best studied. They are small, cysteine rich, amphiphilic proteins typical of filamentous fungi. Eight cysteines forming four disulfide bonds are highly conserved, while they show a high sequence diversity, suggesting multiple biological roles. Their amphipathic tertiary structure provides surfactant-like activity and allow their self-assembly into amphipathic layers at hydrophobic-hydrophilic interfaces (Berger and Sallada 2019). This feature can for example, lead to a stabilization of air bubbles and water/oil emulsions. Nonetheless, characterization of HPBs as effective BS and/or BE is scarce.

Class I HPB assemble into layers with a distinctive rodlet pattern. The rodlet characteristics are common to those of amyloid structures (usually associated with amyloid diseases) and their dissolution is only possible by treatment with strong acids. Class II HPB assemblies are less robust and form layers with varied morphology (Ren et al. 2013). The primary structures of Class I HPB are much less conserved (including size variations) than those of class II, which show a high degree of sequence conservation.

Ceratoplatanins (CP) have been included among the small fungal surface-active proteins (Sunde et al. 2017), even if few studies on this kind of activity have been reported so far, and their function is still a matter of debate. They were originally assumed to be HPB-like proteins, while recent studies highlighted structural and biological differences among these two classes of proteins. CP show four conserved cysteines forming two disulfide bridges, and lack of a large hydrophobic patch, differently from HPB. Another issue concerns the ability of CP to change the wettability of surfaces. HPB layers are known to invert the wettability of surfaces,

while CP can increase the polarity of surfaces, as reported by Frishmann et al. (2013). Another important difference concerns the tendency of HPB to form amyloid-like aggregate, that seems to be completely absent for CP.

Among 100 marine fungi from MUT, 23 were selected for their ability to produce foam in shaken cultures and analysed for the identification of new HPB by Cicatiello et al. (2016). Six fungi were then chosen as the best producers of surface-active proteins endowed with different characteristics. In particular, a protein produced by a facultative marine strain of *Penicillium chrysogenum* (SAP-*Pc*) showed remarkable emulsification ability of a water/olive oil mixture. Indeed, according to literature, marine isolates of *P. chrysogenum* were good sources of new interesting bioactive compounds (Imhoff 2016). SAP-*Pc* was identified as a previously unknown surface-active protein, and was able to form amyloid-like fibrils, like class I HPB. Emulsification ability was tested using "Dectol" (Decane:Toluene 65:35 v/v) as a model oil varying conditions as pH and concentrations, and the best result were obtained in aqueous buffer pH 7 ($E_{24} = 70\%$). What is noteworthy is that E_{24} do not vary even increasing protein concentration from 100 μg/ml to 400 μg/ml. Critical micelle concentration was obtained at 28 μg/ml (2 μM) corresponding in a decrease of surface tension of about 55 mN/m. At protein concentrations higher than about 200 μg/ml, a steep decline of the surface tension indicated the occurrence of another aggregation phenomenon, confirmed by Dynamic Light Scattering (DLS) and Atomic Force Microscopy analysis (Cicatiello et al. 2019).

Two Class I HPB from *Penicillium roseopurpur*eum and *Acremonium sclerotigenum* isolated from marine fungi in the screening previously described (Cicatiello et al. 2016) were purified. Different techniques (circular dichroism, dynamic light scattering and Thioflavin T fluorescence assay) were used to analyse their propensity to form fibrils (Cicatiello et al. 2017). It has been demonstrated that the formation of amyloid fibrils and the assembly morphologies depend on their interaction with specific surfaces. Properties of protein layers can be exploited as bio-coating for different materials.

Two of the fungal strains isolated from the oil spill contaminated site in the Mediterranean Sea, *A. terreus* and *T. harzianum* and selected for their ability to grow on crude oil as sole carbon source (Bovio et al. 2017), were exploited to verify the induction of BS production to solubilize and metabolize organic molecules. Among all the secondary metabolites that could possibly be involved in this process, secreted proteins were explored. Only one secreted protein for each fungal strain was purified and identified. Both proteins were ascribed to the family of CP (Pitocchi et al. 2020). For the first time these proteins were characterized as efficient BE and BS. In particular, the protein from *T. harzianum* identified as *ThCP*, showed a very good capability to decrease the surface tension of water to a minimum value of 36 mN/m at a CMC of 8×10^{-7} M (10 μg/ml).

4.1 Other Biosurfactants Produced by Marine Fungi

BS of different chemical composition are only rarely isolated and identified from marine fungi.

A marine sponge, *Fasciospongia cavernosa*, was collected from the Bay of Bengal region of the Indian peninsular coast (Kiran et al. 2009). Eight sponge-associated marine fungi were isolated from the sponge and screened for BS production, using different tests, hemolytic assay (Carrillo et al. 1996; Moran et al. 2002), drop collapsing test, oil displacement test. Hemolytic activity in blood agar plate (using both human and sheep blood) is an alternative and less used screening method to select BS producers. Indeed, BS can induce hemolysis at a given concentration and activity is revealed as a distinct clearance zone around colony. Among the eight isolated sponge-associated fungi, only one named MSF3 was selected as good BS producer and further characterized. First, different growth conditions were tested with the aim to improve BS production, varying different parameters. BS production in each condition was evaluated through emulsification activity of the cell free supernatant. Once assessed the best culturable conditions, only a partial chemical characterization was performed through TLC analysis. This led to the classification of the isolated BS as glycolipoprotein.

In the work of Luepongpattana et al. (2017b), only one fungal strain was selected from several strains collected in the Gulf of Thailand, as promising BS producers, *Aureobasidium pullulans* YTP6-14, a dimorphic fungus. Different growth conditions were tested for *A. pullulans* varying carbon sources, among which soybean and palm oil. Nevertheless, the maximum BS production yield (1.26 g/L) was achieved with a mixed carbon source (glycerol and glucose). BS production was first assessed through surface tension and oil displacement area measurement on cultural broth. The minimum surface tension was 32 mN/m (Luepongpattana et al. 2017a). Extraction of the crude BS was then performed using ethyl acetate and a critical micelle concentration of 39 mg/L was evaluated on the crude BS. Purification and characterization of the extracted BS led to identification of the compound as 5-hydroxy-2-decenoic acid delta-lactone, commonly named as massoia lactone (whose structure is reported in Fig. 4). This compound shows a great ability in reducing tension and, what is more, surface tension value does not increase neither varying pH of the solution from 2 to 12, neither increasing NaCl concentration up to 12% (w/v).

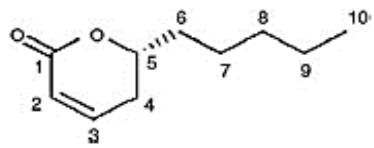

Fig. 4 chemical structure of massoia lactone biosurfactant

5 Future Perspectives

Natural products from some fungal genera, such as *Penicillium* and *Aspergillus*, have been intensively studied, however the great potential of secondary metabolites produced by these fungi has not yet been fully explored. Indeed, the marine microbial world remains largely unexplored even though recent studies have been aimed at exploring the diversity of ecosystems using molecular techniques. The main difficulty concerns the growth of most of marine microorganisms under laboratory conditions (Felczykowska et al. 2012; Jackson et al. 2015). A valid alternative could be culture-independent techniques that can allow the analysis of inaccessible marine microorganisms, avoiding the necessity of culturing them, and the discovery of new natural compounds with important biological activities. One of these molecular techniques is metagenomics that allows culture-independent study of microbial communities through the extraction and analysis of genetic material from any environmental sample, giving access to the total genetic pool of all the microorganisms present in that community and, as consequence, to their biosynthetic capacity (Gudiña et al. 2016).

The growing resource of fungal genome sequences can assist the exploration of new biosynthetic pathways of secondary metabolites and biosynthetic gene clusters. It has been demonstrated that many fungal secondary metabolites show significant differences in bioactivities although closely structurally related. Therefore, it is important to analyse the variety of structures offered by fungi, in order to unravel their biotechnological potential (Imhoff 2016). Interest in BS, as secondary metabolites produced by fungi, has been continuously increasing and the marine environment can be an important source of new and performing compounds.

Recent papers (Sánchez 2020; Spina et al. 2021) have clearly shown that fungi also play a crucial role in the degradation and mineralization of plastics. Indeed, fungi can extend their hyphae through substrates, thus they can explore and grow in places hardly accessible to other microorganisms. Plastics degradation by fungi is favoured not only by their powerful enzymatic system and their ability of adsorption (Karich et al. 2017), but also by the production of natural BS (Sunde et al. 2017), which enable them to use hydrophobic polymers as a source of nutrients.

More recent studies on fungal BS proteins, endowed with very good bioemulsifying activity, can pave the way for their massive production through recombinant expression in highly producing microorganism hosts, thus bringing them closer to their marketability.

References

Abe M (2019) Measurement techniques and practices of colloid and Interface. Springer, Singapore
Amend A et al (2019) Fungi in the marine environment:open questions and unsolved problems. Ecol Evol Sci 10(2):1–15

Aquino SF et al (2008) Methodologies for determining the bioavailability and biodegradability of sludges. Environ Technol 29:855–862. https://doi.org/10.1080/09593330802015508
Berger BW, Sallada ND (2019) Hydrophobins : multifunctional biosurfactants for interface engineering. J Biol Eng 13(10):1–8
Bhardwaj G, Cameotra SS, Chopra HK (2013) Biosurfactants from fungi: a review. J Pet Environ Biotechnol 4(6):1–6. https://doi.org/10.4172/2157-7463.1000160
Blesic M et al (2017) Evaluating the potential of natural surfactants in the petroleum industry: the case of hydrophobins. Pure Appl Chem 2(90):305–314. https://doi.org/10.1515/pac-2017-0703
Bodour AA, Miller-Maier RM (1998) Application of a modified drop-collpase technique for surfactant quantitation and screening of biosurfactant-producing microorganisms. J Microbiol Methods 32:273–280
Bovio E et al (2017) Science of the Total Environment The culturable mycobiota of a Mediterranean marine site after an oil spill : isolation, identi fi cation and potential application in bioremediation. Sci Total Environ 576:310–318. https://doi.org/10.1016/j.scitotenv.2016.10.064
Carrillo PG, Mardaraz C, Giuliett AM (1996) Isolation and selection producing bacteria. World J Microbiol Biotechnol 12(1):62–64
Cicatiello P et al (2016) Marine fungi as source of new hydrophobins. Int J Biol Macromol 92:1229–1233. https://doi.org/10.1016/j.ijbiomac.2016.08.037
Cicatiello P et al (2017) Self-assembly of two Hydrophobins from marine fungi affected by interaction with surfaces. Biotechnol Bioeng 114(10):2173–2186. https://doi.org/10.1002/bit.26344
Cicatiello P et al (2019) Characterization of a surface-active protein extracted from a marine strain of Penicillium chrysogenum. Int J Biol Macromol 20:3242–3255. https://doi.org/10.3390/ijms20133242
Coelho LAS et al (2020) 'Mannosylerythritol lipids : antimicrobial and biomedical properties. Appl Microbiol Biotechnol 104:2297–2318. https://doi.org/10.1007/s00253-020-10354-z
Das P, Mukherjee S, Sen R (2008) Antimicrobial potential of a lipopeptide biosurfactant derived from a marine Bacillus circulans. J Appl Microbiol 104:1675–1684. https://doi.org/10.1111/j.1365-2672.2007.03701.x
Felczykowska A, Bloch SK, Nejman-faleńczyk B (2012) Metagenomic approach in the investigation of new bioactive compounds in the marine environment. ACTA Biochimica Polonia 59(4):501–505
Fenibo EO, Ijoma GN, Selvarajan R (2019) Microbial surfactants:the next generation multifunctional biomolecules for applications in the petroleum industry and its associated environmental remediation. Microorganisms 7:1–29
Frischmann A et al (2013) Self-assembly at air/water interfaces and carbohydrate binding properties of the small secreted protein EPL1 from the fungus Trichoderma atroviride. J Biol Chem 288:4278–4287. https://doi.org/10.1074/jbc.M112.427633
Gudiña EJ, Teixeira JA, Rodrigues LR (2016) Biosurfactants produced by marine microorganisms with therapeutic applications. Mar Drugs 14:38–43. https://doi.org/10.3390/md14020038
Hanson KG, Desai JD, Desai AJ (1993) A rapid and simple screening technique for potential crude oil degrading microorganisms. Biotechnol Tech 7(10):745–748
Harayama S et al (1999) Petroleum biodegradation in marine environments. J Mol Microbiol Biotechnol 1(1):63–70
Imhoff JF (2016) Natural products from marine fungi — still an underrepresented resource. Marine Drugs 14:19–38. https://doi.org/10.3390/md14010019
Jackson SA et al (2015) Metagenomics for the discovery of novel biosurfactants of environmental interest from marine ecosystems. Curr Opin Biotechnol 33:176–182. https://doi.org/10.1016/j.copbio.2015.03.004
Kaczorek E et al (2018) The impact of biosurfactants on microbial cell properties leading to hydrocarbon bioavailability increase. Colloids Interfaces 2:35–57. https://doi.org/10.3390/colloids2030035

Karich A et al (2017) Fungal unspecific Peroxygenases oxidize the majority of organic EPA priority pollutants. Front Microbiol 8(August). https://doi.org/10.3389/fmicb.2017.01463

Karthick A, Roy B, Chattopadhyay P (2019) A review on the application of chemical surfactant and surfactant foam for remediation of petroleum oil contaminated soil. J Environ Manag 243:187–205. https://doi.org/10.1016/j.jenvman.2019.04.092

Kiran GS et al (2009) Optimization and production of a biosurfactant from the sponge-associated marine fungus Aspergillus ustus MSF3. 73. Colloids Surfac B Biointerfac 73:250–256. https://doi.org/10.1016/j.colsurfb.2009.05.025

Kubicki S et al (2019) Marine biosurfactants: biosynthesis, structural diversity and biotechnological applications. Mar Drugs 17:1–30

Luepongpattana S, Thaniyavarn J, Morikawa M (2017a) Production of massoia lactone by Aureobasidium pullulans YTP6-14 isolated from the Gulf of Thailand and its fragrant biosurfactant properties. J Appl Microbiol 132:1448–1497. https://doi.org/10.1111/jam.13598

Luepongpattana S et al (2017b) Screening of biosurfactant production yeast and yeast-like fungi isolated from the coastal areas of Koh Si Chang. In: The 26th Annual Meeting of the Thai Society for Biotechnology and International Conference, pp 469–477

Maamar A et al (2020) Highlighting the crude oil bioremediation potential of marine fungi isolated from the port of Oran (Algeria). Diversity 12:196–215. https://doi.org/10.3390/d12050196

Matthay MA et al (2019) Acute respiratory distress syndrome. Nat Rev Dis Prim 5:18–30. https://doi.org/10.1038/s41572-019-0069-0

McClements DJ, Bai L, Chung C (2017) Recent advances in the utilization of natural emulsifiers to form and stabilize emulsions. Ann Rev Food Sci Technol 8:205–236. https://doi.org/10.1146/annurev-food-030216-030154

Moran AC, Martinez A, Sineriz F (2002) Quantification of surfactin in culture supernatants by hemolytic activity. Biotechnol Lett 24:177–180

Mujumdar S, Joshi P, Karve N (2019) Production, characterization, and applications of bioemulsifiers (BE) and biosurfactants (BS) produced by Acinetobacter spp.: A review. J Basic Microbiol 59:277–287. https://doi.org/10.1002/jobm.201800364

Mukherjee S et al (2009) Antimicrobial biosurfactants from marine Bacillus circulans : extracellular synthesis and purification. Appl Microbiol 48:281–288. https://doi.org/10.1111/j.1472-765X.2008.02485.x

Obi LU, Atagana HI, Adeleke RA (2016) Isolation and characterisation of crude oil sludge degrading bacteria. SpringerPlus 5:1946–1959. https://doi.org/10.1186/s40064-016-3617-z

Pang K et al (2016) " Marine fungi " and " marine-derived fungi " in natural product chemistry research : toward a new consensual definition. Br Mycol Soc 30:163–175. https://doi.org/10.1016/j.fbr.2016.08.001

Perfumo A et al (2010) Production and roles of biosurfactants and bioemulsifiers in accessing hydrophobic substrates. In: Handbook of hydrocarbon and lipid microbiology, pp 1502–1514. https://doi.org/10.1007/978-3-540-77587-4

Pitocchi R et al (2020) Cerato-Platanins from Marine Fungi as Effective Protein Biosurfactants and Bioemulsifiers. Int J Mol Sci 21:2913–2925. https://doi.org/10.3390/ijms21082913

Raghukumar C (2008) Marine fungal biotechnology:an ecological perspective. Fungal Divers 31:19–36

Raghukumar C, Damare SR, Singh P (2010) A review on deep-sea fungi: occurrence, diversity and. Bot Mar 53:479–492. https://doi.org/10.1515/BOT.2010.076

Rédou V et al (2015) Species richness and adaptation of marine fungi from deep-subseafloor sediments. Appl Environ Microbiol 81(10):3571–3583. https://doi.org/10.1128/AEM.04064-14

Ren Q, Kwan AH, Sunde M (2013) Invited review two forms and two faces, multiple states and multiple uses: properties and applications of the self-assembling fungal Hydrophobins. Pept Sci 100(6):601–612. https://doi.org/10.1002/bip.22259

Sánchez C (2020) (2020) 'fungal potential for the degradation of petroleum-based polymers: an overview of macro- and microplastics biodegradation'. Biotechnol Adv 40:107501. https://doi.org/10.1016/j.biotechadv.2019.107501

Satpute SK et al (2010) Biosurfactants, bioemulsifiers and exopolysaccharides from marine microorganisms. Biotechnol Adv 28(4):436–450. https://doi.org/10.1016/j.biotechadv.2010.02.006

Smith ML et al (2020) Biosurfactants:a covid-19 perspective. Front Microbiol 11(1341):1–8. https://doi.org/10.3389/fmicb.2020.01341

Spina F et al (2021) Low density polyethylene degradation by fi lamentous fungi *. Environ Pollut 274:116548. https://doi.org/10.1016/j.envpol.2021.116548

Sunde M, Pham CLL, Kwan AH (2017) Molecular characteristics and biological functions of surface-active and surfactant proteins. Annu Rev Biochem 86:585–608. https://doi.org/10.1146/annurev-biochem-061516-044847

Tao W et al (2019) 'Designer bioemulsifiers based on combinations of different polysaccharides with the novel emulsifying esterase AXE from Bacillus subtilis CICC 20034. Microbial Cell Factories BioMed Central 18:1–10. https://doi.org/10.1186/s12934-019-1221-y

Uzoigwe C et al (2015) Bioemulsifiers are not biosurfactants and require different screening approaches. Front Microbiol 6:1–6. https://doi.org/10.3389/fmicb.2015.00245

Varjani SJ, Upasani VN (2013) Comparative studies on bacterial consortia for hydrocarbon degradation. Int J Innov Res Sci Eng Technol 2(10):5377–5383

Varjani SJ, Upasani VN (2017) Critical review on biosurfactant analysis, purification and characterization using rhamnolipid as a model biosurfactant. *Bioresour Technol* 232:389–397. https://doi.org/10.1016/j.biortech.2017.02.047

Waghmode S et al (2020) Planococcus species – an imminent resource to explore biosurfactant and bioactive metabolites for industrial applications. Front Bioeng Biotechnol 8(August):1–8. https://doi.org/10.3389/fbioe.2020.00996

International Journal of
Molecular Sciences

MDPI

Article

Evidence of Small Fungal Cysteine-Rich Proteins Acting as Biosurfactants and Self-Assembling into Large Fibers

Rossana Pitocchi, Ilaria Stanzione, Anna Illiano, Angela Amoresano, Oreste Tarallo, Paola Cicatiello *, Alessandra Piscitelli and Paola Giardina

Department of Chemical Sciences, University of Naples Federico II, Via Cintia, 80126 Naples, Italy; rossana.pitocchi@unina.it (R.P.); ilaria.stanzione@unina.it (I.S.); anna.illiano@unina.it (A.I.); angela.amoresano@unina.it (A.A.); oreste.tarallo@unina.it (O.T.); alessandra.piscitelli@unina.it (A.P.); paola.giardina@unina.it (P.G.)
* Correspondence: paola.cicatiello@unina.it; Tel.: +39-0817463?7

Abstract: Fungi produce surface-active proteins, among which hydrophobins are the most characterized and attractive also for their ability to form functional amyloids. Our most recent findings show that these abilities are shared with other classes of fungal proteins. Indeed, in this paper, we compared the characteristics of a class I hydrophobin (Vmh2 from *Pleurotus ostreatus*) and an unknown protein (named PAC3), extracted from the marine fungal strain *Acremonium sclerotigenum*, which does not belong to the same protein family based on its sequence features. They both proved to be good biosurfactants, stabilizing emulsions in several conditions (concentration, pH, and salinity) and decreasing surface tension to a comparable value to that of some synthetic surfactants. After that, we observed for both Vmh2 and PAC3 the formation of giant fibers without the need for harsh conditions or long incubation time, a remarkable ability herein reported for the first time.

Keywords: bioemulsifiers; functional amyloids; surface tension; marine fungi

Citation: Pitocchi, R.; Stanzione, I.; Illiano, A.; Amoresano, A.; Tarallo, O.; Cicatiello, P.; Piscitelli, A.; Giardina, P. Evidence of Small Fungal Cysteine-Rich Proteins Acting as Biosurfactants and Self-Assembling into Large Fibers. *Int. J. Mol. Sci.* **2023**, *24*, 13843. https://doi.org/10.3390/ijms241813843

Academic Editor: Artur J.M. Valente

Received: 25 July 2023
Revised: 4 September 2023
Accepted: 6 September 2023
Published: 8 September 2023

1. Introduction

Biosurfactants (BSs) are water-soluble surface-active species, naturally occurring or synthesized from natural components. Their main properties are strong surface activity, adsorption to different interfaces and surfaces, and their ability to self-assemble into aggregates or micelles. In synthetic surfactants, the main structural characteristics are a hydrophilic group, which may be charged, and a hydrophobic group, which is usually an alkyl chain. In bioemulsifiers (BEs), the headgroup can consist of amino acids or saccharide groups, and the hydrophobic portion could be a group of hydrophobic amino acids, an alkyl chain, or other classes of compounds, i.e., the steroid-alkaloid group. The distinct separation between the hydrophilic and hydrophobic regions is often less definite in BSs as compared with synthetic surfactants. Low molecular weight BSs are typically glycolipids or lipopetides and are usually produced by bacteria [1]. The higher molecular weight BSs are often biopolymers, such as polysaccharides, proteins, liposaccharides, or lipoproteins, and are mainly extracellular. They should be more appropriately defined as BEs because they can emulsify two immiscible liquids, even at low concentrations, while not significantly reducing surface or interfacial tension [2].

The wide applications of BEs and BSs in several areas, such as food, agriculture, chemicals, medicine, and energy, have led scientific studies to disclose novel routes to optimize production parameters, increase yields, and cut costs in order to find applications of these compounds at the industrial level. Among other microorganisms, fungi are gaining global interest for their ability to produce these biopolymers at high concentrations under relatively simple production conditions [3].

In particular, filamentous fungi produce and secrete small, amphipathic proteins called hydrophobins (HPBs) (~70–150 residues). HPBs are highly surface-active proteins due to their

asymmetrical distribution of hydrophilic and hydrophobic amino acids on a compact globular protein surface [4]. They spontaneously self-assemble at hydrophobic: hydrophilic interfaces into amphipathic layers, which are functional for fungi because they allow them to breach air and water boundaries; otherwise, surface tension could impede their growth. The structural feature common to all HPBs is the presence of eight conserved cysteine residues that form four disulfide bridges, which connect C1–C6, C2–C5, C3–C4, and C7–C8. The HPB family has been divided into two classes based on the stability of the layer they form and the length of the inter-cysteine spaces [5,6]. Their amino acid sequences show low similarity even when they belong to the same class. For instance, class I hydrophobins share as little as 10% identity in their alignments despite belonging to the same protein family. On the other hand, class II hydrophobins share more sequence identity (48%) and identical cysteine residue spacing [7].

Class I HPBs, produced by ascomycetes and basidiomycetes species, assemble into insoluble layers, which share the cross-β structure and morphology with amyloid fibrils. These extremely stable layers can only be solubilized with harsh acid treatments (formic acid or trifluoroacetic acid) [6]. On the other hand, class II HPBs, produced only by ascomycetes, form aggregates soluble in detergents or alcohols [8]. More recently, this classification has been questioned. Indeed, an intermediate third class has been proposed based on the analysis of hydrophobicity profiles and protein properties [9]. Moreover, a further subdivision of class I HPBs between ascomycete and basidiomycete (class IA and IB, respectively) has been introduced [10].

Class I HPBs are among the first proteins recognized as functional amyloids [11]. These 'functional amyloids' can play physiological roles, being involved in a significant variety of processes, including storage, structural scaffolding, cell signaling, biofilm formation, stabilization, and more.

We studied the self-assembly of the class I HPB Vmh2 from the basidiomycete *Pleurotus ostreatus* in aqueous solutions by using different spectroscopic and microscopic techniques. Vmh2 spontaneously self-assembles into isolated, long, and twisted amyloid fibrils. This process is promoted by acidic pH, temperature, and Ca^{2+} ions [12]. Several applications of this protein, alone or fused with other biotechnologically interesting proteins, have been developed [6]. Furthermore, our research group extracted new putative HFBs from selected marine fungi, since the unique environmental conditions in which they grow lead to the development of proteomes different from those of their terrestrial counterparts, providing new and intriguing biological products [13]. Six HPB-like proteins have been partially isolated and characterized, and their ability to change the wettability of a hydrophobic surface and to stabilize water/oil emulsions have been assessed, suggesting their potential as BS or BE [14]. In particular, a protein isolated from *Acremonium sclerotigenum*, named PAC3, showed a high propensity to form an emulsion with olive oil, form amyloid fibrils, and interact with hydrophobic and hydrophilic surfaces. For these characteristics, PAC3 has been previously classified as class I HPB [15].

In this paper, we analyze the amino acid sequence of PAC3 and observe that it does not belong to the class I HPB, as Vmh2. Nevertheless, we demonstrate that these two proteins can form giant fibers without needing an acidic pH, high temperature, and long incubation time. Moreover, the BS and BE properties of Vmh2 were herein studied for the first time and compared with those of PAC3.

2. Results

Two filamentous fungi, *P. ostreatus* and *A. sclerotigenum*, a terrestrial and a marine strain, are already known to produce amphiphilic self-assembling proteins, Vmh2 and PAC3, respectively. The former is a class I HPB, and the latter, PAC3, shares many characteristics with the HPB proteins family; nonetheless, its sequence is unknown.

2.1. PAC3 Sequence Analysis

The *A. sclerotigenum* genome sequence is unknown; thus, several experiments were performed to determine the de novo amino acid sequencing of PAC3. No results about

the N-terminal sequence were found using the Edman approach, indicating a blocked N-terminus. Classical trypsin hydrolysis protocols, involving denaturation, reduction, and carboxyamidomethylation, did not produce any detectable peptides, neither in solution nor in situ (SDS-PAGE band extraction), probably due to rigid protein conformation that limits the proteolytic action of the digestive enzyme, despite the denaturing environment. Only when the protein was pretreated with 5 mM of dithiothreitol (DTT) at 60 °C for 10 min, it was efficiently denatured and hydrolyzed. The peptide mixture was analyzed by using MALDI-TOF, and the spectrum was recorded in the 400–3500 m/z mass range. It was characterized by the presence of a single intense base peak at 2575 m/z and a limited number of other low signals reported in Figure 1. The MALDI-MS/MS analysis of the fragmentation spectra led to the sequences summarized in Table S1. The fragmentation spectrum of the peptide at 2575 m/z is reported as an example in Figure S2. It can be observed that the 927 m/z signal could be associated with the N-terminus of the protein (Q as the first amino acid) and that only a small portion of the sequence corresponding to the 3204 m/z signal was reconstructed.

A)

m/z	Identified aminoacid sequence
2575	TAYDQVPLATPLPDTSLNEVLYR
1565	CPPDTSLDEVLYR
1130	TELDEVLYR
1037	ELDEVLYR
618	CADLR
927	pGlu-MFDPVR
3204	SLLDDGYETADLR-(partial MS/MS data)

B)

```
peptide1                    ------------------------------------:**-:**-:****TAYDQVPLATP   11
A0A0B7KSF0_BIOOC    MVVKYHSGLAVLLAFSSAVLAQITTFCTYQEYLCGSTLLTNGYAVADLRTAYDANLNSFV   60
peptide2                    ------------------------------------SLLDDGYETADLR****----:--  13

peptide1                    LPDTSLNEVLYR--------------------------------  23
A0A0B7KSF0_BIOOC    IPDTALNKVLFRCTDNVGAIVGNSYCIVGCGVVGDNLVDDNCTM  104
peptide2                    :***:**:**--------------------------------  13
```

Figure 1. (**A**) Table of the identified amino acid sequences from MALDI-TOF analysis; (**B**) alignment of peptide 1 (2575 m/z) and peptide 2 (3204 m/z) with the unknown protein from *B. ochroleuca* resulting from the BLAST research in the Uniprot database. (*) conserved sequence (identical); (:) conservative mutation; (-) Gap.

Homology research regarding the sequence of the peptide at 2575 m/z using the BLAST tool from Uniprot revealed a partial identity with an unknown protein from the fungus *Bionectria ochroleuca* (A0A0B7K0S3_BIOOC), which belongs to the same order (Hypocreales) of *A. sclerotigeum*. Moreover, the partial sequence determined for the 3204 m/z peptide can be effectively aligned to the same protein, using the ClustalW tool, resulting in placement just before the sequence of the peptide at 2575 m/z (Figure 1). The obtained result showed a 44% identity percentage with the A0A0B7K0S3_BIOOC protein in the aligned region.

MALDI-TOF analysis of the reduced and carboxyamidomethylated protein compared to the non-treated one showed an increase in the molecular weight corresponding to the presence of six cysteines (Figure S3), analogously to the protein A0A0B7K0S3_BIOOC. However, it differs significantly from the HPBs family, which exhibits a conserved pattern of eight cysteines.

2.2. *Self-Assembling of Protein into Fibers*

Vmh2, being a class I HPB, forms amyloid fibrils spontaneously. Surprisingly, the small Cys-rich protein PAC3, herein found to not belong to this class, shows the same ability to self-assemble into fibrils [15].

Moreover, the recombinant Vmh2 fused to GFP (green fluorescent protein) was recently drop-cast on a polystyrene surface and analyzed by using laser confocal microscopy, observing fluorescent giant fibers (hundreds of microns long and tens of microns wide) [16]. To understand if similar structures were also formed by the native Vmh2 and by PAC3, the

Thioflavine T (ThT) fluorescent probe (commonly used to detect amyloid fibrils) was added to the protein solutions and analyzed by using a confocal microscope after drop-casting on a polystyrene surface. Again, the presence of large amyloid fibers formed by both proteins, whose width ranged from 20 to 30 µm, with a length in the order of 0.5 mm, was observed. Therefore, to gain deeper insights into the size/morphology of the fibers formed by Vmh2 and PAC3, scanning electron microscopy (SEM) experiments were carried out. SEM analysis of the structures formed by Vmh2 and PAC3 deposited either on polystyrene or aluminum revealed the presence of long, unbranched, twisted ribbon-like filaments (Figures 2, S4 and S5). These filaments are often bent, twisted, or helical in shape and can vary in length and width. They are typically several hundred micrometers to millimeters in length, thus being significantly longer compared to typical fibrils [17]. Moreover, the ribbons are characterized by an average thickness of 5 ± 1 µm and an average width of 25 ± 2 µm. These ribbons seem to exhibit a hierarchical organization in which individual fibrils of nanometric dimension (average diameter around 30 nm) intertwine, align, or bundle together to form larger structures as revealed by examining high-magnification images (Figure S4). The aggregation and bundling of multiple individual fibrils can be considered by the observed rough and irregular surface texture of the ribbons.

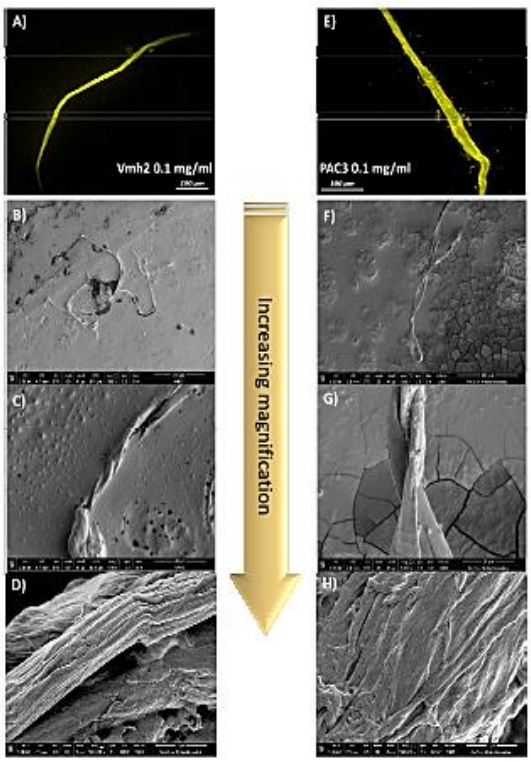

Figure 2. Confocal laser microscope images of Vmh2 (**A**) and PAC3 (E) amyloid fibers stained by ThT. A total of 20 µL of protein solutions containing 3 µM ThT were deposited on a polystyrene support and air-dried prior to visualization. SEM images of Vmh2 (**B–D**) and PAC3 (**F–H**) fibers at different magnifications of 600×, 5000×, and 100,000×, respectively. A total of 20 µL of protein solutions were deposited on the surfaces, air-dried, and Au-Pd-coated prior to visualization.

2.3. Emulsification Ability

To investigate the performances of these proteins as emulsifying agents, hence their ability to disperse oil in water, emulsification tests were performed according to the protocol of Blesic et al. [18]. Firstly, to assess the protein's ability to form stable emulsions, their solutions (0.1 mg/mL) were used, and their good performances as BE were verified, achieving an E_{24} of 78% and 85% for Vmh2 and PAC3, respectively. A buffer (50 mM Tris-HCl, pH 8) and 0.02 mM SDS (equivalent molar concentration to that of the proteins) were used as a negative and positive control, respectively (Figure 3). Protein emulsions were also evaluated in the long term, and they were stable for at least one month.

Figure 3. Emulsions between Dectol and protein solutions (0.1 mg/mL, 50 mM TrisHCl pH 8) 2:1 *v*/*v*. Starting from the left: emulsions formed by Vmh2, PAC3, and Vmh2 after hydrolysis; PAC3 after hydrolysis; and Proteinase K, buffer, and SDS as controls. Images were acquired after 24 h.

A hydrolytic treatment with Proteinase K was performed to ensure that the observed emulsifying capability was due to the presence of proteins. PAC3 hydrolysis was obtained only when the protein was previously treated as described above, as confirmed by SDS-PAGE (Figure S6). The hydrolyzed proteins did not form emulsions, proving their crucial role in emulsion formation.

Emulsions were then made in the presence of the ThT for the confocal microscopy analysis (Figure S7). Images acquired in dried conditions indicate the presence of amyloid aggregates. Moreover, their distribution lets us hypothesize the oil-in water nature of the emulsions, as reported elsewhere [18,19].

2.3.1. Effect of Protein Concentrations

Tests were then conducted at different protein concentrations (0.025, 0.05, 0.1, and 0.2 mg/mL). Both proteins showed a remarkable ability to stabilize emulsions between immiscible phases. As expected, the emulsion indexes increased as the protein concentrations increased, reaching a comparable E_{24} maximum value (Figure 4).

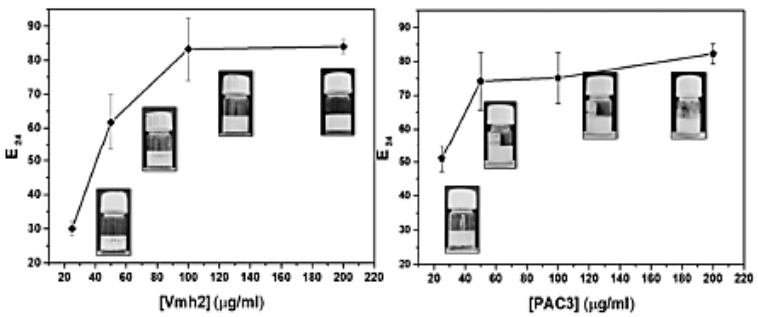

Figure 4. Emulsification index (E_{24}) of Vmh2 and PAC3 versus protein concentrations. At each concentration, an example of the emulsion visible after 24 h is shown. Error bars in the graph represent the standard deviation calculated based on at least two biological and three technical replicates.

2.3.2. Effect of pH and Salt Concentration

As previously reported, both proteins have poor solubility at an acidic pH [12,15]. More specifically, pH ≥ 7.5 is needed to completely solubilize Vmh2, while PAC3 is soluble since pH 6; thus, different ranges of pHs were tested for the two proteins. As reported in Figure 5, the emulsion efficiency of Vmh2 does not vary within the tested pH range; in contrast, PAC3 showed a maximum efficiency between pH 7 and 8. The presence of salt affected the E_{24} values of both proteins, causing their slight reduction at 0.5 M NaCl, while no emulsion at all was formed by doubling the salt concentration (Figure 5).

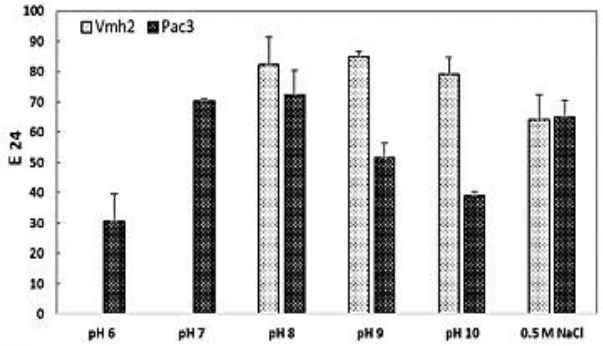

Figure 5. Emulsification index (E_{24}) of Vmh2 and PAC3 solutions at fixed concentration (0.1 mg/mL) versus pHs and in presence of salt. Error bars in the graph represent the standard deviation calculated based on at least two biological and three technical replicates.

2.3.3. Effect of Temperature

The effect of temperature was evaluated by exposing proteins to high temperature (95°) for 20′. Afterward, a substantial decrease in their emulsification ability was observed. However, this ability was restored after prolonged cooling at room temperature. This interesting reversible phenomenon was deepened considering possible changes in the structure of Vmh2 and PAC3, analyzed by using circular dichroism spectroscopy (Figure 6). Results showed changes in the secondary structures right after heating but their restoration (only partially in the case of PAC3) after 60′ at room temperature, highlighting the correlation between the structure and functionality of these proteins.

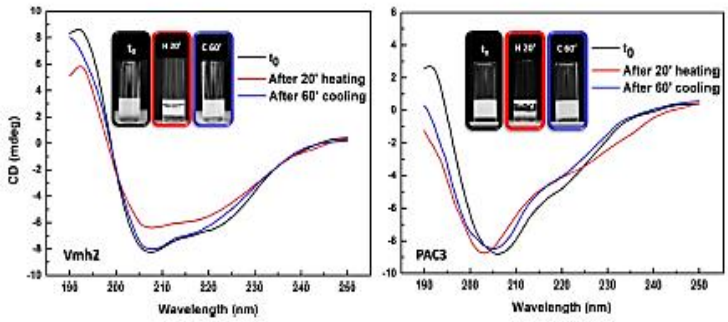

Figure 6. CD spectra of Vmh2 (on the left) and PAC3 (on the right) after heating at 95 °C for 20′ and after cooling at RT for 60′. Emulsions after each thermal treatment were reported as an insert for both proteins.

2.4. Surface Activity

A reduction in surface tension is a fundamental criterion for surfactant characterization and was herein qualitatively measured by using the drop collapse test (Figure 7A) and more accurately using the platinum-iridium ring method (Figure 7B). Protein solutions at their maximal concentration were prepared, reaching 0.14 mg/mL for Vmh2 and 1 mg/mL for PAC3. Then, serial dilutions were carried out starting from these concentrations until the surface tension reached the γ value of the buffer solution.

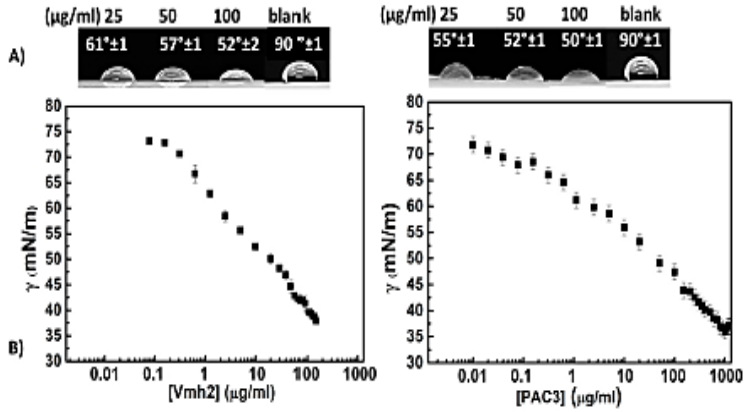

Figure 7. Surface activity. (**A**) Drop collapse tests of Vmh2 solution on the left, PAC3 on the right. A total of 10 µL of protein solution at increasing concentrations was deposited on Parafilm, and pictures were acquired after 10′. Contact angles were estimated using Image J version: 1.8.0. (**B**) Surface tension curves of Vmh2 and PAC3. Each protein was suspended in 50 mM Tris HCl pH 8, and curves were obtained using the Du Noüy ring method. Error bars in the graph represent the standard deviation calculated based on at least two biological and three technical replicates.

The tension curves of Vmh2 and PAC3 showed a constant decrease in the surface tension values as a function of concentration without reaching a critical micellar concentration (CMC). The minimum surface tension value was 38 mN/m for Vmh2 and 35 mN/m for PAC3. However, the surface tension of a PAC3 solution at the same concentration as Vmh2 (0.14 mg/mL) was significantly higher (44 mN/m) than that of Vmh2; thus, Vmh2 can be considered a more efficient surface-active protein than PAC3.

2.5. Surface Adhesion and Wettability Change

It is well known that HPBs can change the wettability of surfaces on which they are deposited [20]. In particular, the ability of PAC3 and Vmh2 to reverse the wettability of a hydrophobic surface, such as polystyrene, was tested. The proteins were deposited on the surface and air-dried; then, the surface was washed as reported in Figure 8, and the contact angle of a water drop was calculated. Both proteins formed stable layers, changing the wettability of the polystyrene surface and maintaining strong adhesion even after SDS washing.

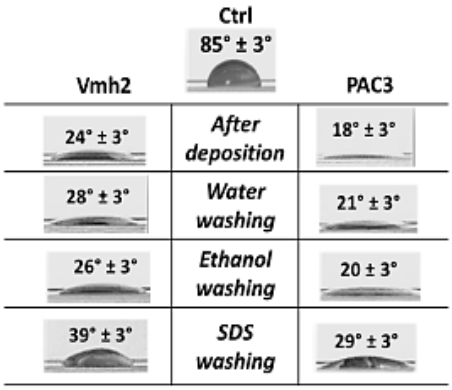

Figure 8. Water contact angle analysis. A total of 50 µL of protein solutions (0.1 mg/mL) was deposited on a polystyrene surface, dried out at RT, and differently washed as indicated. Then, a 10 µL water drop was deposited on the coated surface, and angles were estimated using Image J version: 1.8.0. Errors were calculated on the average of three deposited drops.

3. Discussion

It is worth noting that PAC3 from *A. sclerotigenum* behaves very similarly to HPBs [15,16], even though it does not show the sequence features of that family. Indeed, mass spectrometry studies reported in this paper indicate aminoacidic sequence similarity with an unknown fungal protein. The sequence of Sap-Pc from *Penicillium chrysogenum*, a presumed HPB based on its functional properties, appears to be that of an unknown protein lacking the typical cysteine pattern of HPBs [21]. Both proteins, PAC3 and Sap-Pc, are surface-active and have good emulsification ability. They change their secondary structures, forming aggregate structures positive to the ThT tests, over time and depending on the protein concentration. Analysis by using AFM of PAC3 aggregates shows the rodlet structure, typical of class I HPB, while the morphology of Sap-Pc fibrils looks like a "pearl necklace", originated by an array of interacting aggregates. All of these findings open up new perspectives to discover fungal surface-active proteins beyond the members of the HPB family. In this paper, the characteristics of PAC3 have been compared to those of a canonical HPB, Vmh2.

The first important aspect is the spontaneous formation of large amyloid fibers. To the best of our knowledge, this is the first evidence of giant fibers obtained using a whole protein without the need for harsh conditions or a long incubation time. Indeed, until now, giant fibers have been obtained only upon an engineered control of amyloid fibril assemblies, such as using opportunely mixed protein hydrolysates [22–30], or specific deposition procedures designed to apply external constraints to direct the assembly of protein nanofibrils, such as microfluidics [31,32] and electrospinning [33,34].

As regards the characterization of BE activities, our results indicated that both proteins are good BEs (E_{24}: 70% Vmh2 and 60% PAC3 at 0.1 mg/mL), better or comparable to that of other fungal surfactant proteins. Indeed, the E_{24} value of SapPC at the same concentration was 70%, and the E_{24} of the ceratoplatanins *At*Cp and *Th*Cp was 83% and 70%, respectively. Moreover, the emulsification ability of HFBII, a class II HPB characterized by Blesic et al. [18] using the same protocol, showed an emulsion index of 74% at a concentration of 1 mg/mL, a ten times higher concentration. PAC3 remarkably stabilized emulsions even at lower concentrations (20–50 µg/mL). Regarding the effect of pH, we observed a stronger dependence on the pH of the emulsion activity of PAC3 as compared to Vmh2, whose E_{24} does not change in the tested pH range. On the other hand, they are both negatively affected by salt concentration. In addition, the results showed that incubation at high temperatures has also a negative effect, but emulsification ability can be restored, as well as their secondary structures, when protein solutions are slowly cooled down.

Analysis of the reduction in the surface tension of these proteins is affected by protein solubility and by the aggregation phenomena occurring at relatively high protein concentrations. For these reasons, a constant surface tension value was not reached (Figure 7), noting that Vmh2 possesses a more significant surface activity than PAC3. Compared with synthetic surfactants, Vmh2 showed similar results to Triton X-100®, a non-ionic surfactant that reaches tension values of 31 mN/m at 2×10^{-4} M [35]. As another example, SDS achieves a surface tension of 35 mN/m [36] at 3×10^{-3} M, a significantly higher concentration than that used for the studied proteins.

However, Vmh2 caused weaker surface tension reduction compared with other surfactant proteins, e.g., class I HPB SC3p and class II HPB CTFH1, and decreased surface tension at values of 32 and 33 mN/m for a 0.1 mg/mL solution (6.8×10^{-6} and 2.8×10^{-6} M, respectively), and *Th*CP decreased surface tension until 36 mN/m at 0.01 mg/mL (8×10^{7} M) [37]. According to commonly used grouping, these fungal proteins are more efficient BEs than BSs.

4. Materials and Methods

4.1. Fungal Culture Conditions

P. ostreatus and *A. sclerotigenum* (MUT 4872) were maintained at 4 °C through periodic transfer on potato dextrose agar plates in the presence of 0.5% yeast extract or on agar plates in the presence of XNST30 (malt extract 3 g/L, yeast extract 3 g/L, sodium chloride 30 g/L, 10 g/L glucose, and 5 g/L peptone), respectively. Mycelium disks (10 mm diameter) were taken from the margin of actively growing colonies, inoculated in 1 L flasks containing 500 mL of potato dextrose broth (24 g/L) supplemented with 0.5% yeast extract (*P. ostreatus*) or XNST30 (*A. sclerotigenum*), grown in duplicate at 28 °C in shaken mode (180 rpm).

4.2. Protein Purification

4.2.1. Vmh2

The protein was extracted and purified following the protocol of Gravagnuolo et al. [12]. Briefly, the lyophilized mycelia were washed with 2% SDS and then freeze-dried; upon lyophilization, it was treated with pure TFA, obtaining the raw extract. Then, the extract was solubilized in 60% ethanol and further purified through methanol-chloroform extraction to remove lipids. The protein was finally resuspended in a 60% ethanol solution. This purification protocol yielded 24 mg of protein per gram of mycelium.

4.2.2. PAC3

Purification was performed from the culture broth according to the protocol of Cicatiello et al. [15]. Briefly, the culture broth was stirred using a blender to produce foam. The recovered foam was incubated o.n. with 20% trichloroacetic acid and centrifuged (3000 rcf 60 min). Upon acid precipitation, the pellet was treated with pure TFA and suspended in 60% ethanol to obtain the raw extract. It was extracted in a mixture of water–methanol–chloroform. After centrifugation, the protein was recovered by removal of the liquid phases, treated with TFA for 20 min in a bath sonicator, dried again, and dissolved in 60% ethanol to obtain 20 mg of protein per liter of culture.

Before any experiment, both proteins were dried out, treated with TFA, and solubilized in aqueous buffer (50 mM Tris HCl pH 8 unless otherwise stated).

4.3. MALDI-TOF Analysis of PAC3

A total of 100 µg of extracted PAC3 protein was hydrolyzed with trypsin by using the following procedure. The reduction reaction was performed by adding 20 µL of 100 mM dithiothreitol and 6M urea at 60 °C for 1 h. A total of 20 µL of 120 mM iodoacetamide was added, and the reaction was conducted for 45 min at room temperature in the dark. A total of 500 µL of methanol was used to perform protein precipitation. The solution was centrifuged for 15 min at 13,680 rcf, and the pellet was dried under vacuum and then suspended in 50 µL of 10 mM ammonium bicarbonate (AMBIC) with 2 µL of trypsin

(1 µg/µL in 10 mM AMBIC) at 37 °C for 15 h. A total of 0.5 µL of the peptide mixture was deposited on a MALDI plate with an equal volume (1/1, vol/vol) of a solution of α-cyano-4-hydroxycinnamic acid (20 mg/mL) dissolved in 70:30 acetonitrile:55 mM citric acid in water. MALDI-MS experiments were performed on a 4800 MALDI-TOF ABSciex equipped with a nitrogen laser (337 nm). Spectra were acquired in the reflector-positive mode by using a 400–4000 (m/z) mass range. Laser power was set to 4200 V for MS spectra acquisition. Each spectrum represents the sum of 3000 laser pulses from randomly chosen spots per sample position by covering the entire spot. Calibration was performed by using an AB SCIEX calibration mixture (Monoisotopic (M + nH) n+:904.46 Da des-Arg-Bradykinin, 1296.68 Da Angiotensin I, 1570.67 Da Glu-Fibrinopeptide B, 2093.08 Da ACTH (clip: 1–17), 2465.19 Da ACTH (clip: 18–39), 3657.92 Da ACTH (clip: 7–38)). The data were elaborated using the Data Explorer 5.1 software (Applied Biosystems, Foster City, CA, USA), and the m/z values were reported as monoisotopic masses. The MS/MS spectra were also recorded in positive mode, and air was used as collision gas with a medium pressure of 10–6 Torr for CID experiments. The Glu-Fibrinopeptide peptide (1570.67 Da) was used to calibrate MS/MS acquisition [38,39].

4.4. Confocal Laser Microscopy

Image acquisitions were performed with a confocal laser scanning microscope (CLSM) (LSM700-Zeiss, Oberkochen, Germany) equipped with an Ar laser (488 nm) and a He–Ne laser (555 nm). Images were obtained using a 20×/0.8 objective. The excitation/emission maximum for the ThT dye is 405 nm. Emulsions were visualized by placing samples on a glass slide and letting them dry at room temperature.

4.5. Scanning Electron Microscopy

Scanning electron microscopy (SEM) images were obtained by using a FEI Nova NanoSEM 450 at an accelerating voltage of 1–5 kV with Everhart–Thornley detector (ETD) and through lens detector (TLD) at high magnification (FEI, Austin, TX, USA). Samples were prepared for SEM analyses by depositing proteins onto Al or polystyrene substrates and sputter coating them with a thin layer of Au-Pd (Sputter Coater Denton Vacuum Desk V).

4.6. Emulsification Index Evaluation

Proteins were dissolved in different aqueous buffers and placed in a 5 mL glass vial, and 2 mL of Dectol (Decane:Toluene 65:35) as an emulsifying agent was added [18]. This mixture was homogenized using an IKA T-10 Basic Ultra Turrax Homogenizer for 3 min in a 5 mL glass vial; then, the emulsion ability was reported in terms of emulsification index E_{24}, calculated after 24 h by dividing the final height of the emulsion layer by the total height and multiplying by 100. The emulsification activity was investigated at different protein concentrations; additionally, it was tested by dissolving the proteins at different pH using different solution buffers (50 mM sodium phosphate at pH 6 and pH 7 and 50 mM Tris-HCl from pH 8 to 10). The effect of two different sodium chloride concentrations was tested when the protein was suspended in 50 mM Tris-HCl pH 8. Errors on all of the E_{24} evaluated were calculated as the deviation standard for at least two biological replicates and three technical replicates.

4.7. Effect of Temperature

The effect of temperature was investigated by incubating protein solutions (0.05 mg/mL in 50 mM sodium phosphate pH 7.5) at 95° C for 20 min. Emulsions with Dectol were performed right after heating and after cooling down proteins at room temperature for 60 min.

4.8. Protein Hydrolysis

Hydrolysis with proteinase K was performed after a pretreatment of the sample. A solution of 0.05 mg/mL of the sample was first incubated with 5 mM of dithiothreitol

(DTT) for 10 min at 60 °C. Then, after the solution had cooled, protease K and CaCl2 were added to a final concentration of 1 mg/mL and 0.5 mM, respectively, and the solution was incubated at 40 °C for 1 h.

4.9. Circular Dichroism

CD spectra were recorded on a Jasco J1500 spectropolarimeter (Jasco Corporation), (Jasco Corporation, Cremella (LC), Italy) equipped with a Peltier thermostatic cell holder in a quartz cell (0.1 cm light path) from 190 to 250 nm. Spectra were acquired before and right after the thermal shock at 95 °C for 20′, according to the emulsification tests, under continuous nitrogen flush.

Final spectra (60′ at room temperature) were obtained by averaging six scans using a bandwidth of 1 nm, a step width of 0.5 nm, and a velocity scan of 100 nm/min.

4.10. Surface Tension Measurement

Drop collapse consists of depositing a sample drop onto a hydrophobic surface (polystyrene) and then evaluating the collapsing area. The BS solution should spread on the surface more extensively than water in image analysis on the photos using Image J version: 1.8.0 (Rasband, W.S., ImageJ, U.S. National Institutes of Health, Bethesda, Maryland, USA) [40].

The surface tension γ of the extracted protein solutions was measured with a Sigma 70 tensiometer (KSV, Stockholm, Sweden) using the Du Noüy ring method as described elsewhere (Huh et al., 1975). γ was correlated with the force required to raise the ring from the surface of the air/liquid interface. Aliquots of the proteins suspended in 50 mM pH 8 Tris-HCl buffer were prepared at different concentrations; each sample was filtered with a 0.22 µm filter before testing. A total of 7 mL of the sample was added to the vessel and allowed to equilibrate at least 5 min prior to measuring the surface tension. A 50 mM Tris-HCl buffer with a surface tension of 73 mN/m was used as a control. The results were the average of at least three different measurements.

4.11. Surface Adhesion and Wettability Change

To test the ability of the proteins to adhere to and change the wettability of surfaces, they were deposited on a polystyrene surface, which is highly hydrophobic. A total of 50 µL of proteins was deposited and air-dried, and then the surface was washed with water, 60% ethanol, or 2% sodium dodecyl sulfate (SDS). The contact angle of a drop of water on the surface was calculated after every washing step. The wettability change was evaluated by calculating the contact angle through image analysis on the photos using Image J version: 1.8.0 [40].

5. Conclusions

Besides highlighting the efficiency of Vmh2 and PAC3 as BEs, this paper poses questions about the peculiarity of the HPBs protein family, since other fungal proteins share functional characteristics with this protein family even though they do not share the same sequence features (i.e., the conserved eight cysteines pattern). Among the typical characteristics of the herein-studied proteins, the most remarkable is the spontaneous and easy formation of giant amyloid fibers. This ability could be exploited in the controlled formation of micro- and macro-fibrils through a microfluidic spinning approach or core–shell electrospinning methods [31,41]. The final aim would be the production of functional fibers by using both native and recombinant proteins, also fused with other peptides/proteins of interest. Moreover, the surface-active characteristics shown by the analyzed proteins widen their potential applications. In this context, the use of proteinaceous surfactants could tackle the challenge of large-scale production of BSs and BEs. Indeed, proteinaceous surfactants can be recombinantly produced on low-cost raw materials/wastes as growth substrates and purified using easy processes, leading to cost-effective processes and high production yields [2].

Supplementary Materials: The following supporting information can be downloaded at: https://www.mdpi.com/article/10.3390/ijms241813843/s1.

Author Contributions: Conceptualization, P.G. and A.P.; validation, P.C., R.P. and A.A.; investigation, R.P., I.S., A.I. and O.T.; writing—original draft preparation, R.P. and P.C.; writing—review and editing, A.P., P.G. and P.C. All authors have read and agreed to the published version of the manuscript.

Funding: This research was carried out within the MICS (Made in Italy—Circular and Sustainable) Extended Partnership and received funding from the European Union Next-Generation EU (PIANO NAZIONALE DI RIPRESA E RESILIENZA (PNRR)—MISSIONE 4 COMPONENTE 2, INVESTIMENTO 1.3—D.D. 1551.11-10-2022, PE00000004). This manuscript reflects only the authors' views and opinions; neither the European Union nor the European Commission can be considered responsible for them.

Institutional Review Board Statement: Not applicable.

Informed Consent Statement: Not applicable.

Acknowledgments: The authors thank Giovanna Cristina Varese, Department of Life Sciences and Systems Biology, and Mycotheca Universitatis Taurinensis, University of Turin, Italy, for selecting and supplying the *A. sclerotigenum* strain.

Conflicts of Interest: The authors declare no conflict of interest.

References

1. Otzen, D.E. Biosurfactants and Surfactants Interacting with Membranes and Proteins: Same but Different? *Biochim. Biophys. Acta (BBA) Biomembr.* **2016**, *1859*, 639–649. [CrossRef] [PubMed]
2. Araujo, J.; Monteiro, J.; Silva, D.; Alencar, A.; Silva, K.; Coelho, L.; Pacheco, W.; Silva, D.; Silva, M.; Silva, L.; et al. Surface-Active Compounds Produced by Microorganisms: Promising Molecules for the Development of Antimicrobial, Anti-Inflammatory, and Healing Agents. *Antibiotics* **2022**, *11*, 1106. [CrossRef] [PubMed]
3. Luft, L.; Confortin, T.C.; Todero, I.; Zabot, G.L.; Mazutti, M.A. An Overview of Fungal Biopolymers: Bioemulsifiers and Biosurfactants Compounds Production. *Crit. Rev. Biotechnol.* **2020**, *40*, 1059–1080. [CrossRef]
4. Lo, V.; I-Chun Lai, J.; Sunde, M. Fungal Hydrophobins and Their Self-Assembly into Functional Nanomaterials. *Adv. Exp. Med. Biol.* **2019**, *1174*, 161–185. [CrossRef] [PubMed]
5. Linder, M.B. Hydrophobins: Proteins That Self Assemble at Interfaces. *Curr. Opin. Colloid Interface Sci.* **2009**, *14*, 356–363. [CrossRef]
6. Cicatiello, P.; Sorrentino, I.; Piscitelli, A.; Giardina, P. Spotlight on Class I Hydrophobins: Their Intriguing Biochemical Properties and Industrial Prospects BT. In *Grand Challenges in Fungal Biotechnology*; Nevalainen, H., Ed.; Springer International Publishing: Cham, Switzerland, 2020; pp. 333–347. ISBN 978-3-030-29541-7.
7. Lovett, B.; Kasson, M.T.; Gandier, J. Ecology Drives the Observed Spectrum of Hydrophobin Protein Diversity across Kingdom Fungi Hydrophobins Mediate the Interactions between Fungi and the Elements of Their Ecosystem via Assembly at Interfaces Serving a Wide Range of Diverse Functions. *bioRxiv* **2022**, *2022*, 1–32. [CrossRef]
8. Lo, V.; Ren, Q.; Pham, C.; Morris, V.; Kwan, A.; Sunde, M. Fungal Hydrophobin Proteins Produce Self-Assembling Protein Films with Diverse Structure and Chemical Stability. *Nanomaterials* **2014**, *4*, 827–843. [CrossRef]
9. Winandy, L.; Hilpert, F.; Schlebusch, O.; Fischer, R. Comparative Analysis of Surface Coating Properties of Five Hydrophobins from Aspergillus Nidulans and Trichoderma Reseei. *Sci. Rep.* **2018**, *8*, 12033. [CrossRef]
10. Gandier, J.-A.; Langelaan, D.N.; Won, A.; O'Donnell, K.; Grondin, J.L.; Spencer, H.L.; Wong, P.; Tillier, E.; Yip, C.; Smith, S.P.; et al. Characterization of a Basidiomycota Hydrophobin Reveals the Structural Basis for a High-Similarity Class I Subdivision. *Sci. Rep.* **2017**, *7*, 45863. [CrossRef]
11. Levkovich, S.A.; Gazit, E.; Laor Bar-Yosef, D. Two Decades of Studying Functional Amyloids in Microorganisms. *Trends Microbiol.* **2021**, *29*, 251–265. [CrossRef]
12. Gravagnuolo, A.M.; Longobardi, S.; Luchini, A.; Appavou, M.S.; De Stefano, L.; Notomista, E.; Paduano, L.; Giardina, P. Class i Hydrophobin Vmh2 Adopts Atypical Mechanisms to Self-Assemble into Functional Amyloid Fibrils. *Biomacromolecules* **2016**, *17*, 954–964. [CrossRef] [PubMed]
13. Amend, A.; Burgaud, G.; Cunliffe, M.; Edgcomb, V.P.; Ettinger, C.L.; Gutiérrez, M.H.; Heitman, J.; Hom, E.F.Y.; Ianiri, G.; Jones, A.C.; et al. Fungi in the Marine Environment: Open Questions and Unsolved Problems. *MBio* **2019**, *10*. [CrossRef] [PubMed]
14. Cicatiello, P.; Gravagnuolo, A.M.; Gnavi, G.; Varese, G.C.; Giardina, P. Marine Fungi as Source of New Hydrophobins. *Int. J. Biol. Macromol.* **2016**, *92*, 1229–1233. [CrossRef] [PubMed]
15. Cicatiello, P.; Dardano, P.; Pirozzi, M.; Gravagnuolo, A.M.; De Stefano, L.; Giardina, P. Self-Assembly of Two Hydrophobins from Marine Fungi Affected by Interaction with Surfaces. *Biotechnol. Bioeng.* **2017**, *10*, 2173–2186. [CrossRef] [PubMed]

16. Piscitelli, A.; Pennacchio, A.; Cicatiello, P.; Politi, J.; De Stefano, L.; Giardina, P. Rapid and Ultrasensitive Detection of Active Thrombin Based on the Vmh2 Hydrophobin Fused to a Green Fluorescent Protein. *Biosens. Bioelectron.* **2017**, *87*, 816–822. [CrossRef] [PubMed]
17. Ke, P.C.; Zhou, R.; Serpell, L.C.; Riek, R.; Knowles, T.P.J.; Lashuel, H.A.; Gazit, E.; Hamley, I.W.; Davis, T.P.; Fä, M.; et al. Half a Century of Amyloids: Past, Present and Future †. *Chem. Soc. Rev* **2020**, *49*, 5473. [CrossRef] [PubMed]
18. Blesic, M.; Dichiarante, V.; Milani, R.; Linder, M.; Metrangolo, P. Conference Paper Evaluating the Potential of Natural Surfactants in the Petroleum Industry: The Case of Hydrophobins. *Pure Appl. Chem.* **2018**, *90*, 305–314. [CrossRef]
19. McClements, D.J.; Gumus, C.E. Natural Emulsifiers—Biosurfactants, Phospholipids, Biopolymers, and Colloidal Particles: Molecular and Physicochemical Basis of Functional Performance. *Adv. Colloid Interface Sci.* **2016**, *234*, 3–26. [CrossRef]
20. Wösten, H.A.B.; De Vocht, M.L. Hydrophobins, the Fungal Coat Unravelled. *Biochim. Biophys. Acta Rev. Biomembr.* **2000**, *1469*, 79–86. [CrossRef]
21. Cicatiello, P.; Stanzione, I.; Dardano, P.; De Stefano, L.; Birolo, L.; De Chiaro, A.; Monti, D.M.; Petruk, G.; D'errico, G.; Giardina, P. Characterization of a Surface-Active Protein Extracted from a Marine Strain of Penicillium Chrysogenum. *Int. J. Mol. Sci.* **2019**, *20*, 3242. [CrossRef]
22. Ridgley, D.M.; Ebanks, K.C.; Barone, J.R. Peptide Mixtures Can Self-Assemble into Large Amyloid Fibers of Varying Size and Morphology. *Biomacromolecules* **2011**, *12*, 3770–3779. [CrossRef] [PubMed]
23. Ridgley, D.M.; Claunch, E.C.; Barone, J.R. The Effect of Processing on Large, Self-Assembled Amyloid Fibers. *Soft Matter* **2012**, *8*, 10298–10306. [CrossRef]
24. Ridgley, D.M.; Barone, J.R. Evolution of the Amyloid Fiber over Multiple Length Scales. *ACS Nano* **2013**, *7*, 1006–1015. [CrossRef] [PubMed]
25. Ridgley, D.M.; Freedman, B.G.; Lee, P.W.; Barone, J.R. Genetically Encoded Self-Assembly of Large Amyloid Fibers. *Biomater. Sci.* **2014**, *2*, 560–566. [CrossRef] [PubMed]
26. Ridgley, D.M.; Claunch, E.C.; Lee, P.W.; Barone, J.R. The Role of Protein Hydrophobicity in Conformation Change and Self-Assembly into Large Amyloid Fibers. *Biomacromolecules* **2014**, *15*, 1240–1247. [CrossRef] [PubMed]
27. Ridgley, D.M.; Rippner, C.M.W.; Barone, J.R. Design and Construction of Large Amyloid Fibers. *Fibers* **2015**, *3*, 90–102. [CrossRef]
28. Malgieri, G.; D'Abrosca, G.; Pirone, L.; Toto, A.; Palmieri, M.; Russo, L.; Sciacca, M.F.M.; Tatè, R.; Sivo, V.; Baglivo, I.; et al. Folding Mechanisms Steer the Amyloid Fibril Formation Propensity of Highly Homologous Proteins. *Chem. Sci.* **2018**, *9*, 3290–3298. [CrossRef] [PubMed]
29. Di Natale, C.; La Manna, S.; Malfitano, A.M.; Di Somma, S.; Florio, D.; Scognamiglio, P.L.; Novellino, E.; Netti, P.A.; Marasco, D. Structural Insights into Amyloid Structures of the C-Terminal Region of Nucleophosmin 1 in Type A Mutation of Acute Myeloid Leukemia. *Biochim. Biophys. Acta Proteins Proteom.* **2019**, *1867*, 637–644. [CrossRef]
30. La Manna, S.; Roviello, V.; Scognamiglio, P.L.; Diaferia, C.; Giannini, C.; Sibillano, T.; Morelli, G.; Novellino, E.; Marasco, D. Amyloid Fibers Deriving from the Aromatic Core of C-Terminal Domain of Nucleophosmin 1. *Int. J. Biol. Macromol.* **2019**, *122*, 517–525. [CrossRef]
31. Kamada, A.; Levin, A.; Zenon, T.; Shen, Y.; Lutz-Bueno, V.; Baumann, K.N.; Pezhman, M.; Linder, M.B.; Raffaele, M.; Knowles, T.P.J. Modulating the Mechanical Performance of Macroscale Fibers through Shear-Induced Alignment and Assembly of Protein Nanofibrils. *Small* **2020**, *16*, 1904190. [CrossRef]
32. Shen, Y.; Ruggeri, F.S.; Vigolo, D.; Kamada, A.; Qamar, S.; Levin, A.; Iserman, C.; Alberti, S.; St George-Hyslop, P.; Knowles, T.P.J. Biomolecular Condensates Undergo a Generic Shear-Mediated Liquid-to-Solid Transition. *Nat. Nanotechnol.* **2020**, *15*, 841–847. [CrossRef] [PubMed]
33. Chen, D.; Narayanan, N.; Federici, E.; Yang, Z.; Zuo, X.; Gao, J.; Fang, F.; Deng, M.; Campanella, O.H.; Jones, O.G. Electrospinning Induced Orientation of Protein Fibrils. *Biomacromolecules* **2020**, *21*, 2772–2785. [CrossRef] [PubMed]
34. Wanasekara, N.D.; Santos, R.P.O.; Douch, C.; Frollini, E.; Eichhorn, S.J. Orientation of Cellulose Nanocrystals in Electrospun Polymer Fibres. *J. Mater. Sci.* **2016**, *51*, 218–227. [CrossRef]
35. Giribabu, K.; Ghosh, P. Adsorption of Nonionic Surfactants at Fluid-Fluid Interfaces: Importance in the Coalescence of Bubbles and Drops. *Chem. Eng. Sci.* **2007**, *62*, 3057–3067. [CrossRef]
36. Santos, S.F.; Zanette, D.; Fischer, H.; Itri, R. A Systematic Study of Bovine Serum Albumin (BSA) and Sodium Dodecyl Sulfate (SDS) Interactions by Surface Tension and Small Angle X-Ray Scattering. *J. Colloid Interface Sci.* **2003**, *262*, 400–408. [CrossRef] [PubMed]
37. Pitocchi, R.; Cicatiello, P.; Birolo, L.; Piscitelli, A.; Bovio, E.; Cristina Varese, G.; Giardina, P. Cerato-Platanins from Marine Fungi as Effective Protein Biosurfactants and Bioemulsifiers. *Int. J. Mol. Sci.* **2020**, *21*, 2913. [CrossRef] [PubMed]
38. Luti, S.; Fiaschi, T.; Magherini, F.; Modesti, P.A.; Piomboni, P.; Governini, L.; Luddi, A.; Amoresano, A.; Illiano, A.; Pinto, G.; et al. Relationship between the Metabolic and Lipid Profile in Follicular Fluid of Women Undergoing in Vitro Fertilization. *Mol. Reprod. Dev.* **2020**, *87*, 986–997. [CrossRef] [PubMed]
39. Pinto, G.; Aurilia, M.; Illiano, A.; Fontanarosa, C.; Sannia, G.; Trifuoggi, M.; Lettera, V.; Sperandeo, R.; Pucci, P.; Amoresano, A. From Untargeted Metabolomics to the Multiple Reaction Monitoring-Based Quantification of Polyphenols in Chocolates from Different Geographical Areas. *J. Mass Spectrom.* **2021**, *56*, e4651. [CrossRef]

40. Schneider, C.A.; Rasband, W.S.; Eliceiri, K.W. NIH Image to ImageJ: 25 Years of Image Analysis. *Nat. Methods* **2012**, *9*, 671–675. [CrossRef]
41. Hecker, L.; Wang, W.; Mela, I.; Fathi, S.; Poudel, C.; Soavi, G.; Huang, Y.Y.S.; Kaminski, C.F. Guided Assembly and Patterning of Intrinsically Fluorescent Amyloid Fibers with Long-Range Order. *Nano Lett.* **2021**, *21*, 938–945. [CrossRef]

SUBMITTED TO APPLIED MICROBIAL AND BIOTECHNOLOGY

CHAPTER 3

3.1 INTRODUCTION

BS compounds are very valuable in several industrial fields, however, production on a large scale is the current challenge. One possible route is the production via fermentation, using waste materials, and in particular agrifood wastes, as growth substrates. Generation of agro-industrial byproducts is growing rapidly. In 2019, the industrial activities of bioethanol production, animal slaughter, as well as the processing of cassava, oil palm, and milk together generated more than four billion liters of wastewater [1]. To increase the sustainability of these agro-industrial processes, it is possible to utilize their waste products as substrates for the production of other useful products, such as BS. Another intriguing possibility is the use of BS as adjuvants in the hydrolytic treatment of agro-industrial wastes (see sect 3.2) In medicine technology, bacterial surface colonization represents a big issue, worsened by the spreading of drug-resistant bacteria [2]. Functionalization of surfaces of interest that does not involve the use of chemicals, toxic reagents, harsh conditions, or time-consuming steps, is a significant challenge. In this context, using BS with adhesive properties could be a “greener” way to achieve functionalization. The review in section 3.1 lists all the HPBs surface functionalization to date. In section 3.3 the adhesive capability of the class I HPBs Vmh2 has been tested in the fusion protein with an antimicrobial peptide (GKY20).

Properties such as emulsification, foam formation, phase separation, reduction of surface tension, and viscosity allow biosurfactants to be applied for the cleaning of oil spills in both water and soil. Surfactant molecules can accumulate at the soil-pollutant (or water-soil) interface and change the system’s affinity for water. In addition, at concentrations higher than the CMC, surfactants can incorporate contaminants in micelles and hence favor their partition in the aqueous phase [3,1]. There are plenty of examples in literature about BS as bioremediation agents [4,5,6], therefore, starting from these protocols, preliminary experiments were carried out on the BE proteins extracted from *F. solani* (see sect. 2.3) to test their ability to remove oil from contaminated sands (see appendix)

1. Sarubbo, L.A.; Silva, M. da G.C.; Durval, I.J.B.; Bezerra, K.G.O.; Ribeiro, B.G.; Silva, I.A.; Twigg, M.S.; Banat, I.M. Biosurfactants: Production, Properties, Applications, Trends, and General Perspectives. Biochem Eng J **2022**, 181, 108377 – 108396.
2. Van Epps, J.S.; Younger, J.G. Implantable Device-Related Infection. Shock **2016**, 46, 597–608.
3. Sanches, M.A.; Luzeiro, I.G.; Alves Cortez, A.C.; Simplício De Souza, É.; Albuquerque, P.M.; Chopra, H.K.; Braga De Souza, J.V. Production of Biosurfactants by Ascomycetes. Int J Microbiol **2021**, 6669263, 1-11
4. Chaprão, M.J.; Ferreira, I.N.S.; Correa, P.F.; Rufino, R.D.; Luna, J.M.; Silva, E.J.; Sarubbo, L.A. Application of Bacterial and Yeast Biosurfactants for Enhanced Removal and Biodegradation of Motor Oil from Contaminated Sand. Electronic Journal of Biotechnology **2015**, 18, 471–479.
5. Amani, H. Evaluation of Biosurfactants and Surfactants for Crude Oil Contaminated Sand Washing. Pet Sci Technol **2015**, 33, 510–519.
6. Al-Dhabi, N.A.; Esmail, G.A.; Arasu, M.V. Enhanced Production of Biosurfactant from Bacillus Subtilis Strain Al-Dhabi-130 under Solid-State Fermentation Using Date Molasses from Saudi Arabia for Bioremediation of Crude-Oil-Contaminated Soils. Int J Environ Res Public Health **2020**, 17, 1–20.

frontiers | Frontiers in Molecular Biosciences

TYPE Review
PUBLISHED 11 August 2022
DOI 10.3389/fmolb.2022.959166

OPEN ACCESS

EDITED BY
Greta Faccio,
Independent researcher, Switzerland

REVIEWED BY
Luca Bellucci,
Istituto Nanoscienze, Consiglio Nazionale delle Ricerche, Italy
Cristina Polonschii,
International Centre of Biodynamics, Romania

*CORRESPONDENCE
Alessandra Piscitelli,
apiscite@unina.it

SPECIALTY SECTION
This article was submitted to Biophysics, a section of the journal Frontiers in Molecular Biosciences

RECEIVED 01 June 2022
ACCEPTED 11 July 2022
PUBLISHED 11 August 2022

CITATION
Stanzione I, Pitocchi R, Pennacchio A, Cicatiello P, Piscitelli A and Giardina P (2022), Innovative surface bio-functionalization by fungal hydrophobins and their engineered variants.
Front. Mol. Biosci. 9:959166.
doi: 10.3389/fmolb.2022.959166

Innovative surface bio-functionalization by fungal hydrophobins and their engineered variants

Ilaria Stanzione, Rossana Pitocchi, Anna Pennacchio, Paola Cicatiello, Alessandra Piscitelli* and Paola Giardina

Department of Chemical Sciences, University of Naples Federico II, Naples, Italy

Research on innovative surface functionalization strategies to develop materials with high added value is particularly challenging since this process is a crucial step in a wide range of fields (i.e., biomedical, biosensing, and food packaging). Up to now, the main applied derivatization methods require hazardous and poorly biocompatible reagents, harsh conditions of temperature and pressure, and are time consuming and cost effective. The discovery of biomolecules able to adhere by non-covalent bonds on several surfaces paves the way for their employment as a replacement of chemical processes. A simple, fast, and environment-friendly method of achieving modification of chemically inert surfaces is offered by hydrophobins, small amphiphilic proteins produced by filamentous fungi. Due to their structural characteristics, they form stable protein layers at interfaces, serving as anchoring points that can strongly bind molecules of interest. In addition, genetic engineering techniques allow the production of hydrophobins fused to a wide spectrum of relevant proteins, providing further benefits in term of time and ease of the process. In fact, it is possible to bio-functionalize materials by simply dip-casting, or by direct deposition, rendering them exploitable, for example, in the development of biomedical and biosensing platforms.

KEYWORDS

biosensors, functional amyloid, fusion proteins, coating, protein immobilization

Introduction

The process of surface functionalization plays a pivotal role in a wide range of application fields (i.e., medical, sensing, and food packaging), affecting the quantitative and qualitative aspects of several methodologies and products. That is why the research for innovative functionalization strategies is particularly challenging. Different strategies have been studied and optimized according to the nature of the surface to derivatize and the target application. There are plenty of examples in the literature, ranging from physical techniques (i.e., laser ablation, abrasive blasting, evaporation, and ion-assisted deposition) (Peng et al., 2016; Yang et al., 2017; Letzel et al., 2019; Wolf et al., 2021) to chemical treatments (i.e., chemical vapor deposition, plasma-assisted

surface oxidation, nitration, hydrolyzation, and amination) (Javanbakht et al., 2015; Boaretti et al., 2020), that are commonly used. The mentioned strategies are affected by high costs and environmental impacts due to the inclusion of several time-consuming steps and often using hazardous reagents/solvents under harsh environmental conditions (Lavilla et al., 2014). In the case of biomolecules immobilization, other factors need to be considered such as good orientation of the active sites and retention of biological activity. Nonetheless, immobilized biomolecules (i.e., DNA, enzymes, and antibody) increase their stability against environmental changes and can be easily recycled (Ashkan et al., 2021). Starting from these considerations, the introduction of biocompatible and easy functionalization methodologies is taking place in different working sectors to replace standard methods. The discovery of biomolecules that can adhere to several surfaces with non-covalent bonds paves the way for their employment in these processes. A simple, fast, and environment-friendly means of achieving the modification of chemically inert surfaces is offered by the amphiphilic proteins, produced by filamentous fungi, known as hydrophobins (HPBs) (Fan et al., 2015). HPBs are small cysteine-rich proteins, ranging from 70 to 350 amino acids, expressed at different stages of the fungal life cycle, fulfilling multiple functions in fungal development. These proteins self-assemble at hydrophobic/hydrophilic interfaces into amphipathic layers, changing the wettability of surfaces and playing a role in adhesion and surface modification, acting as coating/protective agents (Cicatiello et al., 2020). It is common knowledge that HPBs can be divided into two classes that correspond to class I HPBs, self-assembling into resistant layers similar to amyloid fibrils that can be solubilized only by means of strong acids, and class II HPBs that form less regular and stable assemblies soluble in solvents and detergents (Ball et al., 2020). Adhesion of HPBs is a very fast process; indeed, they can tightly bind several surfaces by dip-casting or direct deposition. Using an engineered Class II HPB variant (Szilvay et al., 2006) linked to the atomic force microscopy cantilever tip, Paananen et al. demonstrated that interactions between HPB and hydrophobic surfaces are stronger than those formed between two hydrophobin molecules (Paananen et al., 2021). Lo et al. demonstrated that Class I HPB layers formed on a graphite surface are resistant to alcohol, acid, and basic washes (Lo et al., 2014). In contrast, a Class II monolayer is dissociated by alcohol treatment, even if relatively stable towards acid and base washes. However, it is worth noting that HPBs can exhibit various surface binding characteristics, even if they belonged to the same class and to the same organism (Winandy et al., 2018).

These characteristics, together with the capability of the HPB layer to immobilize a plethora of biomolecules by adsorption, make them appealing candidates as biological linkers, exploitable across a wide range of applications. For example, HPB on a polymeric surface can function as an "ink receiving layer," rendering the surface amenable to ink jet printing with desired features (Misra et al., 2015).

More recently, a smart strategy is offered by the production of HPB fusion proteins, obtained using genetic engineering techniques to couple the adhesive capability of HPBs with the biological activity of different target proteins, leading to a rapid and efficient immobilization process (Kurppa et al., 2014; Hennig et al., 2016).

In this work, we provide an overview of the most recent (last ten years) exploitations of wild type and fused HPBs in the development of innovative biosystems in food, environmental, and biomedical fields (Figure 1).

Environmental applications

Biosensors are considered a cutting-edge frontier in environmental diagnostics representing a rapid and cost-effective strategy, alternative to traditional methods (Scognamiglio et al., 2014), for real-time *in situ* analysis. One of the limiting steps in biosensor designing is represented by immobilization of bioreceptors on the transducer elements. The HPBs' ability to bind several biomolecules in their active forms allowed the development of very versatile systems for the detection of a wide range of environmental pollutants by changing the immobilized bioreceptor. For example, the HPB layers were used by Tao et al. to easily functionalize film bulk acoustic wave resonators (FBARs) enabling the development of a sensitive system with the ability to detect volatile organic compounds (VOCs) (Tao et al., 2019). VOCs represent biomarkers of several disorders and diseases (Fitzgerald et al., 2017); thus, their detection and quantification, traditionally carried out by chromatographic strategies, are very useful. The coating obtained by simple droplet casting of the HPB HFBI from *Trichoderma reesei* not only allowed a better adsorption of the analytes, but also their discrimination according to their polarity, due to the negatively charged nature of the HFBI film.

Regarding the exploitation of HPB fusion proteins, Piscitelli et al. (2017b) developed a glutathione-S-transferase (GST)–based biosensor to detect pesticides, such as molinate and captan, in aqueous environmental samples. The authors recombinantly produced in *Escherichia coli* the fusion protein composed by GST and the Class I HPB Vmh2 from *Pleurotus ostreatus*. Vmh2–GST fusion protein can be easily and rapidly immobilized on the polystyrene surface by direct deposition and is able to sense with high sensitivity and accuracy both toxic compounds, which act as competitors of an enzyme substrate. With a similar aim, Doring et al. (2019) fused the target protein 5-enolpyruvylshikimate-3-phosphate synthase (EPSPS) to the HPB Ccg2 (also known as EAS from *Neurospora crassa*) to functionalize both glass and polystyrene surfaces. Using this biosystem, the widespread herbicide glyphosate (Kanissery et al., 2019), which inhibits the enzyme

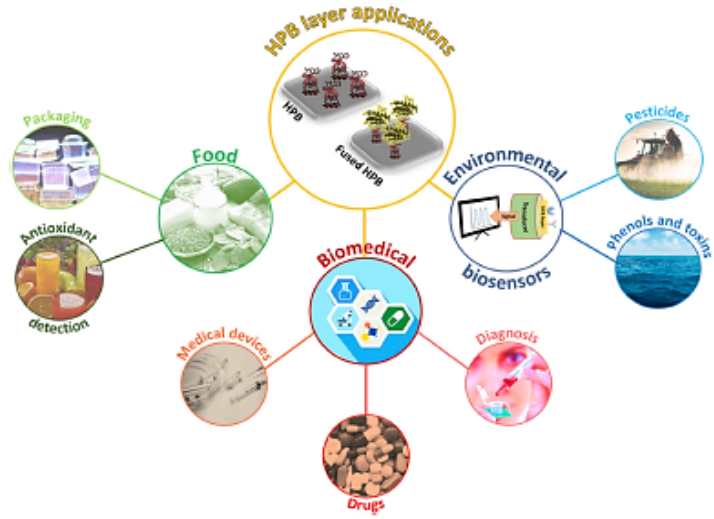

FIGURE 1
Schematic representation of HPB layer exploitation in different application fields.

activity (Murtaza and William, 2001), was detected at a nanomolar sensitivity. The surfaces were also functionalized with a mixture of the fusion protein and the wild type HPB to avoid steric hindrance, achieving better signal-to-noise (S/N) ratio. The same fusion protein was later used by Rettke et al. (2020) to functionalize a glass slide by direct deposition, thus developing an ultrasensitive optical particle-based biosensor. A straightforward approach to quantify the analyte was set up as a competitive binding assay between glyphosate immobilized on soft colloidal probe and the free one.

Among the well-known environmental pollutants, heavy metals are highly toxic, persistent, and capable of bioaccumulation in nature (Ali et al., 2019). Quantification of mercury, arsenic, cadmium, and nickel in aqueous samples is currently performed using elaborate methods. Biosensors based on the Vmh2 fusion proteins were set up as alternative methods for the detection of heavy metals. Puopolo et al. coupled the HPB Vmh2 with a thermophilic arsenate reductase, able to reduce As(V) to As(III) (Puopolo et al., 2021). The functionalized gold electrodes were used by the authors as innovative platforms for the detection of arsenic. Moreover, Pennacchio et al. (2022) developed a fluorescence-based biosensor based on Vmh2 fused to a mercury-binding peptide. The immobilized fusion protein was able to bind to mercury in the presence of other metals, leading to a decrease in the fluorescence intensity and achieving a nanomolar sensitivity both in tap and seawater. The real innovation of this biosensor is related to the combination of the fluorescence detection with machine learning methodologies to predict the mercury (II) concentration by analyzing the image of a multiwell plate, without the need of classical reader devices.

Stanzione et al. (2021) designed and expressed in *E. coli* two Vmh2 fusion proteins in which the HPB partners were single-chain fragment variables (ScFvs) of antibodies, able to recognize two marine neurotoxins, saxitoxin and domoic acid. These algal toxins are associated with algal blooms and can be bioaccumulated in fish or shellfish, leading to heavy consequences for human health (Vilariño et al., 2009). By immobilizing the proteins on pristine magnetic nanoparticles, both optical and electrochemical biosensors, able to detect the two neurotoxins, were developed.

Highly sensitive detection of catechol and poly aromatic hydrocarbons (PAH), widespread contaminants of the environment, was progressively developed starting from the fusion of Vmh2 with a laccase enzyme. Laccase is able to oxidize aromatic and phenolic compounds by reducing molecular oxygen to water. In this case, an added value of the system was the enzyme immobilization on carbon nanomaterials, thereby endowed with a high surface-to-volume ratio. Starting from previous experimental works that demonstrated the successful functionalization of nanomaterials with Vmh2 (Gravagnuolo et al., 2015), Sorrentino et al. (2020b) produced

few-layer graphene functionalized with the Vmh2–laccase fusion protein through a "one-pot" approach. Once the immobilization conditions were optimized, biofunctionalized few-layer graphene was deposited on glass carbon electrodes to detect catechol at micromolar sensitivity. An improvement of this biosensor was later developed by immobilizing the same fusion protein on multi-walled carbon nanotubes reaching higher sensitivity (Sorrentino et al., 2021). More recently, Vmh2–laccase fusion protein was also immobilized on magnetic beads and used to detect three PAHs, upon their oxidation into quinones in the presence of a redox mediator. Owing to the efficient adsorption of quinones at carbon nanotube–modified electrodes, PAHs were detected at picomolar sensitivity (Sorrentino et al., 2022).

Biomedical applications

HPBs are widely used for the formulation and the administration of hydrophobic drugs, for the development of biomedical devices, and for the detection of targeted biomarkers in diagnostics. Although many examples regarding the use of HPBs as effective adjuvants for improved hydrophobic drug solubility, stability, and bioavailability are reported (Weiszhár et al., 2012; Valo et al., 2013; Fang et al., 2014; Paukkonen et al., 2017), in this review, we will focus on HPB exploitation in the functionalization of drug carrier surfaces. Class II HPBs were used to functionalize silicon, gold, and other carriers, providing several benefits in terms of drug stability, biodistribution, and targeting. The coating of porous silicon with the HPB HFBII modified the hydrophobicity of the nanoparticles, improved intravenous biodistribution with respect to non-functionalized particles, and altered the adsorption profile of plasma proteins on the particle surface (Sarparanta et al., 2012). Maiolo et al. (2017) functionalized dodecanethyl-protected gold nanoparticles with the same HPB, obtaining exceptionally stable encapsulated drugs, whose release was selectively triggered in the tissues by the cytoplasmic glutathione reduction. More recently, Barani and coworkers coated the surface of doxorubicin-loaded niosomes with HFB-1, a vesicular system made from nonionic surfactants, presenting a promising drug delivery system for sustained drug release in cancer (Barani et al., 2020). Using a different approach, Reuter et al. (2017) improved drug delivery to specific target cells by functionalizing porous silicon nanoparticles with a fusion protein combining the coating ability of the HPB HFBIV with the targeting ability of the human transferrin. The nanoparticles were stable, degradable, non-immunogenic, and specifically reached their targets. The HPB–transferrin coating also affected the biodistribution of the nanoparticles when administered intravenously to rats and allowed decrease in the adsorption of plasma proteins around the nanoparticles and, consequently, their aggregation and loss of activity (Reuter et al., 2017). Furthermore, the Class I HPB HGFI from *Grifola frondosa* and its mutant were used to easily modify halloysite clay nanotubes loaded with an anticancer drug: results confirmed that the HPB coating enhanced the dispersion stability, the pH-dependent prolonging drug release, and the effective cytotoxicity (Wang et al., 2021).

Despite many breakthroughs in science and technology, a significant proportion of medical implants are still infected by bacteria. Implant infection is estimated to cause around one-fifth of implant failures, which can occur at any time post-implantation (VanEpps and Younger, 2016). Surface contamination represents a serious concern both in material science and in medicine; therefore, prevention and control of nonspecific protein adsorption and of microbial growth on surfaces is a key issue, currently addressed by many researchers (Wang et al., 2017). As the cell number keeps increasing on a surface, microbes usually start to build up a biofilm, namely, a complex structure consisting of polysaccharides, proteins, and extracellular DNA in which cells are embedded. The biofilm is characterized by a strong resistance to many treatments and consequently, is extremely hard to remove (Maan et al., 2020). Several approaches to prevent biofilm formation on implants include applying chemical surface coatings that kill bacteria such as antibiotics, antimicrobial peptides, and metal nanoparticles (Maan et al., 2020). The ability of Class I HPBs to reduce the thickness of the biofilm formed by different strains of *Staphylococcus epidermidis* on plastic-, metal-, and glass-coated surfaces has been demonstrated first by Artini et al. with confocal laser scanning microscope analysis (Artini et al., 2017). The HPB SC3 was used to coat a medical-grade nitric oxide (NO)–releasing polymer, providing an antifouling layer which works synergistically with NO's antibacterial and antiplatelet activities (Devine et al., 2019). Moreover, fusion protein containing HPB and antimicrobial peptides went one step further. Wang and coworkers fused the HPB HGFI to the antimicrobial peptide pediocin PA-1 and proved the ability of the fusion protein against two Gram-positive bacteria (Wang et al., 2017). Sorrentino et al. (2020a) developed a chimeric protein combining the assessed capabilities of the HPB Vmh2 with those of the human antimicrobial peptide LL37. The so-developed fusion protein enhances and enlarges the anti-biofilm activity against both Gram-positive and Gram-negative pathogenic bacteria, and also displays biocidal activity, since dead cells were found in the biofilm layer.

In other fields of research, HPBs were fused to different protein motifs, and the coating they formed was used for the development of biocompatible surfaces able to allow both adhesion of human cells and tissue regeneration (Huang et al., 2013; Zhao et al., 2016; Wang et al., 2017). Boeuf et al. (2012) used the Class I HPB from *Aspergillus nidulans* to functionalize orthopedic implant surfaces. Two HPB variants were produced, one with fibronectin receptor sites (RGD) and another one with the laminin domain (LG3) and showed continuous adhesion of human cells without increasing the adhesion of bacterial cells

(Bouef et al., 2012). In the patent of Shufang et al. (2017), the inventors set up a method to prepare a novel bioactive protein-loaded stent material using the amphiphilic protein HFBI. The stent material improves its biocompatibility and promotes cell migration and vascularization.

As far as medical diagnostics are concerned, different HPB functionalization strategies were adopted. Functionalization of optical fibers was achieved by exploiting the self-assembly of HPB and the immobilization of goat-anti-rabbit IgG for the development of a label-free immunosensor. HGFI allows the formation of a self-assembled amphipathic film on the fiber surface, which can adsorb antibodies with desirable advantages such as ease of use, quick response, good stability, good repeatability, good specificity, and no side effects (Duan et al., 2020). Following a different approach, the class II HPB HFBI was fused to Protein A, a protein known to bind different immunoglobulin subclasses, and the HFBI–Protein A monolayer was proven to bind to immunoglobin; thus, a highly sensitive label-free graphene biosensor was built (Soikkeli et al., 2016). Moreover, a Vmh2–fusion protein was used to detect thrombin in human plasma (Piscitelli et al., 2017a). In this case, the HPB was fused to the green fluorescent protein (GFP) and immobilized on multiwell plates. Since the two proteins are linked by the specific cleavage site of thrombin, the higher the protease concentration, the lower the fluorescence intensity measured in the well, due to the release of GFP from the surface, thus developing an ultrasensitive biosensor. A very similar approach was used by Zhang and coworkers by using a HGFI-fusion protein (Zhang et al., 2020). Mirzaei et al. coated glassy carbon electrodes with HFBI and used it as a glue to immobilize the lactate dehydrogenase enzyme developing a biosensor for pyruvate, whose concentration is an index of circulatory disorders (Mirzaei et al., 2019). The HPB layer improved enzyme stability and allowed the achievement of low detection limits. In the recent invention of a CRISPR high-throughput biochip for detecting single gene mutation, an HPB is used for modifying a chip substrate (Zefang et al., 2019). Compared with a common substrate, this chip allows a uniform spread of the protein on the surface, avoiding the waste of biomolecules.

Food applications

The exploitation of HPBs in food industry is mainly related to their ability to stabilize emulsions, for instance, in the design of aerated foods (e.g., mayonnaise, shelf-stable milk shakes, smoothies and other beverages, yoghurt, and gelatin-free mousse), with benefits such as fat/calorie reduction or improved/new product textures. With regard to their capability to functionalize surfaces, HPBs were recently exploited to enable a biosensor to detect antioxidant compounds in beverages. These compounds are used to maintain the color stability and to protect beverages from oxidative deterioration. Nonetheless, high concentration of these can have negative effects on human health. Thus, to overcome the traditional chromatographic methods often used for their analysis, Sorrentino et al. (2019) developed an innovative, easy-to-use, and rapid colorimetric biosensor, immobilizing the already mentioned Vmh2–laccase on the polystyrene surface. A competitive assay between a chromogenic substrate of the laccase enzyme and the caffeic acid as inhibitor allowed reaching micromolar sensitivity in real samples, such as ACE juice and tea infusion.

A completely different application of HPBs was developed to improve the degradation of plastic materials used in food packaging. Polyethylene terephthalate (PET) is the most widely used plastic for beverage bottles and food packaging, although its low level of degradation has a heavy impact on the environmental pollution. Puspitasari et al. (2021) discovered that an HPB layer on a PET surface, not only changed its wettability, making the plastic component more hydrophilic, but also made its degradation by PETase enzyme easier. Thus, the HPB RolA, extracted from the fungus *Aspergillus oryzae*, was successfully immobilized on the PET surface, obtaining faster and enhanced activity of the PETase enzyme when compared to its performance without the HPB layer. Moreover, a comparison between the effects of three free HPBs and of their fusion proteins with the cutinase enzyme was studied by Ribitsch et al. (2015) based both on the ability of cutinase enzyme to hydrolyze PET and of HPB to enhance its degradation. The authors demonstrated that the genetic fusion between the HPBs and the cutinase leads to a better performance of the enzyme. The HPB role should be the creation of a more hydrophilic surface, leading to a better binding and targeting of the cutinases to PET.

Protein structure analysis and proteomic applications

The HPB layers were successfully exploited to improve the adhesion of proteins on supports used in different structural analysis techniques (Figure 2).

Using the class II HPB HFBI, a cryo-EM support film was developed. The HFBI film, spontaneously formed on top of a solution drop, was transferred onto the cryo-EM grid, with a simple and highly reproducible procedure, avoiding the need for conventional grid treatments before cryo-vitrification. The hydrophilic side of HFBI film adsorbs proteins via electrostatic interactions, allowing high-quality data collection. Using this support, the authors determined high resolution structures of some proteins (e.g., aldolase 150 kDa, hemoglobin 64 kDa), demonstrating the potentiality of HFBI films in increasing the success rate and efficiency of cryo-EM analyses (Fan et al., 2021).

10.3389/fmolb.2022.959166

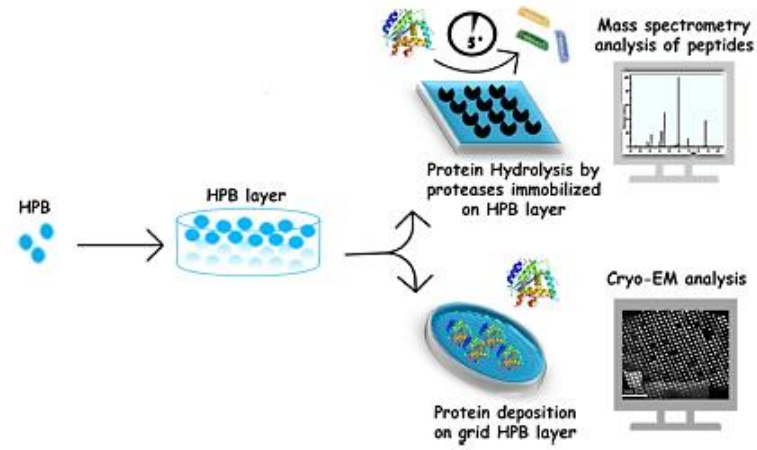

FIGURE 2
HPB layer used in protein structure analysis and proteomic applications.

Regarding mass spectrometry analysis, the self-assembled layer of the Class I HPB Vmh2 was successfully used to functionalize the conductive supports used in direct matrix-assisted laser desorption/ionization (MALDI) mass spectrometry. Indeed, the Vmh2 coating enables an efficient on-plate desalting and, consequently, a fast analysis with a good S/N ratio of a wide mass range of molecules (from small peptides to intact proteins), thus representing a very simple alternative to other known methods (Longobardi et al., 2014). In a different scenario, Vmh2-coated MALDI sample plates were exploited as a lab-on-plate platform for a stable non-covalent and non-destructive immobilization of enzymes commonly involved in proteomic studies (such as trypsin, V8 protease, PNGaseF, and alkaline phosphatase). Efficient, fast, and reproducible protein digestion is of utmost importance in bottom-up proteomics. Immobilization of proteolytic enzymes has gained an increasing interest owing to its several advantages over soluble enzyme reactions. Most importantly, it allows online mass spectrometric (MS) analysis of the proteolytic digests and effectively suppresses autoproteolysis even at high enzyme-to-substrate ratios (Tähkä et al., 2019). Rapid and efficient on-plate reactions were performed on Vmh2-coated MALDI plates, using very low sample volumes (some microliters) achieving high protein sequence coverage in few minutes, even when multi-proteolysis steps were performed directly on the same plate (Longobardi et al., 2015). This approach was exploited for *in situ* detection on a MALDI plate of blood as a real sample. In particular, the authors demonstrated the opportunity to discriminate the blood provenance even when present in a mixture (Patel et al., 2016).

In the field of cultural heritage preservation, the self-assembled Vmh2 layer was employed to bio-functionalize a flexible cellulose acetate sheet with trypsin, to digest proteins and capture peptides from paintings and ancient archeological artifacts with good efficiency. This flexible tool was fully portable without the need of microsampling the works of art; indeed, it is only necessary to moisten the biofunctionalized sheet just before use, and put it in contact with the work of art. The released peptides are captured onto the film surface and then analyzed when required, by a simple MALDI-TOF analysis or, eventually, by more resolutive and informative LC–MS/MS analyses (Cicatiello et al., 2018). Additionally, this lab-on-plate method was implemented immobilizing the glycosidases PNGaseF on the Vmh2-coated sheet for a two-step procedure in which the deglycosylation pretreatment allows an improved proteolysis and detection of glycosylated proteins (Ntasi et al., 2021).

Because of HPBs' natural abilities, these interesting proteins can be used to replace conventional strategies generally adopted in surface derivatization processes. Nonetheless, some weak points of HPB exploitation have to be considered, for example, the unpredictability of the ligand–HPB layer interactions and the low production yield of native HPBs, which hinder their employment at industrial scale. Therefore, the recombinant production of HPBs, wild type or fused to target proteins, can allow researchers to tackle these issues. However, this strategy still carries some problems since it is not feasible for

non-protein ligands and production of functional HPB fusion proteins cannot be assumed *a priori*.

Further studies on the potential of HPBs can encourage their use, even in unexplored fields of application, making them building blocks for macroscopic functional materials.

Author contributions

IS, RP, AP, and PC were involved in the literature search and in writing the review draft. AP and PG were involved in reviewing and editing the manuscript.

Funding

This work was supported by grants from the University of Naples Federico II, Italy (000,023_ALTRI_CDA_75_2021_FRA_PISCITELLI) "Intelligent biosensors based on chimeric proteins (BIOCHIP)."

Conflict of interest

The authors declare that the research was conducted in the absence of any commercial or financial relationships that could be construed as a potential conflict of interest.

Publisher's note

All claims expressed in this article are solely those of the authors and do not necessarily represent those of their affiliated organizations, or those of the publisher, the editors, and the reviewers. Any product that may be evaluated in this article, or claim that may be made by its manufacturer, is not guaranteed or endorsed by the publisher.

References

Ali, H., Khan, E., and Ilahi, I. (2019). Environmental chemistry and ecotoxicology of hazardous heavy metals: Environmental persistence, toxicity, and bioaccumulation. *J. Chem.* 2019, 6730305. doi:10.1155/2019/6730305

Artini, M., Cicatiello, P., Ricciardelli, A., Papa, R., Selan, L., Dardano, P., et al. (2017). Hydrophobin coating prevents Staphylococcus epidermidis biofilm formation on different surfaces. *Biofouling* 33, 601–611. doi:10.1080/08927014.2017.1338690

Ashkan, Z., Hemmati, R., Homaei, A., Dinari, A., Jamlidoost, M., Tashakor, A., et al. (2021). Immobilization of enzymes on nanoinorganic support materials: An update. *Int. J. Biol. Macromol.* 168, 708–721. doi:10.1016/j.ijbiomac.2020.11.127

Ball, S. R., Kwan, A. H., and Sunde, M. (2020). Hydrophobin rodlets on the fungal cell wall. *Curr. Top. Microbiol. Immunol.* 425, 29–51. doi:10.1007/82_2019_186

Barani, M., Mirzaei, M., Torkzadeh-Mahani, M., Lohrasbi-Nejad, A., and Nematollahi, M. H. (2020). A new formulation of hydrophobin-coated niosome as a drug carrier to cancer cells. *Mat. Sci. Eng. C Mat. Biol. Appl.* 113, 110975. doi:10.1016/j.msec.2020.110975

Boaretti, C., Roso, M., Bonora, R., Modesti, M., and Lorenzetti, A. (2020). Investigation of plasma-assisted functionalization of graphitic materials for epoxy composites. *Nanomaterials* 10, E78. doi:10.3390/nano10010078

Boeuf, S., Throm, T., Gutt, B., Strunk, T., Hoffmann, M., Seebach, E., et al. (2012). Engineering hydrophobin DewA to generate surfaces that enhance adhesion of human but not bacterial cells. *Acta Biomater.* 8, 1037–1047. doi:10.1016/j.actbio.2011.11.022

Cicatiello, P., Ntasi, G., Rossi, M., Marino, G., Giardina, P., Birolo, L., et al. (2018). Minimally invasive and portable method for the identification of proteins in ancient paintings. *Anal. Chem.* 90, 10128–10133. doi:10.1021/acs.analchem.8b01718

Cicatiello, P., Sorrentino, I., Piscitelli, A., and Giardina, P. (2020). "Spotlight on class I hydrophobins: Their intriguing biochemical properties and industrial prospects BT," in *Grand challenges in fungal biotechnology*. Editor H. Nevalainen (Cham: Springer International Publishing), 333–347. doi:10.1007/978-3-030-29541-7_12

Devine, R., Singha, P., and Handa, H. (2019). Versatile biomimetic medical device surface: Hydrophobin coated, nitric oxide-releasing polymer for antimicrobial and hemocompatible applications. *Biomater. Sci.* 7, 3438–3449. doi:10.1039/c9bm00469f

Döring, J., Rettke, D., Rödel, G., Pompe, T., and Ostermann, K. (2019). Surface functionalization by hydrophobin-EPSPS fusion protein allows for the fast and simple detection of glyphosate. *Biosensors* 9, E104. doi:10.3390/bios9030104

Duan, S., Wang, R., Qiao, M., Zhang, X., Liu, B., Zhang, H., et al. (2020). Hydrophobin HGFI – based fibre-optic biosensor for detection of antigen – antibody interaction. *Nanophotonics* 9, 177–186. doi:10.1515/nanoph-2019-0370

Fan, H., Wang, B., Zhang, Y., Zhu, Y., Song, B., Xu, H., et al. (2021). *A novel cryo-electron microscopy support film based on 2D crystal of HFBI protein*. Cold Spring Harbor Laboratory, United States. doi:10.1101/2021.11.09.467987

Fan, L., Zheng, Y., and Victoria, R. (2015). Hydrophobin composition and process for treating surfaces. patent WO2015051121A1. United States: Du Pont. Available at: (Accessed May 25, 2022).

Fang, G., Tang, B., Liu, Z., Gou, J., Zhang, Y., Xu, H., et al. (2014). Novel hydrophobin-coated docetaxel nanoparticles for intravenous delivery: *In vitro* characteristics and *in vivo* performance. *Eur. J. Pharm. Sci.* 60, 1–9. doi:10.1016/j.ejps.2014.04.016

Fitzgerald, J. E., Bui, E. T. H., Simon, N. M., and Fenniri, H. (2017). Artificial nose technology: Status and prospects in diagnostics. *Trends Biotechnol.* 35, 33–42. doi:10.1016/j.tibtech.2016.08.005

Gravagnuolo, A. M., Morales-Narváez, E., Longobardi, S., Da Silva, E. T., Giardina, P., Merkoçi, A., et al. (2015). *In situ* production of biofunctionalized few-layer defect-free microsheets of graphene. *Adv. Funct. Mat.* 25, 2771–2779. doi:10.1002/adfm.201500016

Hennig, S., Rödel, G., and Ostermann, K. (2016). Hydrophobin-based surface engineering for sensitive and robust quantification of yeast pheromones. doi:10.3390/s16050602

Huang, Y., Zhang, S., Niu, B., Wang, D., Wang, Z., Feng, S., et al. (2013). Poly(ε-caprolactone) modified with fusion protein containing self-assembled hydrophobin and functional peptide for selective capture of human blood outgrowth endothelial cells. *Colloids Surf. B Biointerfaces* 101, 361–369. doi:10.1016/j.colsurfb.2012.06.034

Javanbakht, T., Laurent, S., Stanicki, D., Raphael, W., and Tavares, J. R. (2015). Charge effect of superparamagnetic iron oxide nanoparticles on their surface functionalization by photo-initiated chemical vapour deposition. *J. Nanopart. Res.* 17, 462. doi:10.1007/s11051-015-3276-y

Kanissery, R., Gairhe, B., Kadyampakeni, D., Batuman, O., and Alferez, F. (2019). Glyphosate: Its environmental persistence and impact on crop health and nutrition. *Plants (Basel, Switz.* 8, 499. doi:10.3390/plants8110499

Kurppa, K., Hytönen, V. P., Nakari-Setälä, T., Kulomaa, M. S., and Linder, M. B. (2014). Molecular engineering of avidin and hydrophobin for functional self-assembling interfaces. *Colloids Surf. B Biointerfaces* 120, 102–109. doi:10.1016/j.colsurfb.2014.05.010

Lavilla, I., Romero, V., Costas, I., and Bendicho, C. (2014). Greener derivatization in analytical chemistry. *TrAC Trends Anal. Chem.* 61, 1–10. doi:10.1016/j.trac.2014.05.007

Letzel, A., Reich, S., dos Santos Rolo, T., Kanitz, A., Hoppius, J., Rack, A., et al. (2019). Time and mechanism of nanoparticle functionalization by macromolecular ligands during pulsed laser ablation in liquids. *Langmuir* 35, 3038–3047. doi:10.1021/acs.langmuir.8b01585

Lo, V. C., Ren, Q., Pham, C. L. L., Morris, V. K., Kwan, A. H., Sunde, M., et al. (2014). Fungal hydrophobin proteins produce self-assembling protein films with diverse structure and chemical stability. *Nanomaterials* 4, 827–843. doi:10.3390/nano4030827

Longobardi, S., Gravagnuolo, A. M., Punzi, R., Della Ventura, B., Pane, F., Galano, E., et al. (2015). A simple MALDI plate functionalization by Vmh2 hydrophobin for serial multi-enzymatic protein digestions. *Anal. Bioanal. Chem.* 407, 487–496. doi:10.1007/s00216-014-8309-3

Longobardi, S., Gravagnuolo, A. M., Rea, I., De Stefano, L., Marino, G., Giardina, P., et al. (2014). Hydrophobin-coated plates as matrix-assisted laser desorption/ionization sample support for peptide/protein analysis. *Anal. Biochem.* 449, 9–16. doi:10.1016/j.ab.2013.11.021

Maan, A. M. C., Hofman, A. H., de Vos, W. M., and Kamperman, M. (2020). Recent developments and practical feasibility of polymer-based antifouling coatings. *Adv. Funct. Mat.* 30, 2000936. doi:10.1002/adfm.202000936

Maiolo, D., Pigliacelli, C., Sánchez Moreno, P., Violatto, M. B., Talamini, L., Tirotta, I., et al. (2017). Bioreducible hydrophobin-stabilized supraparticles for selective intracellular release. *ACS Nano* 11, 9413–9423. doi:10.1021/acsnano.7b04979

Mirzaei, F., Mirzaei, M., and Torkzadeh-mahani, M. (2019). A hydrophobin-based biosensor layered by an immobilized lactate dehydrogenase enzyme for electrochemical determination of pyruvate. *Bioelectrochemistry* 130, 107323. doi:10.1016/j.bioelechem.2019.06.008

Misra, Anuradha, Misra, Rahul, and ReddyManohar, Esukapalli (2015). *Print quality of polymeric surfaces with amphiphilic protein coating*. patent US20160082A1. United States: El Du Pont de Nemours and Co. Available at: (Accessed May 25, 2022).

Murtaza, Alibhai, and William, Stallings (2001). Closing down on glyphosate inhibition—With a new structure for drug discovery. *Proc. Natl. Acad. Sci. U. S. A.* 98, 2944–2946. doi:10.1073/pnas.061025898

Ntasi, G., Kirby, D. P., Stanzione, I., Carpentieri, A., Somma, P., Cicatiello, P., et al. (2021). A versatile and user-friendly approach for the analysis of proteins in ancient and historical objects. *J. Proteomics* 231, 104039. doi:10.1016/j.jprot.2020.104039

Paananen, A., Weich, S., Szilvay, G. R., Leitner, M., Tappura, K., Ebner, A., et al. (2021). Quantifying biomolecular hydrophobicity: Single molecule force spectroscopy of class II hydrophobins. *J. Biol. Chem.* 296, 100728. doi:10.1016/j.jbc.2021.100728

Patel, E., Cicatiello, P., Deininger, L., Clench, M. R., Marino, G., Giardina, P., et al. (2016). A proteomic approach for the rapid, multi-informative and reliable identification of blood. *Analyst* 141, 191–198. doi:10.1039/c5an01016f

Paulkonen, H., Ulkonen, A., Szilvay, G., Yliperttula, M., and Laaksonen, T. (2017). European Journal of Pharmaceutical Sciences Hydrophobin-nano fi brillated cellulose stabilized emulsions for encapsulation and release of BCS class II drugs. *Eur. J. Pharm. Sci.* 100, 238–248. doi:10.1016/j.ejps.2017.01.029

Peng, L., Gao, R., Lan, J., Jiang, S., and Lin, S. (2016). Microwave-assisted deposition of silver nanoparticles on bamboo pulp fabric through dopamine functionalization. *Appl. Surf. Sci.* 386, 151–159. doi:10.1016/j.apsusc.2016.05.170

Pennacchio, A., Giampaolo, F., Piccialli, F., Cuomo, S., Notomista, E., Spinelli, M., et al. (2022). A machine learning-enhanced biosensor for mercury detection based on an hydrophobin chimera. *Biosens. Bioelectron.* 196, 113696. doi:10.1016/j.bios.2021.113696

Piscitelli, A., Pennacchio, A., Cicatiello, P., Politi, J., De Stefano, L., Giardina, P., et al. (2017a). Rapid and ultrasensitive detection of active thrombin based on the Vmh2 hydrophobin fused to a Green Fluorescent Protein. *Biosens. Bioelectron.* 87, 816–822. doi:10.1016/j.bios.2016.09.052

Piscitelli, A., Pennacchio, A., Longobardi, S., Velotta, R., and Giardina, P. (2017b). Vmh2 hydrophobin as a tool for the development of "self-immobilizing" enzymes for biosensing. *Biotechnol. Bioeng.* 114, 46–52. doi:10.1002/bit.26049

Puopolo, R., Sorrentino, I., Gallo, G., Piscitelli, A., Giardina, P., Le Goff, A., et al. (2021). Self-assembling thermostable chimeras as new platform for arsenic biosensing. *Sci. Rep.* 11, 2991. doi:10.1038/s41598-021-82648-9

Puspitasari, N., Tsai, S.-L., and Lee, C.-K. (2021). Fungal hydrophobin RolA enhanced PETase hydrolysis of polyethylene terephthalate. *Appl. Biochem. Biotechnol.* 193, 1284–1295. doi:10.1007/s12010-020-03358-y

Rettke, D., Döring, J., Martin, S., Venus, T., Estrela-Lopis, I., Schmidt, S., et al. (2020). Picomolar glyphosate sensitivity of an optical particle-based sensor utilizing biomimetic interaction principles. *Biosens. Bioelectron.* 165, 112262. doi:10.1016/j.bios.2020.112262

Reuter, L. J., Shahbazi, M.-A., Mäkilä, E. M., Salonen, J. J., Saberianfar, R., Menassa, R., et al. (2017). Coating nanoparticles with plant-produced transferrin-hydrophobin fusion protein enhances their uptake in cancer cells. *Bioconjug. Chem.* 28, 1639–1648. doi:10.1021/acs.bioconjchem.7b00075

Ribitsch, D., Herrero Acero, E., Przylucka, A., Zitzenbacher, S., Marold, A., Gamerith, C., et al. (2015). Enhanced cutinase-catalyzed hydrolysis of polyethylene terephthalate by covalent fusion to hydrophobins. *Appl. Environ. Microbiol.* 81, 3586–3592. doi:10.1128/AEM.04111-14

Sarparanta, M., Bimbo, L. M., Rytkönen, J., Mäkilä, E., Laaksonen, T. J., Laaksonen, P., et al. (2012). Intravenous delivery of hydrophobin-functionalized porous silicon nanoparticles: Stability, plasma protein adsorption and biodistribution. *Mol Pharm.* 9, 654–663. doi:10.1021/mp200611d

Scognamiglio, V., Arduini, F., Palleschi, G., and Rea, G. (2014). Biosensing technology for sustainable food safety. *Trac. Trends Anal. Chem.* 62, 1–10. doi:10.1016/j.trac.2014.07.007

Shufang, W., Li, J., and Tang, D. (2017). *Method for loading bioactive protein on hydrophobic stent material*. patent CN107308501A. China: Nankai University. Available at:.

Sofkoli, M., Kurppa, K., Kainlauri, M., Arpiainen, S., Paananen, A., Gunnarsson, D., et al. (2016). Graphene biosensor programming with genetically engineered fusion protein monolayers. *ACS Appl. Mat. Interfaces* 8, 8257–8264. doi:10.1021/acsami.6b00123

Sorrentino, I., Carrière, M., Jamet, H., Stanzione, I., Piscitelli, A., Giardina, P., et al. (2022). The laccase mediator system at carbon nanotubes for anthracene oxidation and femtomolar electrochemical biosensing. *Analyst* 147, 897–904. doi:10.1039/D1AN02091A

Sorrentino, I., Gargano, M., Ricciardelli, A., Parrilli, E., Buonocore, C., de Pascale, D., et al. (2020a). Development of anti-bacterial surfaces using a hydrophobin chimeric protein. *Int. J. Biol. Macromol.* 164, 2293–2300. doi:10.1016/j.ijbiomac.2020.07.301

Sorrentino, I., Giardina, P., and Piscitelli, A. (2019). Development of a biosensing platform based on a laccase-hydrophobin chimera. *Appl. Microbiol. Biotechnol.* 103, 3061–3071. doi:10.1007/s00253-019-09678-2

Sorrentino, I., Stanzione, I., Nedellec, Y., Piscitelli, A., Giardina, P., Le Goff, A., et al. (2020b). From graphite to laccase biofunctionalized few-layer graphene: A "one pot" approach using a chimeric enzyme. *Int. J. Mol. Sci.* 21, E3741. doi:10.3390/ijms21113741

Sorrentino, I., Stanzione, I., Piscitelli, A., Giardina, P., and Goff, A. L. (2021). Carbon-nanotube-supported POXA1b laccase and its hydrophobin chimera for oxygen reduction and picomolar phenol biosensing. *Biosens. Bioelectron. X* 8, 100074. doi:10.1016/j.biosx.2021.100074

Stanzione, I., Izquierdo-Bote, D., González García, M. B., Giardina, P., and Piscitelli, A. (2021). Immobilization of antibodies by genetic fusion to a fungal self-assembling adhesive protein. *Front. Mol Biosci.* 8, 725697. doi:10.3389/fmolb.2021.725697

Szilvay, G. R., Nakari-Setälä, T., and Linder, M. B. (2006). Behavior of Trichoderma reesei hydrophobins in solution: Interactions, dynamics, and multimer formation. *Biochemistry* 45, 8590–8598. doi:10.1021/bi060620y

Tähkä, S., Sarfraz, J., Urvas, L., Provenzani, R., Wiedmer, S. K., Peltonen, J., et al. (2019). Immobilization of proteolytic enzymes on replica-molded thiol-ene micropillar reactors via thiol-gold interaction. *Anal. Bioanal. Chem.* 411, 2339–2349. doi:10.1007/s00216-019-01674-9

Tao, J., Chang, Y., Liang, J., Duan, X., Pang, W., Wang, Y., et al. (2019). Hydrophobin-functionalized film bulk acoustic wave resonators for sensitive and polarity-sensitive sensing of volatile organic compounds. *Appl. Phys. Lett.* 115, 163502. doi:10.1063/1.5124525

Valo, H., Arola, S., Laaksonen, P., Torkkeli, M., Peltonen, L., Linder, M. B., et al. (2013). Drug release from nanoparticles embedded in four different nanofibrillar cellulose aerogels. *Eur. J. Pharm. Sci. Off. J. Eur. Fed. Pharm. Sci.* 50, 69–77. doi:10.1016/j.ejps.2013.02.023

VanEpps, J. S., and Younger, J. G. (2016). Implantable device-related infection. *Shock* 46, 597–608. doi:10.1097/SHK.0000000000000692

Vilariño, N., Fonfría, E. S., Louzao, M. C., and Botana, L. M. (2009). Use of biosensors as alternatives to current regulatory methods for marine biotoxins. *Sensors* 9, 9414–9443. doi:10.3390/s91109414

Wang, B., Han, Z., Song, B., Yu, L., Ma, Z., Xu, H., et al. (2021). Colloids and Surfaces A : Physicochemical and Engineering Aspects Effective drug delivery system based on hydrophobin and halloysite clay nanotubes for sustained release of doxorubicin. *Colloids Surfaces A Physicochem. Eng. Aspects* 628, 127351. doi:10.1016/j.colsurfa.2021.127351

Wang, K., Zhang, Q., Zhao, L., Pan, Y., Wang, T., Zhi, D., et al. (2017). Functional modification of electrospun poly(ε-caprolactone) vascular grafts with the fusion protein VEGF-HGF1 enhanced vascular regeneration. *ACS Appl. Mat. Interfaces* 9, 11415–11427. doi:10.1021/acsami.6b16713

Weiszhár, Z., Czúcz, J., Révész, C., Rosivall, L., Szebeni, J., Rozsnyay, Z., et al. (2012). Complement activation by polyethoxylated pharmaceutical surfactants: Cremophor-EL, tween-80 and tween-20. *Eur. J. Pharm. Sci.* 45, 492–498. doi:10.1016/j.ejps.2011.09.016

Winandy, L., Hilpert, F., Schlebusch, O., and Fischer, R. (2018). Comparative analysis of surface coating properties of five hydrophobins from Aspergillus nidulans and Trichoderma reesei. *Sci. Rep.* 8, 1–11. doi:10.1038/s41598-018-29749-0

Wolf, A., Lorrmann, H., Flegler, A., Wolf, A. J., Guerfi, A., Mandel, K., et al. (2021). Abrasive blasting of lithium metal surfaces yields clean and 3D-structured lithium metal anodes with superior properties. *Energy Technol.* 9, 2100455. doi:10.1002/ente.202100455

Yang, J., Pang, Y., Huang, W., Shaw, S. K., Schiffbauer, J., Pillers, M. A., et al. (2017). Functionalized graphene enables highly efficient solar thermal steam generation. *ACS Nano* 11, 5510–5518. doi:10.1021/acsnano.7b00867

Zefang, W., Xuechun, G., Linpeng, C., and Yang, H. (2019). *CRISPR high-throughput biochip for detecting single gene mutation*. patent CN110117818A. China: Tianjin University. Available at.

Zhang, H., Yang, L., Zhu, X., Wang, Y., Yang, H., Wang, Z., et al. (2020). A rapid and ultrasensitive thrombin biosensor based on a rationally designed trifunctional protein. *Adv. Healthc. Mat.* 9, 1–9. doi:10.1002/adhm.202000364

Zhao, W., Li, J., Jin, K., Liu, W., Qiu, X., Li, C., et al. (2016). Fabrication of functional PLGA-based electrospun scaffolds and their applications in biomedical engineering. *Mat. Sci. Eng. C Mat. Biol. Appl.* 59, 1181–1194. doi:10.1016/j.msec.2015.11.026

microbial biotechnology

Open Access

Trichoderma harzianum cerato-platanin enhances hydrolysis of lignocellulosic materials

Anna Pennacchio,[1,†] Rossana Pitocchi,[1,†] Giovanna Cristina Varese,[2] Paola Giardina[1] and Alessandra Piscitelli[1]

[1]*Department of Chemical Sciences, University of Naples Federico II, Via Cintia 4, Naples, 80126, Italy.*

[2]*Department of Life Sciences and Systems Biology, University of Turin, viale P.A. Mattioli 25, Turin, 10125, Italy.*

Summary

Considering its worldwide abundance, cellulose can be a suitable candidate to replace the fossil oil-based materials, even if its potential is still untapped, due to some scientific and technical gaps. This work offers new possibilities demonstrating for the first time the ability of a cerato-platanin, a small fungal protein, to valorize lignocellulosic Agri-food Wastes. Indeed, cerato-platanins can loosen cellulose rendering it more accessible to hydrolytic attack. The cerato-platanin *Th*CP from a marine strain of *Trichoderma harzianum*, characterized as an efficient biosurfactant protein, has proven able to efficiently pre-treat apple pomace, obtaining a sugar conversion yield of 65%. Moreover, when used in combination with a laccase enzyme, a notable increase in the sugar conversion yield was measured. Similar results were also obtained when other wastes, coffee silverskin and potato peel, were pre-treated. With respect to the widespread laccase pre-treatments, this new pre-treatment approach minimizes process time, increasing energy efficiency.

Introduction

The continuous increase in energy consumption needs for effective alternatives to gradually replace the fossil fuels, as encouraged by the EU Bioeconomy Strategy. The valorization of inexpensive, abundant, and renewable biomass wastes could provide benefits reducing both fossil fuel demands and environmental concerns.

In this regard, the possibility to recover fermentable sugars from lignocellulosic biomass has long been deemed as a sustainable alternative to obtain biofuels and other biomaterials from different microorganisms (Chohan *et al.*, 2020; Hyväkkö *et al.*, 2020). Moreover, lignocellulosic raw materials, including forest residues, agricultural wastes and agri-food wastes (AFW), are the most abundant source of organic material in the world (Giacobbe *et al.*, 2020).

In this direction, some hurdles still exist, such as physico-chemical, structural and compositional factors hindering the hydrolysis of cellulose present in biomasses, beyond other economic aspects (Kahn *et al.*, 2020). A necessary step is the removal or reduction of any obstacle to hydrolysis, in order to maximize the yields of fermentable sugars from cellulose or hemicellulose (Mosier *et al.*, 2005). This step is still a matter of investigation, since an effective pre-treatment able to combine environmental sustainability, sugar recovery and cost-effectiveness is still missing (Fillat *et al.*, 2017). A number of physical and chemical pre-treatment methods have been tested; however, they are often expensive, high-energy demanding and cause loss of carbohydrates and/or formation of unfavourable by-products. Laccases do the lion's share of the biological pre-treatment approaches, since they have been used in the valorization of many lignocellulosic biomasses alone, or in mixture with other ligninolytic enzymes and in combination with physical and chemical treatment methods (Giacobbe *et al.*, 2020).

In the last years, cerato-platanin family proteins have proven able to weaken filter paper, acting similarly to another class of fungal proteins, the expansins (Luti *et al.*, 2019). Cerato-platanin is small, cysteine-rich, non-catalytic fungal proteins (Gaderer and Bonazza, 2014). Their structure shows a double-ψ β-barrel structurally related to the expansin domain D1 (De Oliveira *et al.*, 2011). Their physiological role is still a matter of debate, indeed they are reported to act both as virulence factor and as elicitors, even if other study suggests that their main biological functions are also related to other, more general aspects of fungal growth (Djonovic *et al.*, 2007).

Biochemical analysis of the properties of cerato-platanins showed that they have both carbohydrate-

Received 5 February, 2021; revised 3 April, 2021; accepted 10 May, 2021.
For correspondence. E-mail apiscite@unina.it; Tel. +39 081 674475; Fax +39 081674313.
[†]Equally contributing authors.
Microbial Biotechnology (2021) **14**(4), 1699–1706
doi:10.1111/1751-7915.13836
Funding Information
No funding information provided.

binding/carbohydrate-loosening properties (Baccelli *et al.*, 2014), and the ability to self-assemble and change the polarity of surfaces (Frischmann *et al.*, 2013).

The ability to weaken cellulose derived substrates in the absence of hydrolytic activity has been reported till now for several cerato-platanins, such as CP from *Ceratocystis platani*, Pop1 from *Ceratocystis populicola* (Baccelli *et al.*, 2014), MpCP2 from *Moniliophthora perniciosa* (Barsottini *et al.*, 2013), FgCPPs from *Fusarium graminearum* (Quarantin *et al.*, 2019) and recently for *Th*CP from *Trichoderma harzianum* (Pitocchi *et al.*, 2020). Luti and coworkers carried out an analysis of site-directed mutants of CP from *C. platani* and figured out that it weakly binds cellulose while performing its non-lytic loosening, like other single domain expansin-like proteins, and its expansin-like activity depends on its net charge (Luti *et al.*, 2020). This ability is potentially very interesting for biotechnological applications, since cerato-platanin may contribute to the valorization of lignocellulosic waste materials, but we did not find out any ongoing efforts in this respect yet.

The cerato-platanin *Th*CP was recently isolated from *T. harzianum* grown on oil as sole carbon source and characterized as an efficient biosurfactant protein (Pitocchi *et al.*, 2020). This work explores for the first time the potential of a cerato-platanin in the valorization of lignocellulosic biomasses promoting enzymatic attack of cellulose. Three AFWs, apple pomace (AP), coffee silverskin (CS) and potato peels (PP) endowed with different lignin and carbohydrate contents and already used in biorefinery approaches, were successfully pre-treated with *Th*CP confirming that cerato-platanins could play an important role in the future of waste valorization circle.

Results and discussion

Valorization of Apple Pomace (AP)

*Th*CP was produced in the presence of lampante oil as sole carbon source and was purified by simple ultrafiltration to remove high molecular weight proteins (> 30 kDa), and then concentrated and dialyzed. As a matter of fact, only one band was observed when this sample was loaded on SDS-PAGE (Fig. 1A).

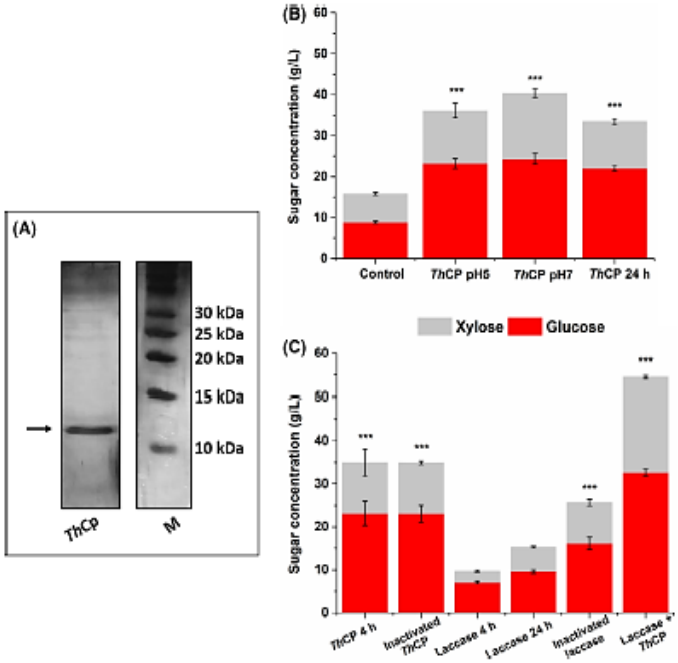

Fig. 1. (A) SDS-PAGE of the cerato-platanin *Th*CP purified from *T. harzianum* used for the pre-treatment. (B) Glucose and xylose concentration obtained after 72 h enzymatic hydrolysis by commercial enzymes of pre-treated Apple Pomace biomass. *Th*CP (4×10^{-6} M) pre-treatment was performed for 4 h at pH 5 and 7 and for 24 h at pH5. BSA (4×10^{-6} M) was used as control (4 h at pH 5). (C) Glucose and xylose concentration obtained after enzymatic hydrolysis of pre-treated Apple Pomace biomass by cellulolytic commercial enzymes. *Th*CP pre-treatment (4 h), laccase pre-treatment (24 h) and laccase+ *Th*CP pre-treatment (24 h) were followed by 6 h inactivation at 50°C. Results of two technical replicates of at least three biological replicates were analysed. The mean values were compared to the control and considered significant when $P < 0.05$ ($^{*}P < 0.05$, $^{**}P < 0.01$, $^{***}P < 0.001$) according to Student's *t*-test.

The purified *Th*CP was firstly tested on AP, considering that it shows a high sugar content (52%) with a high percentage (16%) of soluble carbohydrates, along with a low lignin content (18%) (Giacobbe *et al.*, 2018a). With the aim to set up the process conditions avoiding intermediate steps between pre-treatment and hydrolysis, the effect of time, temperature and pH were considered, taking into account that cellulolytic enzymes are reported to efficiently work at 50°C and pH 5 (Procentese *et al.*, 2017). The solubility of *Th*CP was evaluated by measuring the protein concentration at different temperatures: *Th*CP was soluble at 30°C for at least 4 h, while its concentration was quickly reduced about one fourth at 40°C and 50°C, therefore, the temperature of 30°C was selected for the pre-treatment. As for the pH, two different pHs were tested: 7.0, the pH of the solution containing *Th*CP, and 5.0, the pH needed for the enzymatic hydrolysis. After a 4h *Th*CP pre-treatment, the saccharification experiments were carried out for 72 h, obtaining the release of about 40 gl^{-1} of total sugars (corresponding to 65% sugar yield) at both pH 5.0 and 7.0, indicating that this pH variation did not affect the pre-treatment step (Fig. 1B). Increasing the duration of the *Th*CP pre-treatment did not increase the efficiency of the process. Considering these results, the selected pre-treatment conditions were 4 h at 30°C, at pH 5.0, thus avoiding the need of buffer exchange.

These results demonstrate for the first time that the action of *Th*CP in loosening cellulose increases its availability for the hydrolysis by a tailored mix of hydrolytic enzymes in AFW. Giacobbe *et al.* (2018b) reported a very efficient AP pre-treatment with laccase after a 24 h process at 28°C followed by a 6 h inactivation step at 50°C. Indeed, when the laccase pre-treatment was 4 h long (the same duration of cerato-platanin pre-treatment, a negligible amount of sugars was released (Fig. 1C). Moreover, the laccase thermal inactivation is necessary to maintain cellulase activity, while the thermal inactivation is not necessary when the cerato-platanin was used to pre-treat AP.

A mix of *Th*CP and laccase in a pre-treatment process was used (Fig. 1C), in order to evaluate their synergistic action, setting conditions suitable to highlight the contribution of both proteins (5 U of laccase, 24 h pre-treatment followed by 6 h inactivation at 50°C). A very relevant sugars conversion yield (95%) was achieved (Table 1), thanks to the action of laccase in lignin removal and of cerato-platanin in loosening cellulose, making cellulose biomass fully accessible to cellulases.

To further analyse the process, Klason-lignin (KL) content was evaluated after pre-treatment with cerato-platanin or laccase enzyme. As expected, the reduction of lignin content (5% decrease) was negligible when the cerato-platanin was used, while a higher decrease of lignin content (15%) was observed after laccase pre-treatment (Table 1).

Table 1. Lignin removal of pre-treated biomass waste as percentage respect to control samples. Results of two technical replicates of at least three biological replicates were analysed.

AFW	Pre-treatment	Lignin removal (%)	Sugar conversion yield (%)
AP	*Th*CP	5	65 ± 2
	Laccase	15	56 ± 7
	Laccase + *Th*CP	n. a.	95 ± 1
CS	*Th*CP	11	54 ± 2
	Laccase	25	42 ± 2
	Laccase + *Th*CP	n. a.	99 ± 1
PP	*Th*CP	15	59 ± 4
	Laccase	28	45 ± 6
	Laccase + *Th*CP	n. a.	94 ± 2

n. a., not analysed.

Process optimization

With the aim to optimize the conditions of cerato-platanin pre-treatment and to improve the sugar yield from the biomasses, different experiments were performed. Table 2 reports results obtained after *Th*CP pre-treatment and enzymatic hydrolysis at higher biomass loading, compared with those obtained using laccase alone and in combination with the cerato-platanin. Albeit an increased amount of released sugars was obtained at higher biomass loading (15% w/v), the sugar conversion yield was lower. Moreover, a further decrease was observed at 20% (w/v) biomass loading, leading to an amount of released sugars comparable to that obtained at 10% (w/v) biomass loading (Table 2). Since high-water absorption at such high biomass loading was observed, the lower availability of free water can affect the protein efficiency. At all the tested biomass loadings, the combined action of cerato-platanin and laccase is very effective.

In addition, in order to assess the reusability of the proteins in the pre-treatment process, several successive cycles of pre-treatment were performed recovering the soluble part and adding it to fresh biomass. After each pre-treatment step, the insoluble recovered biomass underwent the enzymatic hydrolysis (Fig. 2A). After four

Table 2. Sugar conversion yield obtained after enzymatic hydrolysis by commercial enzymes of AP biomass pre-treated at different biomass loading. Results of two technical replicates of at least three biological replicates were analysed.

	Sugar conversion yield (%)		
	10% AP	15% AP	20% AP
*Th*CP	65 ± 2	50 ± 1	33 ± 1
Laccase	56 ± 7	40 ± 1	27 ± 1
Laccase + *Th*CP	95 ± 1	69 ± 1	46 ± 1

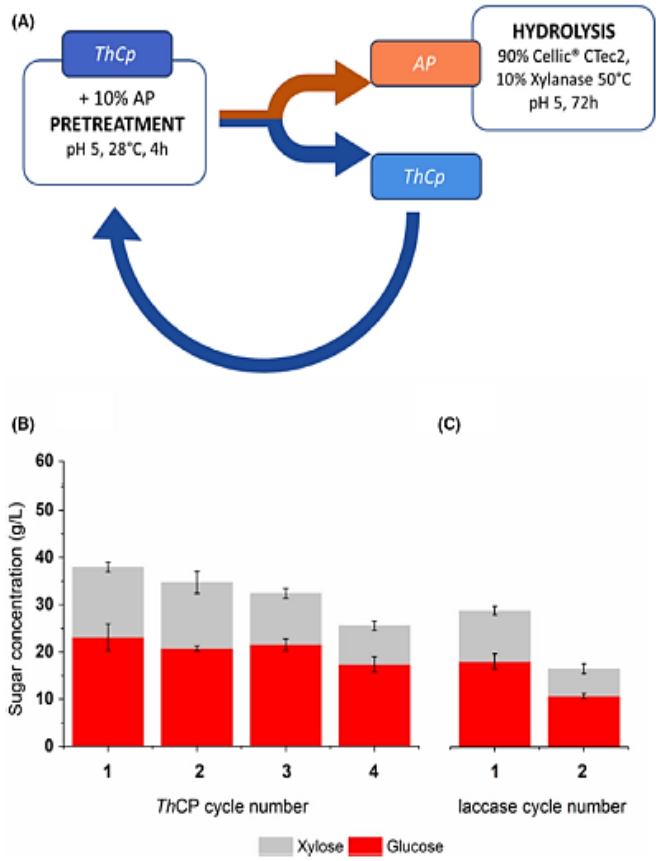

Fig. 2. (A) Scheme of the recycling protocol. Glucose and xylose concentration obtained after enzymatic hydrolysis of Apple Pomace biomass pre-treated by cerato-platanin (B) or laccase (C). Results of two technical replicates of at least three biological replicates were analysed.

cycles with cerato-platanin, a sugar conversion yield of 45% was still obtained (Fig. 2B), while laccase ability dropped already at the second cycle (Fig. 2C).

The amount of cerato-platanin recovered up to the third cycle is 75% compared to the initial concentration, while it decreased up to 50% after four cycles. On the other hand, laccase activity decreased to 40% in the second cycle.

Protein production optimization

Different culture conditions were tested to increase protein yield production growing the fungus *T. harzianum* in rich media. In the condition reported above (§ 2.2 Production of cerato-platanin), an increase of about five-fold mycelium biomass, and about two-fold total protein production was obtained in half time, moreover, several protein bands were evident in the sample loaded on SDS-PAGE (Fig. 3A).

Nonetheless, different amounts of these secreted proteins were used for AP pre-treatment. A yield comparable to that obtained with the purified *Th*CP was achievable when the protein amounts of the secreted proteins were doubled (Fig. 3B), and a slight increase of the sugar yield conversion was obtained after further doubling the protein amount.

These results indicate that the use of this rich medium to produce the protein does not confer a real advantage to the process, therefore, other strategies to increase the sustainability of the process must be explored, for example, *Th*CP recombinant expression.

Valorization of other agri-food wastes

To test the versatility of the process, cerato-platanin was also tested using two other biomasses, CS and PP, endowed with a lower sugar and a higher lignin content

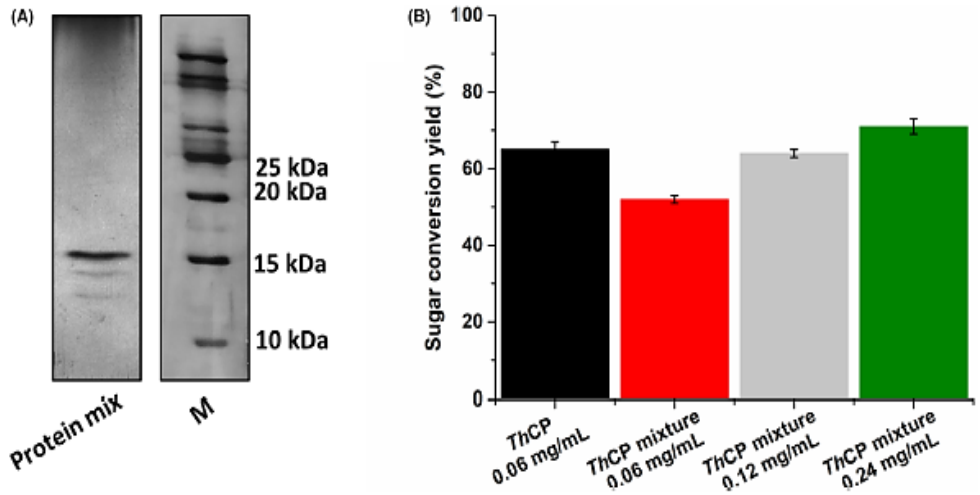

Fig. 3. (A) SDS-PAGE of *T. harzianum* protein mixtures used for the pre-treatment. (B) Sugar conversion yields (%) obtained after enzymatic hydrolysis by commercial enzymes of Apple Pomace biomass pre-treated with purified *Th*CP and *Th*CP in mixture at different total protein amount. Results of two technical replicates of at least three biological replicates were analysed.

with respect to AP. In particular, PP showed the highest lignin content (33%) also characterized by the presence of suberin, a very complex polymer (Liang and McDonald, 2014).

As already observed for AP, the cerato-platanin pre-treatment of CS and PP allowed a good sugar release (Fig. 4), even if lower compared to that obtained with AP, as a consequence of their higher lignin content. Analysis of Klason-lignin (KL) content and sugar yield (Table 1) suggests that the presence of lignin barrier is not the only obstacle to the accessibility of cellulose by cellulolytic enzymes, and other side effects must be taken into account.

It is worth noting that 99% and 94% sugar conversion yield was achieved when the combined action of laccase enzyme and cerato-platanin was tested on CS and PP respectively (Table 1).

The sugar conversion yield obtained after cerato-platanin pre-treatment is comparable or higher to that reported on the same biomasses by Giacobbe *et al.*

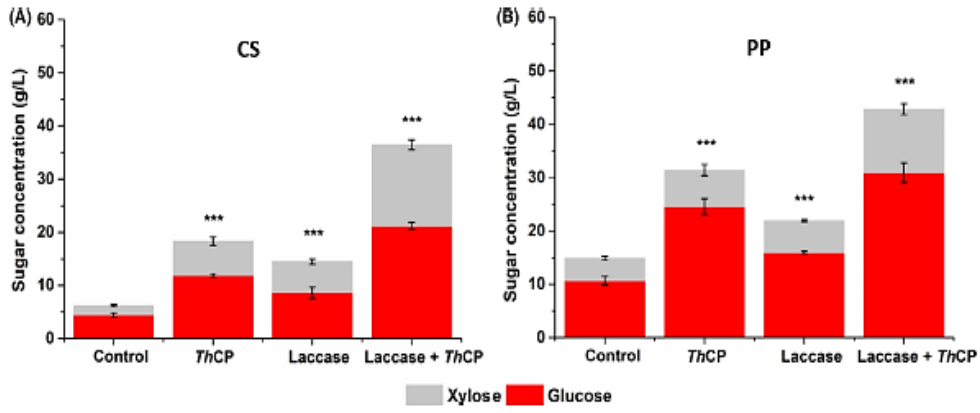

Fig. 4. Glucose and xylose concentration obtained after enzymatic hydrolysis by commercial enzymes of pre-treated Coffee Silverskin (A) and Potato Peels (B) biomass. *Th*CP (4×10^{-6} M) pre-treatment was performed for 4 h at pH 5. BSA (4×10^{-6} M) was used as control. Laccase and laccase+ *Th*CP pre-treatment was performed for 24 h followed by 6 h inactivation at 50°C. Results of two technical replicates of at least three biological replicates were analysed. The mean values were compared to the control and considered significant when $P < 0.05$ (*$P < 0.05$, **$P < 0.01$, ***$P < 0.001$) according to Student's *t*-test.

(2018b) and by Hijosa-Valsero *et al.* (2018a) (Hijosa-Valsero, 2017; Hijosa-Valsero *et al.*, 2018a,b,) after enzymatic and physico-chemical pre-treatments respectively. Moreover, the combination of cerato-platanin and laccase allowed a significant improvement of these results, demonstrating that the action of cerato-platanin is very efficient and versatile.

Conclusion

Recent findings suggest that surfactants supplementation during saccharification is an effective strategy to achieve higher saccharification yields, since they can reduce non-specific binding of enzymes on lignin (Singhania *et al.*, 2017), promoting physico-chemical and biological delignification and enzyme recovery (Agrawal *et al.*, 2017). However, the mechanism of action of surfactants for improved saccharification is far to be well understood.

The biosurfactant properties recently demonstrated for *Th*CP (Pitocchi *et al.*, 2020) can explain its ability to loosen cellulose rendering it more accessible to hydrolytic attack. This work offers new possibilities to improve the biological pre-treatment of lignocellulolytic biomasses. the herein developed process ensures high chemical efficiency and minimizes operative time, increasing energy efficiency.

Experimental procedures

Materials

Reagents were purchased from Sigma-Aldrich Corp. (St. Louis, MO) unless otherwise specified. The commercial enzymes used in this study were cellulolytic enzyme cocktail Cellic®CTec2 (kindly supplied by Novozyme); endo-1,4-β-Xylanase M1 from *Trichoderma viride* (Megazyme, Bray, Ireland); α-amylase from *Bacillus licheniformis* (Megazyme). Dry apple pomace (AP) was provided by Muns Agroindustrial S.L. (Lleida, Spain). Coffee silverskin (CS) was kindly provided by Illy S.p.A (Trieste, Italy). Fresh potato peel (PP) containing 76.94% moisture was kindly provided by Aperitivos Gus S.L. (Riego de la Vega, León, Spain). The supplied biomasses were oven-dried, milled and stored as specified by Giacobbe *et al.* (2018b).

Production of cerato-platanin

Trichoderma harzianum MUT 290 was maintained through periodic transfer on agar plate at 28°C, using XNST30 agar medium (3 g l^{-1} malt extract; 3 g l^{-1} yeast extract; 30 g l^{-1} NaCl; 10 g l^{-1} glucose; 5 g l^{-1} peptone; 15 g l^{-1} agar).

Protein production and isolation was performed as described elsewhere (Pitocchi *et al.*, 2020). Mycelium plugs (10 mm diameter) cut from the actively growing colonies were pre-inoculated in 100 ml flasks containing 50 ml of ONR7 mineral medium (30 g of NaCl, 3.98 g of Na_2SO_4, 1.3 g of HEPES (4-(2-hydroxyethyl)-1-piperazineethanesulfonic acid), 0.72 g of KCl, 0.27 g of NH_4Cl, 47 mg of Na_2HPO_4, 83 mg of NaBr, 2.6 mg of NaF, 31 mg of $NaHCO_3$, 27 mg of H_3B0_3, 24 mg of $SrCl_2{\cdot}6H_20$, 11.18 g of $MgCl_2{\cdot}6H_2O$, 1.46 g of $CaCl_2{\cdot}2H_2O$ and 2.0 mg of $FeCl_2{\cdot}4H_20$ per litre of distillate water) supplemented with 10 g l^{-1} glucose, 2 g l^{-1} peptone, and incubated at 28°C for 3 days. Then, 50 ml of these pre-inoculum were inoculated in 1 l flasks containing ONR7 mineral medium (500 ml) supplemented with 1% v/v lampante oil and 0.1% v/v Tween 80. Lampante oil is used to avoid corrosion of industrial and laboratory machines. Flasks were incubated in the dark at 28°C for 14 days, then mycelia were separated from the culture broth using a Whatman 3MM paper filters (Termo Fischer Scientific, Rodano (MI), Italy). Culture broth was filtered using Stericup GP vacuum filtration system (0.22 μm pore size, Merck KGaA, Darmstadt, Germany), and *Th*CP was concentrated by air bubbling, using a Waring blender. The formed foam was separated, collected and loaded in an Amicon Ultrafiltration cell equipped with a 30 kDa cut-off PES Millipore Ultrafiltration Disc (Merck KGaA, Darmstadt, Germany). The ultrafiltrate, containing low molecular weight proteins (<30 kDa), was concentrated using a 3 kDa cut-off disc and dialyzed against 10 mM sodium phosphate buffer pH 7.0.

Another culture condition was tested with the aim to increase protein yield, using a rich medium (1 g l^{-1} yeast extract, 1 g l^{-1} of peptone, 1 g l^{-1} gelatine, 5 g l^{-1} glucose, 30 g l NaCl). Flasks were incubated in the dark at 28°C for 7 days and mycelia were separated from the culture broth using a Whatman 3MM paper filters (Termo Fischer Scientific). Then proteins were overnight precipitated by the addition of $(NH_4)_2SO_4$ up to 50% saturation at 4°C and centrifuged at 10 000 rpm for 20 min. The ammonium sulphate precipitate was resuspended in 10 mM sodium phosphate buffer (pH 7.0) and extensively dialysed against the same buffer, using regenerated Cellulose dialysis tube with 3.5 kDa cut-off (Spectrum Spectra/Por, Thermo Fischer Scientific).

Production of laccase

The *Pleurotus ostreatus* laccases adopted in this study was the recombinant POXA1b expressed in *Pichia pastoris* and secreted in the cultural broth as reported in Pezzella *et al.* (2017). The broth was ultrafiltered and dialyzed towards 50 mM Tris HCl pH8, using Centricon (Merck KGaA, Darmstadt, Germany), cut-off 10 kDa. Laccase activity against ABTS was assayed as reported by (Macellaro *et al.*, 2014).

(2018b) and by Hijosa-Valsero *et al.* (2018a) (Hijosa-Valsero, 2017; Hijosa-Valsero *et al.*, 2018a,b,) after enzymatic and physico-chemical pre-treatments respectively. Moreover, the combination of cerato-platanin and laccase allowed a significant improvement of these results, demonstrating that the action of cerato-platanin is very efficient and versatile.

Conclusion

Recent findings suggest that surfactants supplementation during saccharification is an effective strategy to achieve higher saccharification yields, since they can reduce non-specific binding of enzymes on lignin (Singhania *et al.*, 2017), promoting physico-chemical and biological delignification and enzyme recovery (Agrawal *et al.*, 2017). However, the mechanism of action of surfactants for improved saccharification is far to be well understood.

The biosurfactant properties recently demonstrated for *Th*CP (Pitocchi *et al.*, 2020) can explain its ability to loosen cellulose rendering it more accessible to hydrolytic attack. This work offers new possibilities to improve the biological pre-treatment of lignocellulolytic biomasses. the herein developed process ensures high chemical efficiency and minimizes operative time, increasing energy efficiency.

Experimental procedures

Materials

Reagents were purchased from Sigma-Aldrich Corp. (St. Louis, MO) unless otherwise specified. The commercial enzymes used in this study were cellulolytic enzyme cocktail Cellic®CTec2 (kindly supplied by Novozyme); endo-1,4-β-Xylanase M1 from *Trichoderma viride* (Megazyme, Bray, Ireland); α-amylase from *Bacillus licheniformis* (Megazyme). Dry apple pomace (AP) was provided by Muns Agroindustrial S.L. (Lleida, Spain). Coffee silverskin (CS) was kindly provided by Illy S.p.A (Trieste, Italy). Fresh potato peel (PP) containing 76.94% moisture was kindly provided by Aperitivos Gus S.L. (Riego de la Vega, León, Spain). The supplied biomasses were oven-dried, milled and stored as specified by Giacobbe *et al.* (2018b).

Production of cerato-platanin

Trichoderma harzianum MUT 290 was maintained through periodic transfer on agar plate at 28°C, using XNST30 agar medium (3 g l^{-1} malt extract; 3 g l^{-1} yeast extract; 30 g l^{-1} NaCl; 10 g l^{-1} glucose; 5 g l^{-1} peptone; 15 g l^{-1} agar).

Protein production and isolation was performed as described elsewhere (Pitocchi *et al.*, 2020). Mycelium plugs (10 mm diameter) cut from the actively growing colonies were pre-inoculated in 100 ml flasks containing 50 ml of ONR7 mineral medium (30 g of NaCl, 3.98 g of Na_2SO_4, 1.3 g of HEPES (4-(2-hydroxyethyl)-1-piperazineethanesulfonic acid), 0.72 g of KCl, 0.27 g of NH_4Cl, 47 mg of Na_2HPO_4, 83 mg of NaBr, 2.6 mg of NaF, 31 mg of $NaHCO_3$, 27 mg of H_3B0_3, 24 mg of $SrCl_2{\cdot}6H_20$, 11.18 g of $MgCl_2{\cdot}6H_2O$, 1.46 g of $CaCl_2{\cdot}2H_2O$ and 2.0 mg of $FeCl_2{\cdot}4H_20$ per litre of distillate water) supplemented with 10 g l^{-1} glucose, 2 g l^{-1} peptone, and incubated at 28°C for 3 days. Then, 50 ml of these pre-inoculum were inoculated in 1 l flasks containing ONR7 mineral medium (500 ml) supplemented with 1% v/v lampante oil and 0.1% v/v Tween 80. Lampante oil is used to avoid corrosion of industrial and laboratory machines. Flasks were incubated in the dark at 28°C for 14 days, then mycelia were separated from the culture broth using a Whatman 3MM paper filters (Termo Fischer Scientific, Rodano (MI), Italy). Culture broth was filtered using Stericup GP vacuum filtration system (0.22 μm pore size, Merck KGaA, Darmstadt, Germany), and *Th*CP was concentrated by air bubbling, using a Waring blender. The formed foam was separated, collected and loaded in an Amicon Ultrafiltration cell equipped with a 30 kDa cut-off PES Millipore Ultrafiltration Disc (Merck KGaA, Darmstadt, Germany). The ultrafiltrate, containing low molecular weight proteins (<30 kDa), was concentrated using a 3 kDa cut-off disc and dialyzed against 10 mM sodium phosphate buffer pH 7.0.

Another culture condition was tested with the aim to increase protein yield, using a rich medium (1 g l^{-1} yeast extract, 1 g l^{-1} of peptone, 1 g l^{-1} gelatine, 5 g l^{-1} glucose, 30 g l NaCl). Flasks were incubated in the dark at 28°C for 7 days and mycelia were separated from the culture broth using a Whatman 3MM paper filters (Termo Fischer Scientific). Then proteins were overnight precipitated by the addition of $(NH_4)_2SO_4$ up to 50% saturation at 4°C and centrifuged at 10 000 rpm for 20 min. The ammonium sulphate precipitate was resuspended in 10 mM sodium phosphate buffer (pH 7.0) and extensively dialysed against the same buffer, using regenerated Cellulose dialysis tube with 3.5 kDa cut-off (Spectrum Spectra/Por, Thermo Fischer Scientific).

Production of laccase

The *Pleurotus ostreatus* laccases adopted in this study was the recombinant POXA1b expressed in *Pichia pastoris* and secreted in the cultural broth as reported in Pezzella *et al.* (2017). The broth was ultrafiltered and dialyzed towards 50 mM Tris HCl pH8, using Centricon (Merck KGaA, Darmstadt, Germany), cut-off 10 kDa. Laccase activity against ABTS was assayed as reported by (Macellaro *et al.*, 2014).

Determination of protein concentration

Protein concentration was determined with the Pierce Protein Assay (Thermo Fischer Scientific, Rodano (MI), Italy) using Bovine Serum Albumin (BSA) as standard.

Pre-treatment experiments

*Th*CP pre-treatments were carried out at 10% (w/v) of AP and CS, at 30°C for 4 and 24 h in a total volume of 2.5 ml at two different pHs, pH 5.0 in 50 mM sodium citrate and 7.0 in 50 mM sodium phosphate. In the case of PP, due to its high-water absorption, the pre-treatments were carried at 5% (w/v).

Laccase pre-treatments were carried out at 10% (w/v) of AP and CS at 28°C for 4 and 24 h in a total volume of 2.5 ml followed by an inactivation step of 6 h at 50°C.

Trials at 15 and 20%w/v AP were also performed. The reuse of cerato-platanin and laccase enzyme was tested: after biomass pre-treatment, the solution was centrifuged, and the supernatant transferred to another 10% biomass waste.

About 0.06 mg ml^{-1} (4×10^{-6} M) of *Th*CP and 5 U of POXA1b were used for each-pre-treatment experiment. Control assays were performed under the same conditions using BSA (0.24 mg ml^{-1}, 4×10^{-6} M). Results represent the mean ± the SD of at least three independent samples.

Klason lignin evaluation

The Klason lignin content of treated and untreated biomass waste was determined according to NREL LAPs (Sluiter *et al.*, 2012). Percentage of lignin reduction with respect to untreated samples was reported.

Enzymatic hydrolysis and sugar concentration

Enzymatic hydrolysis of pre-treated biomasses was carried out in the presence of 0.5 mM sodium azide to prevent microbial and fungal growth. According to Giacobbe *et al.* (2018b), the hydrolytic enzymatic cocktail was composed by 90% of Cellic® CTec2 and 10% of xylanase for AP and CS, while in the case of PP, the enzyme mixture contained 80% of amylase, 10% of Cellic® CTec2 and 10% of xylanase.

Samples were collected after 72 h, cooled on ice, centrifuged at 16 500 × *g* for 30 min at 4°C and the amount of sugars released was determined and quantified in the recovered supernatant, by high-performance liquid chromatography (HPLC) using a system 7Q (Dionex, California, USA), equipped with an anionic exchange column (Carbopac PA-100) and a pulsed electrochemical detector. Glucose and xylose were separated with 16 mM sodium hydroxide at a flow rate of 0.25 ml min^{-1} and identified by the respective standards. Fucose was used as internal standard. The total amount of reducing sugars was determined using a Dionex CarboPac MA1 column with pulsed amperometric detection. Standard sugar solutions were prepared separately by dissolving different concentration of glucose, xylose, fructose, arabinose, mannose and sucrose.

The saccharification yields, that are means of three replicates, were expressed as percentages with respect to the sugar content of the pre-treated material before the hydrolysis using the formula (Santhi *et al.*, 2014):

$$\text{Sugar conversion yield} = \left(\frac{\text{Amount of reducing sugar}*0.9}{\text{Carbohydrate content of the biomass}}\right)*100$$

Statistics

The data reported were statistically validated using the Student's *t*-test comparing the sugar concentration obtained after pre-treatment with control BSA and that obtained after pre-treatment with cerato-platanin and/or laccase. The significance of the differences between the values was calculated using a two-tailed Student's *t*-test. A *P*-value of < 0.05 was considered significant.

Acknowledgements

The authors thank Prof. Antonio Marzocchella, Department of Chemical, Materials and Production Engineering of the University of Naples Federico II for kindly making available coffee silverskin; Dr. Rebeca Díez-Antolínez and Dr. María Hijosa-Valsero of the Centre of Biofuels and Bioproducts. Agricultural Technological Institute of Castilla y León, Spain, for kindly making available apple pomace and potato peels.

Conflict of interest

The authors declare that they have no conflict of interest.

References

Agrawal, R., Satlewal, A., Kapoor, M., Mondal, S., and Basu, B. (2017) Investigating the enzyme-lignin binding with surfactants for improved saccharification of pilot scale pretreated wheat straw. *Bioresour Technol* **224:** 411–418.

Baccelli, I., Luti, S., Bernardi, R., Scala, A., and Pazzagli, L. (2014) Cerato-platanin shows expansin-like activity on cellulosic materials. *Appl Microbiol Biotechnol* **98:** 175–184.

Barsottini, M.R.D.O., De Oliveira, J.F., Adamoski, D., Teixeira, P.J.P.L., Prado, P.F.V., Tiezzi, H.O., *et al.* (2013) Functional diversification of cerato-platanins in Moniliophthora perniciosa as seen by differential expression and protein function specialization. *Mol Plant-Microbe Interact* **26:** 1281–1293.

Chohan, N.A., Aruwajoye, G.S., Sewsynker-Sukai, Y., and Gueguim Kana, E.B. (2020) Valorisation of potato peel wastes for bioethanol production using simultaneous saccharification and fermentation: process optimization and kinetic assessment. *Renew Energy* **146:** 1031–1040.

De Oliveira, A.L., Gallo, M., Pazzagli, L., Benedetti, C.E., Cappugi, G., Scala, A., *et al.* (2011) The structure of the elicitor Cerato-platanin (CP), the first member of the CP fungal protein family, reveals a double ψβ-Barrel fold and carbohydrate binding. *J Biol Chem* **286:** 17560–21756.

Djonovic, S., Vargas, W.A., Kolomiets, M.V., and Horndeski, M. (2007) A proteinaceous Elicitor Sm1 from the beneficial fungus *Trichoderma virens* is required for induced systemic resistance in maize. *Plant Physiol* **145:** 875–889.

Fillat, Ú., Ibarra, D., Eugenio, M., Moreno, A., Tomás-Pejó, E., and Martín-Sampedro, R. (2017) Laccases as a potential tool for the efficient conversion of Lignocellulosic biomass: a review. *Fermentation* **3:** 17–47.

Frischmann, A., Neudl, S., Gaderer, R., Bonazza, K., Zach, S., Gruber, S., *et al.* (2013) Self-assembly at air/water interfaces and carbohydrate binding properties of the small secreted protein EPL1 from the fungus Trichoderma atroviride. *J Biol Chem* **288:4278–4287.**

Gaderer, R., Bonazza, K., and Seidl-Seiboth, V. (2014) Cerato-platanins: a fungal protein family with intriguing properties and application potential. *Appl Microbiol Biotechnol* **98:** 4795–4803.

Giacobbe, S., Pezzella, C., Lettera, V., Sannia, G., and Piscitelli, A. (2018a) Bioresource Technology Laccase pretreatment for agrofood wastes valorization. *Bioresour Technol* **265:** 59–65.

Giacobbe, S., Pezzella, C., Lettera, V., Sannia, G., and Piscitelli, A. (2018b) Laccase pretreatment for agrofood wastes valorization. *Bioresour Technol* **265:** 59–65.

Giacobbe, S., Pezzella, C., Sannia, G., and Piscitelli, A. (2020) Old enzymes at the forefront of Lignocellulosic waste valorization. In *Laccases in Bioremediation and Waste Valorisation*. Cham, Switzerland: Springer Nature, pp. 57–78. https://doi.org/10.1007/978-3-030-47906-0_3

Hijosa-Valsero, M., Cambronero, J.G., García, A.I.P., and Antolínez, R.D. (2018a) Biobutanol production from coffee silverskin. *Microb Cell Fact* **17:** 154–163.

Hijosa-Valsero, M., Paniagua-García, A.I., and Díez-Antolínez, R. (2018b) Industrial potato peel as a feedstock for biobutanol production. *N Biotechnol* **46:** 54–56.

Hijosa-Valsero, M., Paniagua-García, A.I., and Díez-Antolínez, R. (2017) Biobutanol production from apple pomace: the importance of pretreatment methods on the fermentability of lignocellulosic agro-food wastes. *Appl Microbiol Biotechnol* **101:** 8041–8052.

Hyväkkö, U., Maltari, R., Kakko, T., Kontro, J., Mikkilä, J., Kilpeläinen, P., *et al.* (2020) On the effect of hot-water pretreatment in sulfur-free pulping of aspen and wheat straw. *ACS Omega* **5:** 265–273.

Kahn, A., Moraïs, S., Chung, D., Sarai, N.S., Hengge, N.N., Kahn, A., *et al.* (2020) Glycosylation of hyperthermostable designer cellulosome components yields enhanced stability and cellulose hydrolysis. *FEBS J* **287:** 4370–4388.

Liang, S., and McDonald, A.G. (2014) Chemical and thermal characterization of potato peel waste and its fermentation residue as potential resources for biofuel and bioproducts production. *J Agric Food Chem* **62:** 8421–8429.

Luti, S., Bemporad, F., Vivoli Vega, M., Leri, M., Musiani, F., Baccelli, I., and Pazzagli, L. (2020) Partitioning the structural features that underlie expansin-like and elicitor activities of cerato-platanin. *Int J Biol Macromol* **165:** 2845–2854.

Luti, S., Sella, L., Quarantin, A., Pazzagli, L., and Baccelli, I. (2019) Twenty years of research on cerato-platanin family proteins: clues, conclusions, and unsolved issues. *Fungal Biol Rev* **34:** 13–24.

Macellaro, G., Pezzella, C., Cicatiello, P., Sannia, G., and Piscitelli, A. (2014) Fungal laccases degradation of endocrine disrupting compounds. *Biomed Res Int* **2014:** 1–8.

Mosier, N., Wyman, C., Dale, B., Elander, R., Lee, Y.Y., Holtzapple, M., *et al.* (2005) Features of promising technologies for pretreatment of lignocellulosic biomass. *Bioresour Technol* **96:** 673–686.

Pezzella, C., Giacobelli, V.G., Lettera, V., Olivieri, G., Cicatiello, P., Sannia, G., and Piscitelli, A. (2017) A step forward in laccase exploitation: recombinant production and evaluation of techno-economic feasibility of the process. *J Biotechnol* **259:** 175–181.

Pitocchi, R., Cicatiello, P., Birolo, L., Piscitelli, A., Bovio, E., Varese, G.C., and Giardina, P. (2020) Cerato-platanins from marine fungi as effective protein biosurfactants and bioemulsifiers. *Int J Mol Sci* **21:** 2913–2925.

Procentese, A., Raganati, F., Olivieri, G., Elena Russo, M., and Marzocchella, A. (2017) Pre-treatment and enzymatic hydrolysis of lettuce residues as feedstock for bio-butanol production biomass and bioenergy pre-treatment and enzymatic hydrolysis of lettuce residues as feedstock for bio-butanol production. *Biomass Bioenerg* **96:** 172–179.

Quarantin, A., Castiglioni, C., Schäfer, W., Favaron, F., and Sella, L. (2019) The *Fusarium graminearum* cerato-platanins loosen cellulose substrates enhancing fungal cellulase activity as expansin-like proteins. *Plant Physiol Biochem* **139:** 229–238.

Satheeja Santhi, V., Bhagat, A.K., Saranya, S., Govindarajan, G., and Jebakumar, S.R.D. (2014) Seaweed (*Eucheuma cottonii*) associated microorganisms, a versatile enzyme source for the lignocellulosic biomass processing. *Int Biodeterior Biodegrad* **96:** 144–151.

Singhania, R.R., Patel, A.K., Saini, R., and Pandey, A. (2017) 5-Industrial enzymes: β-glucosidases. In *Current Developments in Biotechnology and Bioengineering*. Amsterdam, Netherlands: Elsevier, pp. 103–125. https://doi.org/10.1016/B978-0-444-63662-1.00005-1

Sluiter, A.D., Hames, B., Ruiz, R., and Scarlata, C. (2012) Determination of Structural Carbohydrates and Lignin in Biomass Laboratory Analytical Procedure (LAP). Natl Anal Energy Lab.

(SUBMITTED TO ACS APPLIED BIOMATERIALS)

CHAPTER 4

4. CONCLUSIONS

The predicted outcomes of the present PhD project, i.e. the identification of new fungal biosurfactant proteins and the proof of their possible applications in biomedical and bioremediation fields, were successfully achieved.
In the research of new biosurfactant proteins produced by filamentous fungi, different fungal strains have been investigated. On one hand, two *F. solani* isolated from hostile environments, such as plastic dumpsites, were analyzed. Following a common BS extraction technique, it was possible to separate a low molecular weight protein that has been demonstrated to form aggregates, responsible for the good emulsifying properties. The two extracts were thereafter tested on a small scale as bioremediation agents, for the cleaning of oil-contaminated soil. Other two fungal proteins, named Vmh2 and PAC3, previously isolated and characterized as amyloid-forming proteins, were analyzed in terms of surfactant activities. Both showed great performances in reducing surface tension and stabilizing emulsions between oil and water. While the Vmh2 sequence was already known, only a partial sequence of PAC3 was obtained, since the genome of its producing fungus is not sequenced yet. Results obtained from both works represent evidence that there might be other new fungal proteins, behind HPBs or CPs families, with good BS/BE properties.
As for the applications side, a BS native protein in one case and an engineered one in the other, have been successfully used in two different fields. The native Ceratoplatanin from *T. harzianum*, has been included in the hydrolysis process of lignocellulosic substrates, as a pretreatment step. Tightly packed cellulose fibers can be “loosened” by the non-enzymatic action of CP, being hence more prone to enzyme attacks. With the right scale-up system, CPs can be valuable resources for the valorization of agrifood wastes, or the extraction of cellulose from plants and other substrates. On the other hand, a recombinant fusion protein was designed to combine the adhesive properties of the HPB Vmh2, from *P. ostreatus* with the antimicrobial peptide GKY20. Exploiting the capability of Vmh2 to form stable layers on several surfaces, the designed chimera Vmh2-GKY20 has been used to functionalize polystyrene and bacterial cellulose. Vmh2-GKY20 successfully adhered on both surfaces, imparting antibiofilm or antibacterial activity against different nosocomial pathogens.
The work carried out within this PhD project has highlighted once more how filamentous fungi are a valuable and still untapped resource of compounds of biotechnological interest, just like BS/BE. Indeed, to achieve full valorization of these compounds, research must focus on sustainable large-scale production, *e.g.* by using genetically modified organisms, or through circular bioeconomy approaches. Particularly interesting in the case of BS proteins, is the possibility of using genetic engineering techniques to heterologously produce these proteins, allowing their large-scale production more easily. Moreover, these DNA recombinant techniques offer the possibility to design whole new proteins, combining the BS characteristics with those of other proteins/peptides, imparting them new functionalities.

On the other hand, circular bioeconomy approaches can imply fungal growth using wastes from different sources, as an inexpensive and abundant carbon source. This approach is particularly useful, for example, in an environmental context (i.e. bioremediation processes) where BS do not need to be pure. In this case, industrial waste materials, such as agrifood wastes, can be used as cheap and otherwise non-reusable growth substrates. Indeed, it is of fundamental importance to target the specific application field, in order to make BS industrial production truly viable.

Synergy work of microbial biobanks, addressed to the identification and preservation of fungal strains of interest, and research focused on the isolation and characterization of new compounds, paves the way for the applicability of filamentous fungi and their products in the bio-industry.

APPENDIX

5.1 Preliminary results on *F. solani* BS as bioremediation agents

Protocol reported by Chaprao et al. [33], with slight modification, was used to assess ability of the raw extracts of *F. solani* strains to enhance oil recovery from sand samples. Contaminated sand samples were simulated by adding 20% w/w of exhausted motor oil to 100 g of silica (SiLibeads), and then let stand for one week prior any experiments. Raw extracts were incubated for different hours with contaminated sand samples, under magnetic stirring. Thereafter the supernatant was extracted using hexane. Percentage of oil removal was calculated as the ratio between weight of oil extracted by hexane (O_{rim}) and initial oil weight (O_{tot}).

$$O_{rim}\% = \frac{O_{rim}}{O_{tot}} * 100$$

Both *F. solani* extracts showed a great enhancing in oil removal, even at low protein concentration (30 µM). BS from the strain MUT 6181 showed the highest percentage of oil removal already after 1h of incubation; while extract from the other strain reached the maximum extraction yield after 3h (figure 5). Control was performed using SDS at the same concentration (30 µM). Removed oil percentage calculated was 18 and 23% for 1h and 3h of incubation.

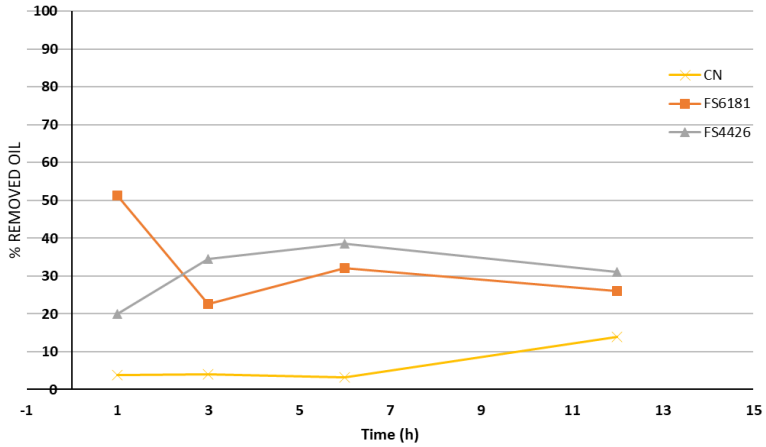

Figure 5: Percentage of oil removed from oil contaminated sand by the two extract of *F. solani* strains (MUT6181 and MUT4426), varying incubation time. Water was used as negative control (CN).

The BS produced by *Candida sphaerica* in the work of Chaprao 2015 caused a 70% removal of the oil present in sands, but at a fourfold higher concentration compared to that presently used.
Experiments were herein conducted on a lab scale, using small amount of sand and extracts, as preliminary analysis. However, they represent a promising indication about the applicability of this fungal BS for bioremediation purposes.

Evidence of small fungal cysteine-rich proteins acting as biosurfactants and self-assembling into large fibers.

Rossana Pitocchi[1], Ilaria Stanzione[1], Anna Illiano[1], Angela Amoresano[1], Oreste Tarallo[1], Paola Cicatiello[1*], Alessandra Piscitelli[1], Paola Giardina[1]

[1] Department of Chemical Sciences, University of Naples Federico II, Via Cintia, 80126 Naples, Italy.
* Correspondence: paola.cicatiello@unina.it; Tel. +3908174327

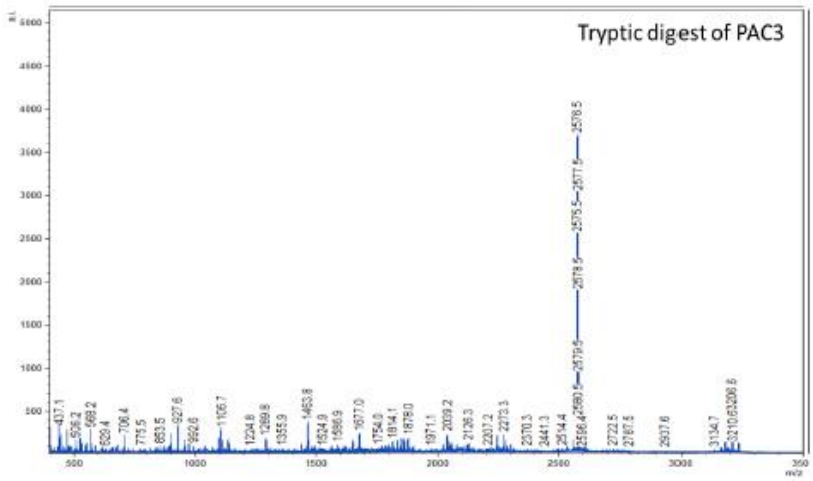

Figure S1. MALDI-MS spectrum of tryptic peptides of PAC3 acquired in the range 400 - 3500 m/z.

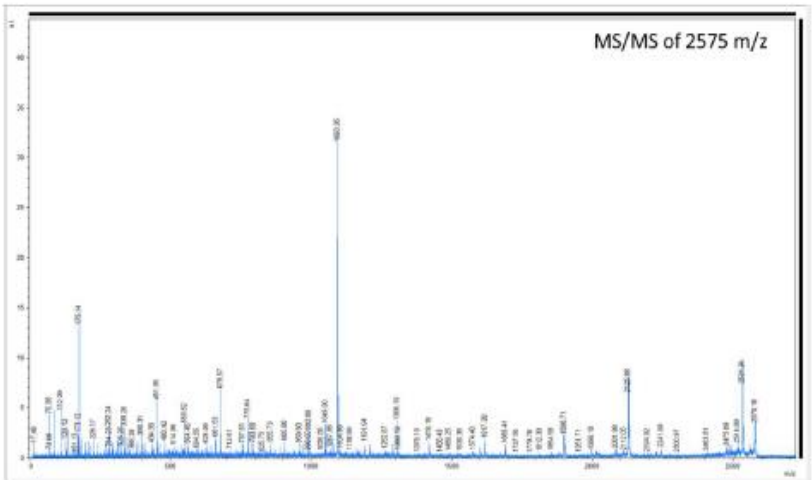

Figure S2. MALDI MS-MS fragmentation spectrum of the 2575 m/z PAC3 tryptic peptide (named peptide 1).

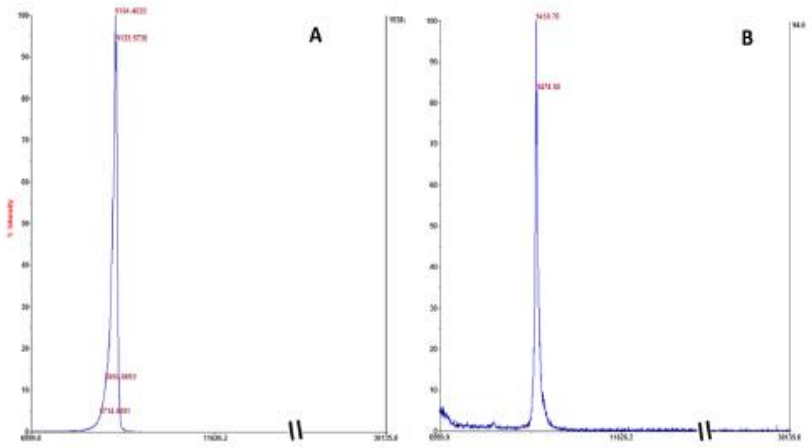

Figure S3. MALDI-TOF spectrum of PAC3 protein. The spectrum A is related to the untreated PAC3, while the spectrum B is related to the reduced and carbamidomethylated PAC3.

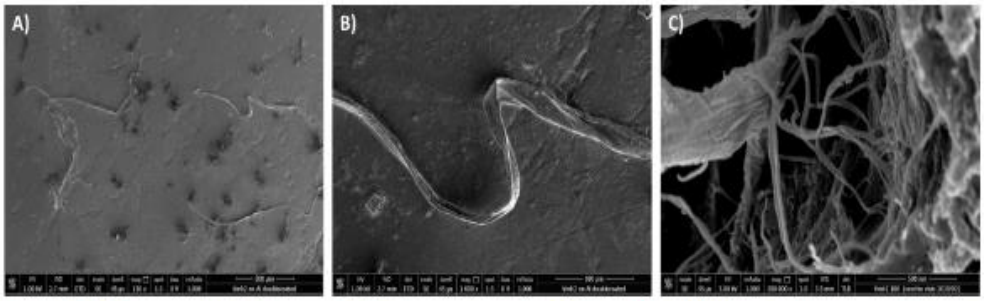

Figure S4. SEM images of Vmh2 fibers at different magnification (A, B, C, at 150X, 1000X, 200000X respectively). 20 µl of protein solutions were deposited on the surfaces, air dried and Au-Pd coated prior visualization.

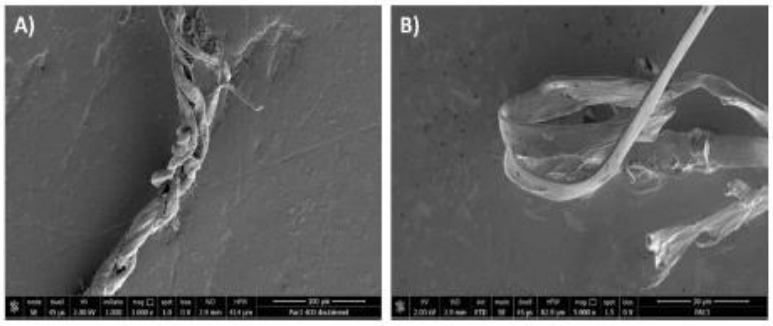

Figure S5. SEM images of PAC3 fibers at different magnification (A, B, at 1000X, 5000X respectively). 20 µl of protein solutions were deposited on the surfaces, air dried and Au-Pd coated prior visualization.

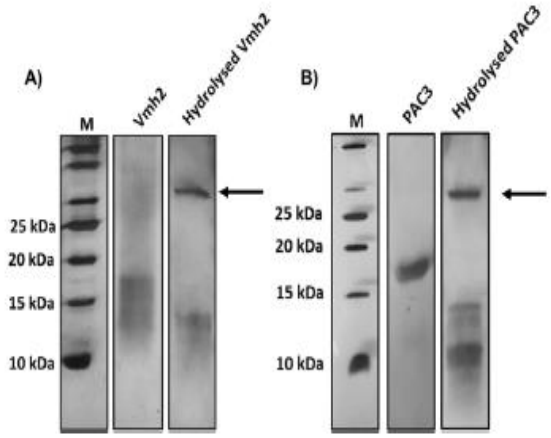

Figure S6. SDS-PAGE before (first lane) and after hydrolysis (second lane) of Vmh2 (A) and Pac3 (B) with Proteinase K, indicated in the figure by the arrows.

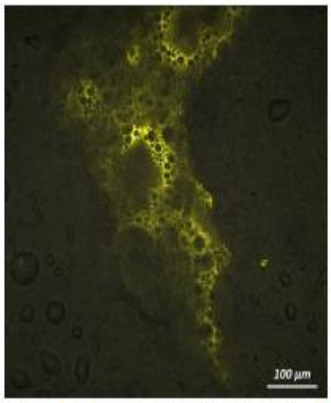

Figure S7. Emulsions of PAC3 solution (0.05 mg/ml) containing 3µM ThT mixed with Dectol (2:1 v/v), analysed by confocal laser microscopy. Image was acquired depositing the foam on a glass slide and drying at RT.

Applied Microbiology and Biotechnology

Supplementary Information

IDENTIFICATION OF A SMALL CYS-RICH PROTEIN FROM *FUSARIUM SOLANI* AND THE ESSENTIAL ROLE OF ITS AGGREGATION FOR EMULSIFYING ABILITY

Rossana Pitocchi[1], Paola Cicatiello[1]*, Anna Illiano[1], Carolina Fontanarosa[1], Federica Spina[2], Giovanna Cristina Varese[2], Angela Amoresano[1], Alessandra Piscitelli[1], Paola Giardina[1]

[1]Department of Chemical Sciences, University of Naples Federico II, Via Cintia, 80126 Naples, Italy.
[2]Department of Life Sciences and Systems Biology, University of Turin, Viale P.A. Mattioli 25, 10125 Turin, Italy
*Correspondence: paola.cicatiello@unina.it; Tel. +3908174327

Table S.1: List of precursor ion, product ions, collision energy and declustering potential parameters for the analysis of the phenolic compounds using LC-MRM-MS/MS in negative (ESI-) ionization modes.

precursor	product	Dwell	Analyte	DP	CE
285.000	151.000	50.0	Kaempferol	-86.000	-28.000
285.000	92.800	50.0	Kaempferol	-86.000	-28.000
285.000	133.000	50.0	Kaempferol	-60.000	-28.000
242.800	158.900	50.0	Piceatannol	-36.000	-38.000
242.800	201.000	50.0	Piceatannol	-36.000	-38.000
431.000	268.700	50.0	Genistin	-86.000	-18.000
431.000	132.800	50.0	Genistin	-86.000	-18.000
609.000	301.000	50.0	Rutin	-60.000	-30.000
609.000	299.800	50.0	Rutin	-61.000	-50.000
609.000	270.900	50.0	Rutin	-61.000	-50.000
579.100	270.800	50.0	Naringin	-96.000	-56.000
579.100	150.800	50.0	Naringin	-96.000	-56.000
227.000	185.000	50.0	Resveratrol	-96.000	-32.000
227.000	143.000	50.0	Resveratrol	-96.000	-32.000
316.800	150.800	50.0	Myricetin	-56.000	-36.000
316.800	178.900	50.0	Myricetin	-56.000	-36.000
286.800	150.700	50.0	Eriodictyol	-31.000	-22.000
286.800	134.900	50.0	Eriodictyol	-31.000	-22.000
356.900	82.900	50.0	Matairesinol	-31.000	-36.000
356.900	137.000	50.0	Matairesinol	-31.000	-36.000
301.000	252.900	50.0	Enterodiol	-56.000	-26.000
301.000	106.000	50.0	Enterodiol	-56.000	-26.000
300.900	150.900	50.0	Quercetin	-56.000	-32.000
300.900	178.600	50.0	Quercetin	-56.000	-32.000
284.900	174.900	50.0	Cyanidin	-61.000	-32.000
284.900	240.800	50.0	Cyanidin	-61.000	-32.000
285.000	132.900	50.0	Luteolin	-61.000	-46.000
285.000	150.900	50.0	Luteolin	-61.000	-46.000
285.000	217.000	50.0	Luteolin	-60.000	-46.000
285.000	199.000	50.0	Luteolin	-60.000	-46.000
296.900	106.900	50.0	Enterolactone	-46.000	-46.000
296.900	253.000	50.0	Enterolactone	-46.000	-46.000
288.800	245.000	50.0	Catechin	-71.000	-22.000
288.800	108.900	50.0	Catechin	-71.000	-22.000
166.600	123.100	50.0	Vanillic acid	-61.000	-18.000
166.600	107.800	50.0	Vanillic acid	-61.000	-18.000
178.700	107.200	50.0	Caffeic acid	-21.000	-22.000
288.800	244.800	50.0	Epicatechin	-76.000	-22.000
288.800	109.100	50.0	Epicatechin	-76.000	-22.000
300.900	256.700	50.0	Delphinidin	-51.000	-20.000

300.900	190.800	50.0	Delphinidin	-51.000	-20.000
268.800	240.900	50.0	Pelargonidin	-61.000	-26.000
268.800	200.700	50.0	Pelargonidin	-61.000	-26.000
163.000	162.000	50.0	transpCoumaric acid	-35.000	-20.000
163.000	119.000	50.0	transpCoumaric acid	-35.000	-20.000
300.800	163.900	50.0	Haesperetin	-51.000	-34.000
300.800	150.900	50.0	Haesperetin	-51.000	-34.000
268.600	132.900	50.0	Genistein	-101.000	-44.000
268.600	159.000	50.0	Genistein	-101.000	-44.000
267.000	210.900	50.0	Coumestrol	-81.000	-38.000
267.000	238.800	50.0	Coumestrol	-80.000	-44.000
268.800	116.900	50.0	Apigenin	-46.000	-44.000
268.800	150.800	50.0	Apigenin	-45.000	-30.000
266.800	251.700	50.0	Formonetin	-91.000	-30.000
266.800	222.800	50.0	Formonetin	-90.000	-28.000
282.800	267.500	50.0	Glycitein	-101.000	-28.000
282.800	240.000	50.0	Glycitein	-100.000	-32.000
282.900	267.800	50.0	Biochanin A	-76.000	-28.000
282.900	238.800	50.0	Biochanin A	-76.000	-28.000
254.900	239.900	50.0	Pterosilbene	-31.000	-28.000
449.000	431.000	50.0	luteolin6cglucoside (ISOORIENTIN)	-60.000	-30.000
449.000	285.000	50.0	luteolin6cglucoside (ISOORIENTIN)	-60.000	-30.000
449.000	377.000	50.0	luteolin6cglucoside (ISOORIENTIN)	-60.000	-30.000
431.000	311.000	50.0	Apigenin8cglucoside (VITEXIN)	-55.000	-30.000
431.000	269.000	50.0	Apigenin8cglucoside (VITEXIN)	-55.000	-30.000
431.000	341.000	50.0	Apigenin8cglucoside (VITEXIN)	-55.000	-30.000
464.000	301.000	50.0	Quercetin3Ogalactoside	-60.000	-38.000
464.000	463.000	50.0	Quercetin3Ogalactoside	-60.000	-38.000
594.000	593.000	50.0	kaempferol3Orutinoside	-65.000	-45.000
594.000	285.000	50.0	kaempferol3Orutinoside	-65.000	-45.000
316.000	300.000	50.0	Isorhamnetin	-60.000	-30.000
316.000	151.000	50.0	Isorhamnetin	-60.000	-30.000
316.000	315.000	50.0	Isorhamnetin	-60.000	-30.000
538.000	537.000	50.0	Amentoflavone	-60.000	-40.000
538.000	375.000	50.0	Amentoflavone	-60.000	-40.000
353.000	191.000	50.0	caffeoylquinic acid derivative	-60.000	-30.000
353.000	179.000	50.0	caffeoylquinic acid derivative	-60.000	-30.000
609.000	463.000	50.0	quercetin rutinoside	-60.000	-30.000
609.000	300.000	50.0	quercetin rutinoside	-60.000	-30.000
505.000	463.000	50.0	Quercetin acetylhexoside	-60.000	-30.000
505.000	445.000	50.0	Quercetin acetylhexoside	-60.000	-30.000
183.000	169.000	50.0	methyl gallate	-60.000	-20.000
183.000	125.000	50.0	methyl gallate	-60.000	-20.000
593.000	425.000	50.0	EGCepicatechin dimer	-60.000	-30.000
197.000	169.000	50.0	ethyl gallate	-60.000	-20.000
197.000	125.000	50.0	ethyl gallate	-60.000	-20.000

729.000	577.000	50.0	Procyanidin dimer gallate	-60.000	-30.000
493.000	317.000	50.0	Myricetin3Oglucuronide	-40.000	-25.000
479.000	317.000	50.0	Myricetin3Oglucoside	-40.000	-25.000
441.000	289.000	50.0	EC3Ogallate	-60.000	-30.000
441.000	169.000	50.0	EC3Ogallate	-60.000	-30.000
389.000	227.000	50.0	cisresveratrol3Oglucoside	-40.000	-25.000
561.000	289.000	50.0	EfisetinidolEC isomer 2	-71.000	-22.000
561.000	273.000	50.0	EfisetinidolEC isomer 3	-71.000	-22.000
745.000	457.000	50.0	EGCEGC gallate	-60.000	-20.000
745.000	169.000	50.0	EGCEGC gallate	-60.000	-20.000
619.000	457.000	50.0	EGC gallate glucoside	-60.000	-20.000
619.000	305.000	50.0	EGC gallate glucoside	-60.000	-20.000
609.000	457.000	50.0	EGC digallate	-60.000	-20.000
609.000	305.000	50.0	EGC digallate	-60.000	-30.000
455.000	289.000	50.0	EC methyl gallate	-60.000	-30.000
455.000	183.000	50.0	EC methyl gallate	-60.000	-30.000
425.000	169.000	50.0	EAfzelechin gallate	-60.000	-30.000
715.000	563.000	50.0	Theaflavin gallate	-60.000	-30.000
715.000	545.000	50.0	Theaflavin gallate	-60.000	-30.000
867.000	715.000	50.0	Theaflavin diglallate	-60.000	-30.000
867.000	563.000	50.0	Theaflavin diglallate	-60.000	-30.000
563.000	545.000	50.0	Theaflavin	-60.000	-30.000
153.100	133.000	50.0	Protocatechuic Acid	-40.000	-20.000
153.100	109.000	50.0	Protocatechuic Acid	-40.000	-20.000
153.100	93.000	50.0	Protocatechuic Acid	-40.000	-20.000
353.300	191.000	50.0	Chlorogenic Acid	-50.000	-20.000
353.300	163.000	50.0	Chlorogenic Acid	-50.000	-20.000
353.300	145.000	50.0	Chlorogenic Acid	-50.000	-20.000
353.300	179.000	50.0	Chlorogenic Acid	-50.000	-30.000
353.300	135.000	50.0	Chlorogenic Acid	-50.000	-30.000
335.300	179.000	50.0	Caffeoyliquinic Acid Lactone	-60.000	-30.000
335.300	161.000	50.0	Caffeoyliquinic Acid Lactone	-60.000	-30.000
193.200	149.000	50.0	Ferulic Acid	-40.000	-20.000
193.200	134.000	50.0	Ferulic Acid	-40.000	-20.000
591.200	283.000	50.0	Linarin	-40.000	-18.000
591.200	447.000	50.0	Linarin	-40.000	-18.000
591.200	420.000	50.0	Linarin	-40.000	-18.000
415.400	295.000	50.0	Puerarin	-40.000	-30.000
415.400	325.000	50.0	Puerarin	-40.000	-30.000
415.400	399.000	50.0	Puerarin	-40.000	-45.000
415.400	381.000	50.0	Puerarin	-40.000	-45.000
299.300	284.000	50.0	Diosmetin	-40.000	-26.000
299.300	153.000	50.0	Diosmetin	-40.000	-26.000
299.300	201.000	50.0	Diosmetin	-40.000	-26.000
299.300	55.000	50.0	Diosmetin	-40.000	-26.000
769.700	768.000	50.0	Typhanoside	-40.000	-35.000

769.700	314.000	50.0	Typhanoside	-40.000	-35.000
447.400	327.000	50.0	Astragalin	-40.000	-35.000
447.400	284.000	50.0	Astragalin	-40.000	-35.000
163.200	147.000	50.0	Coumaric Acid	-40.000	-20.000
163.200	119.000	50.0	Coumaric Acid	-40.000	-20.000
163.200	91.000	50.0	Coumaric Acid	-40.000	-20.000
337.300	191.000	50.0	3PCoumaroylquinic Acid	-40.000	-30.000
337.300	163.000	50.0	3PCoumaroylquinic Acid	-40.000	-30.000
447.300	431.000	50.0	Orientin	-40.000	-30.000
447.300	413.000	50.0	Orientin	-40.000	-30.000
447.300	357.000	50.0	Orientin	-40.000	-30.000
447.300	285.000	50.0	Orientin	-40.000	-30.000
447.400	285.000	50.0	Luteolin7OGlucoside	-60.000	-30.000
447.400	153.000	50.0	Luteolin7OGlucoside	-60.000	-30.000
447.400	60.000	50.0	Luteolin7OGlucoside	-60.000	-30.000
577.500	270.000	50.0	Isorhoifolin	-60.000	-40.000
577.500	269.000	50.0	Isorhoifolin	-60.000	-40.000
577.500	45.000	50.0	Isorhoifolin	-60.000	-40.000
463.400	43.000	50.0	Hyperoside	-60.000	-38.000
463.400	301.000	50.0	Hyperoside	-60.000	-38.000
447.400	301.000	50.0	QuercetinORhamnoside	-60.000	-30.000
447.400	431.000	50.0	QuercetinORhamnoside	-60.000	-30.000
461.900	299.000	50.0	QuercetinOHexoside	-60.000	-30.000
593.500	285.000	50.0	Nicotinflorin	-60.000	-45.000
593.500	257.000	50.0	Nicotinflorin	-60.000	-45.000
593.500	449.000	50.0	Nicotinflorin	-60.000	-45.000
431.100	285.000	50.0	Kaempeferol3ORhamnoside	-60.000	-30.000
271.200	153.000	50.0	Naringenin	-60.000	-30.000
271.200	177.000	50.0	Naringenin	-60.000	-30.000
271.200	119.000	50.0	Naringenin	-60.000	-30.000
271.200	107.000	50.0	Naringenin	-60.000	-30.000
271.200	93.000	50.0	Naringenin	-60.000	-30.000
271.200	83.000	50.0	Naringenin	-60.000	-30.000
433.400	271.000	50.0	Naringenin7OGlucoside	-60.000	-20.000
433.400	295.000	50.0	Naringenin7OGlucoside	-60.000	-20.000
433.400	270.000	50.0	Naringenin7OGlucoside	-60.000	-20.000
579.500	271.000	50.0	Naringenin7ONeohesperidoside	-80.000	-35.000
579.500	459.000	50.0	Naringenin7ONeohesperidoside	-80.000	-35.000
623.500	314.000	50.0	Isorhamentin3ONeohesperidoside	-80.000	-43.000
179.200	67.000	50.0	Theobromine	-45.000	-30.000
179.200	109.000	50.0	Theobromine	-45.000	-30.000
179.200	83.000	50.0	Theobromine	-45.000	-30.000
179.200	69.000	50.0	Theobromine	-45.000	-30.000
179.200	138.000	50.0	Theobromine	-45.000	-30.000
193.200	109.000	50.0	Caffeine	-45.000	-30.000
193.200	123.000	50.0	Caffeine	-45.000	-30.000

193.200	153.000	50.0	Caffeine	-45.000	-30.000
193.200	60.000	50.0	Procynadin B2	-45.000	-22.000
135.200	54.000	50.0	Tetramethyl Pyrazine	-45.000	-22.000
135.200	80.000	50.0	Tetramethyl Pyrazine	-45.000	-22.000
135.200	121.000	50.0	Tetramethyl Pyrazine	-45.000	-22.000
135.200	96.000	50.0	Tetramethyl Pyrazine	-45.000	-22.000
121.200	54.000	50.0	Trimethyl Pyrazine	-45.000	-22.000
121.200	42.000	50.0	Trimethyl Pyrazine	-45.000	-22.000
121.200	39.000	50.0	Trimethyl Pyrazine	-45.000	-22.000
865.800	289.000	50.0	Procynadin C1	-45.000	-22.000
865.800	393.000	50.0	Procynadin C1	-45.000	-22.000
865.800	713.000	50.0	Procynadin C1	-45.000	-22.000
865.800	849.000	50.0	Procynadin C1	-45.000	-22.000
865.800	577.000	50.0	Procynadin C1	-45.000	-22.000
577.500	427.000	50.0	Procynadin B2	-45.000	-22.000
577.500	291.000	50.0	Procynadin B2	-45.000	-22.000
577.500	561.000	50.0	Procynadin B2	-45.000	-22.000
575.500	109.000	50.0	Proanthocyanidin A2	-45.000	-22.000
575.500	139.000	50.0	Proanthocyanidin A2	-45.000	-22.000
575.500	559.000	50.0	Proanthocyanidin A2	-45.000	-22.000
169.000	52.000	50.0	Gallic acid	-64.000	-45.000
169.000	125.000	50.0	Gallic acid	-64.000	-20.000
169.000	80.000	50.0	Gallic acid	-64.000	-30.000
169.000	126.000	50.0	Gallic acid	-49.000	-21.000
169.000	124.900	50.0	Gallic acid	-66.000	-20.000
169.000	106.800	50.0	Gallic acid	-66.000	-18.000

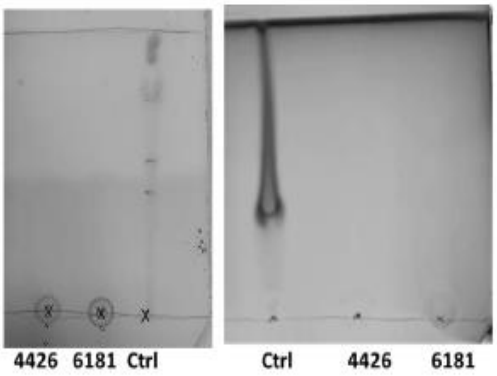

Figure S.1: TLC of the extracted broths, stained by Phosphomolybdic acid (10% w/v EtOH) for lipids detection on the right, and Sulfuric acid (3% v/v) for sugars detection on the left. Olive oil was used as a control in both experiments.

FS 4426		
Identified peptides	**Protein sequence coverage**	**Protein accession number**
K.TCTEANMFLCMCKIK.A	41%	C7Z2B1_NECH7 gi|302897631 **C7Z2B1**
K.IKALTLAYR.D		
K.DCACSSCLTPQSKLDAIATGK.D		
K.ALTLAYR.D		
K.ALTLAYRDCACSSCLTPQSK.L		
K.LDAIATGK.D		

FS 6181		
Identified peptides	**Protein sequence coverage**	**Protein accession number**
K. DICNQYQAPVAWLPDTCPA	47%	C7Z2B1_NECH7 gi|302897631 **C7Z2B1**
K. LDAIATGK.D		
K.DCACSSCLTPQSK.L		
K.ALTLAYR.D		

MKVSAFLSSVAVTLASIGSANAATPLCAITCFTAVMNHEAAKTCTEANMFLCM
CKIKALTLAYRDCACSSCLTPQSKLDAIATGKDICNQYQAPVAWLPDTCPA

Figure S.2: overview tables of the identified proteins in the two extracts, with the respective peptides, sequence coverage and UniProt accession number. Protein sequence is reported below tables; in yellow are highlighted the Cys typical of CFEM domain, in red the additional Cys.

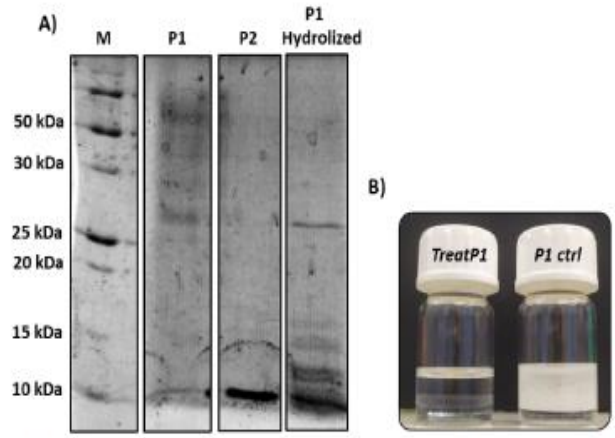

Figure S.3: A) SDS-PAGE of P1 after incubation with proteinase K (P1 hydrolized); P1 and P2 were loaded as controls. B) emulsion formed after (Treat P1) and before (P1 ctrl) hydrolysis with Proteinase K.

Table S.2: List of the polyphenols detected in the chromatographic peaks successive gel chromatography, with LC-MS/MS, MRM mode. The standard used to perform the quantitative analysis is gallic acid.

	P1	P2	P3
Poliphenol	ug/L		
Kaempferol	12.37	8.34	nd
Rutin	8.45	5.59	13.37
Quercetin	7.95	2.21	78.37
Cyanidin	8.84	0.36	177.9
Luteolin	41.64	2.91	23.75
Delphinidin	nd	nd	363.64
Pelargonidin	nd	nd	nd
Haesperetin	5.52	1.62	46.65
luteolin6cglucoside (ISOORIENTIN)	8.29	6.63	150.42
Quercetin acetylhexoside	2.64	2.09	15.35
EGCEGC gallate	0.06	0.86	2.88
EGC gallate glucoside	0.69	0.37	5.58
Theaflavin gallate	1.04	0.95	17.89
Theaflavin diglallate	2.03	1.35	9.15
Chlorogenic Acid	6.77	34.31	617.9
Linarin	2.24	1.66	10.5
Diosmetin	2.03	6.09	226.72
3P-Coumaroylquinic Acid	nd	nd	128.45
Orientin	nd	1.5	27.47
Luteolin$_7$O-Glucoside	3.13	1.35	nd
Nicotinflorin	0.61	0.31	22.19
Naringenin	9.3	32.27	5645.34
Naringenin$_7$O-Glucoside	nd	1.29	19.75
Procynadin C_1	4.42	3.1	4.65
Proanthocyanidin A_2	0.74	0.55	3.01

Identified peptides	Sequence coverage	Unique peptides	Score sequest
LDAIATGKDICNQYQAPVAWLPDTCPA	58%	7	33.05
DCACSSCLTPQSK			
TCTEANMFLCMCK			
ALTLAYRDCACSSCLTPQSK			
LDAIATGK			
ATLAYR			
DICNQYQAPVAWLPDTCPA			

Identified peptides	Sequence coverage	Unique peptides	Score sequest
TCTEANMFLCMCK	40%	6	51.65
ALTLAYRDCACSSCLTPQSK			
TCTEANMFLCMCK			
DCACSSCLTPQSK			
DCACSSCLTPQSKLDAIATGK			
LDAIATGK			
ALTLAYR			

Figure S.4: identification of proteins presents in P2*, after anionic exchange. The same protein initially identified, C7Z2B1, was found within two independent experiments, with a good sequence coverage and number of peptides.

(TO BE SUBMITTED TO ACS APPLIED BIOMATERIALS)

ANTIMICROBIAL FUNCTIONALIZATION OF SURFACES BY A CHIMERIC ADHESIVE PROTEIN

Pitocchi Rossana[a], Pennacchio Anna[a], Zuber Flavia[b], Ren Qun[b], Notomista Ennio[a], Campioni Silvia[c], Nystrom Gustav[c], Giardina Paola[a], Piscitelli Alessandra[a].*

AUTHOR ADDRESS

[a]Department of Chemical Sciences, University of Naples Federico II, Napoli, Italy

[b] Laboratories for Materials Science and Technology, St. Gallen

[c] Department of Biology, University of Naples Federico II, Napoli, Italy

[d] Laboratory for Cellulose and Wood Materials, Empa, Dübendorf, Switzerland

SUPPORTING INFORMATION.

1 table

5 figures

Table S1. Immobilization yield of Vmh2-GKY20 on polystyrene multiwell.

Number of depositions		Amount of deposited protein (µg)	Amount of bounded protein (µg)	Immobilization yield(%)
1		**10**	**5±1**	**54±9**
2	first		4.0±1.0	
	second		7.0±1.0	
	total	**20**	**11±1**	**53±6**
1		**20**	**12±1**	**58±4**
2	first		10±1	
	second		14±1	
	total	**40**	**24±1**	**60±3**
1		**30**	**16.0±0.8**	**53±3**
2	first		11±1	
	second		21±1	
	total	**60**	**32±2**	**52±4**

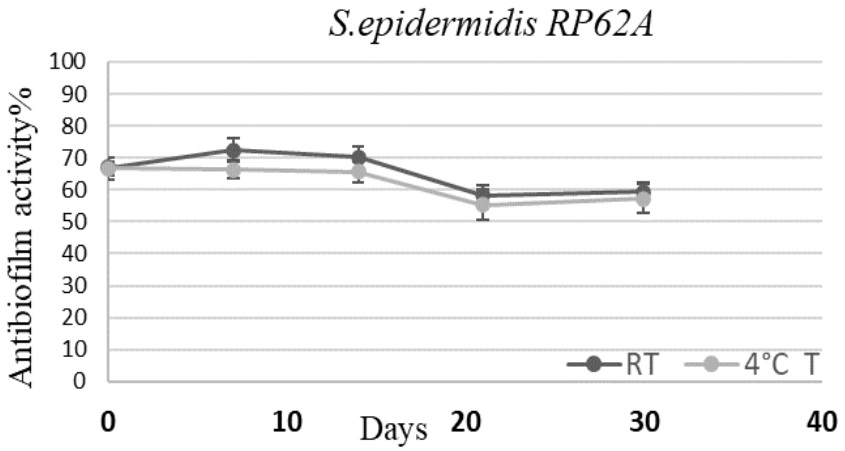

Figure S.1: Antibiofilm activity tested at different time intervals on plates functionalized with Vmh2-GKY20 and incubated at 4 ºC and room temperature (RT).

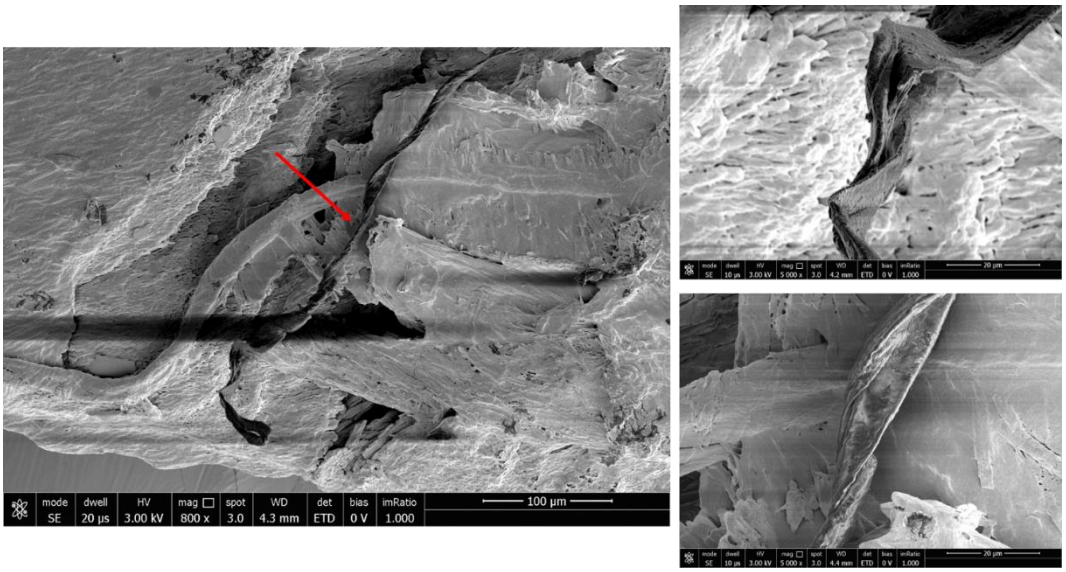

Figure S.2: SEM images of Vmh2-GKY20 fibril formed on BCps functionalized in 7 µM protein solution. The red arrow points the fibril observed, two different details of the fibril, at different magnification are reported on the right.

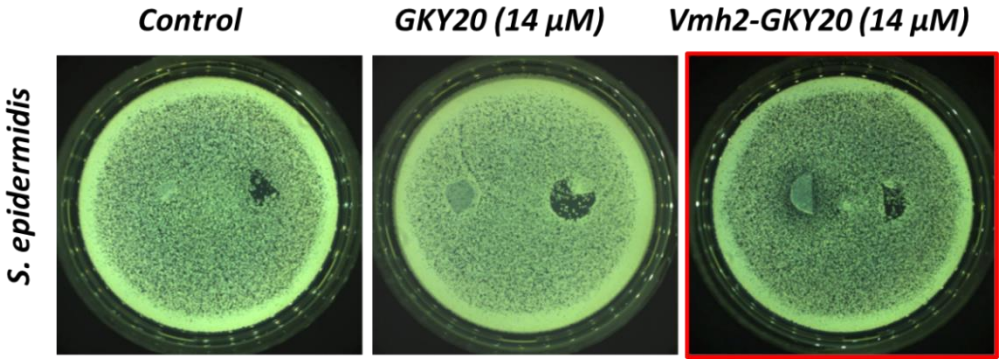

Figure S.3: Diffusion (left) and touch (right) assays against *S. epidermidis* for BCPs functionalized with fusion protein and the peptide GKY20, using the same initial molar concentration 14 µM. Control is untreated BCps.

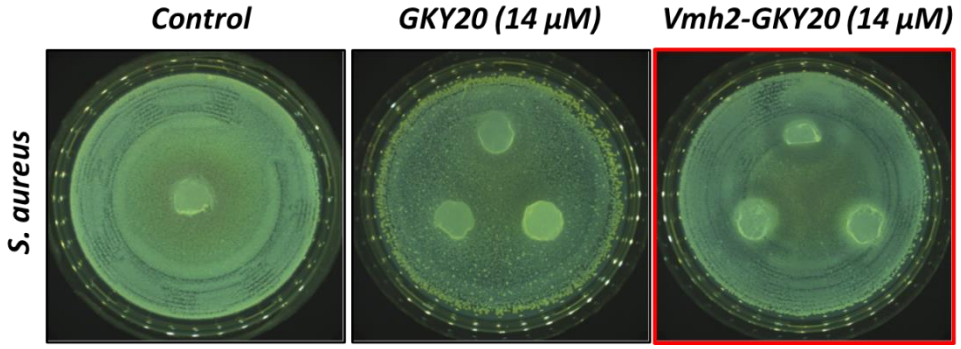

Figure S.4: Diffusion assays against *S. aureus* for BCPs functionalized with fusion protein and the peptide GKY20, using the same initial molar concentration 14 µM. Control is untreated BCps.

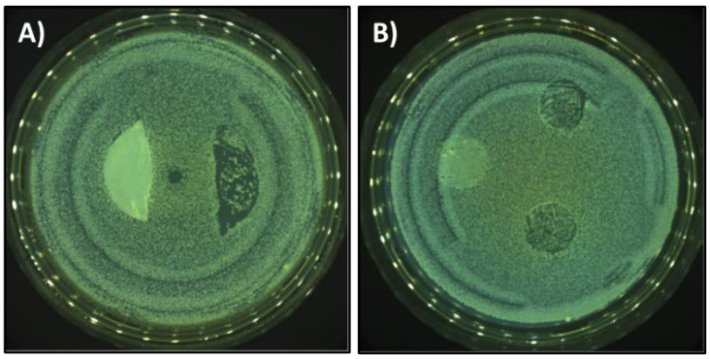

Figure S.5: Diffusion and touch tests against *S. aureus* for untreated BCp (A) and those functionalized with 14 µM of native Vmh2 (B). Samples on the left, diffusion test; samples on the right, touch test.

International Journal of
Molecular Sciences

MDPI

Article

Cerato-Platanins from Marine Fungi as Effective Protein Biosurfactants and Bioemulsifiers

Rossana Pitocchi [1], Paola Cicatiello [1], Leila Birolo [1], Alessandra Piscitelli [1], Elena Bovio [2], Giovanna Cristina Varese [2] and Paola Giardina [1,*]

[1] Department of Chemical Sciences, University of Naples Federico II, Via Cintia, 80126 Naples, Italy; rosspitocchi@gmail.com (R.P.); p.cicatiello@gmail.com (P.C.); birolo@unina.it (L.B.); apiscite@unina.it (A.P.)
[2] Department of Life Sciences and Systems Biology, University of Turin, viale P.A. Mattioli 25, 10125 Turin, Italy; elena.bovio@unito.it (E.B.); cristina.varese@unito.it (G.C.V.)
* Correspondence: giardina@unina.it; Tel.: +39-081-674319

Received: 3 March 2020; Accepted: 20 April 2020; Published: 21 April 2020

check for updates

Abstract: Two fungal strains, *Aspergillus terreus* MUT 271 and *Trichoderma harzianum* MUT 290, isolated from a Mediterranean marine site chronically pervaded by oil spills, can use crude oil as sole carbon source. Herein, these strains were investigated as producers of biosurfactants, apt to solubilize organic molecules as a preliminary step to metabolize them. Both fungi secreted low molecular weight proteins identified as cerato-platanins, small, conserved, hydrophobic proteins, included among the fungal surface-active proteins. Both proteins were able to stabilize emulsions, and their capacity was comparable to that of other biosurfactant proteins and to commercially available surfactants. Moreover, the cerato-platanin from *T. harzianum* was able to lower the surface tension value to a larger extent than the similar protein from *A. terreus* and other amphiphilic proteins from fungi. Both cerato-platanins were able to make hydrophilic a hydrophobic surface, such as hydrophobins, and to form a stable layer, not removable even after surface washing. To the best of our knowledge, the ability of cerato-platanins to work both as biosurfactant and bioemulsifier is herein demonstrated for the first time.

Keywords: cerato-platanin; surface tension; foam stabilizer; surface coating; hydrophobin

1. Introduction

Marine fungi (MF) have been recognized as a diverse group and an excellent source of natural products. Obligate MF grow and sporulate exclusively in sea water and their spores are capable of germinating in sea water. On the other hand, facultative MF have undergone physiological adaptations to live either in fresh water or terrestrial environment that allow them to grow and possibly also sporulate in the marine environment [1]. MF grow in stressful habitats, such as under cold, lightless and high-pressure conditions or in association with other organisms, sometimes even in oil-spill polluted site. In order to survive in different environmental conditions, they produce many interesting secondary metabolites, with relevant bioactivities, making them attractive in different application fields [2].

Our oceans, seas and coastal zones are under great stress and pollution, particularly because of crude oil, which is a major threat to the sustainability of the planet. However, the presence of crude oil in the environment for millions of years have led to the evolution of many microorganisms able to activate their metabolism to use it as a major or sole source of carbon and energy [3]. The study of these microorganisms is gaining more and more interest in the last decades, in view of developing a completely environmentally friendly bioremediation. In this respect, the Mycotheca Universitatis Taurinensis (MUT) studied the fungal community from a Mediterranean marine site chronically

pervaded by oil spills. Some of the fungal isolates were able to use crude oil as their sole carbon source, and *Aspergillus terreus* MUT 271, and *Trichoderma harzianum* MUT 290 were selected because they could represent potential bioremediation agents with strong crude oil degrading capabilities [4].

Many microorganisms have developed mechanism to access hydrocarbons more easily. One way is to increase the bioavailability of these compounds through the production of biosurfactants (BS) [5,6]. BS-producing microorganisms are ubiquitous, inhabiting water (sea, fresh water, groundwater) and land, as well as extreme environments (e.g., oil reservoirs), and thriving at a wide range of temperatures, pH values and salinity. BS offer significant industrial advantages over chemical surfactants thanks to lower toxicity, higher biodegradability, extreme temperatures, varying pH and salinity resistance. They are known to lower the surface and interfacial tension between different phases, possessing a low critical micelle concentration (CMC) and allowing the formation of stable emulsions. Bioemulsifiers (BE) are usually higher in molecular weight than BS as they are complex mixtures of heteropolysaccharides, lipopolysaccharides, lipoproteins and proteins. They can efficiently emulsify immiscible liquids even at low concentrations and thus they possess a good emulsifying activity, but are less effective at surface tension reduction, hence they show a low surface activity [7].

Among the high-molecular weight BS, hydrophobins (HFBs), self-assembling proteins typical of filamentous fungi, are described as the most powerful surface-active proteins. HFBs are small (about 100 amino acids) amphiphilic proteins that play multiple biological roles in fungal biology, lowering the surface tension of the liquid medium in their soluble form and coating aerial structures such as hyphae, fruiting bodies and spores for their easy growth and dispersal in the air, for fungal adhesion to surfaces and host-pathogen interactions [8,9].

Cerato-platanins (CP) are another class of fungal proteins known as surface-active biomolecules [10]. They are small (about 120 amino acids) cysteine-containing proteins (two disulfide bonds), released into the culture filtrate, but also found in the cell wall of fungal hyphae and spores. CP proteins constitute a well-conserved family, with a 70% similarity at some conserved motifs [11]. Similar to HFBs, their solutions lead to strong foam formation and they self-assemble at hydrophobic:hydrophilic interfaces into ordered, amphipathic layers [12,13]. However, they are not HFB-like proteins, and some studies indicated that their behavior is opposite to that of HFBs, i.e., it has been reported that the CP EPL1 from *Trichoderma atroviride* increased the polarity of solutions and surfaces [12,14]. Moreover, structural analysis of CP from *Ceratocystis platani* revealed that there are significant structural differences between CPs and HFBs, i.e., the surface of the molecule shows no large hydrophobic patch [11]. On the other hand, the CP structure (a double ψβ-barrel fold with six β-strands and two α-helices) is homologous to the N-terminal domain of expansins, which are proteins associated with carbohydrate binding and loosening of the cellulose scaffolds in plant cell walls [15]. Expansins are mainly found in plants, where they have various roles in growth and developmental processes, beyond the cell wall-loosening activity. Their action was shown for the first time as a weakening activity on filter paper [16]. Similar to expansins, CPs are able to weaken cellulose substrate, disrupting its non-covalent bonds without any hydrolytic activity. This action could be useful to efficiently hydrolyze cellulosic substrates; in fact, cellulases must have complete access to the cellulose chains that are tightly packed [17]. However, gene knockout experiments have not yet permitted the identification of a clear biological function of CPs, and to date, it is not easy to answer the question of why fungi produce these proteins. CPs can act both as virulence factor and as elicitors. In some plant pathogenic fungi, CPs have been reported to act as phytotoxins inducing cell necrosis. On the other hand, beneficial fungi of the genus *Trichoderma* were shown to induce plant defense responses, activity known as eliciting activity [8,18]. However, the presence and abundant expression of CPs in fungi with all types of lifestyle suggests that the main biological functions are not solely related to fungal–plant interactions but to other, more general aspects of fungal growth.

In this work, we isolated the proteins secreted by *A. terreus* MUT 271 and *T. harzianum* MUT 290 using crude oil as sole carbon source, identified them as CPs (named *At*CP and *Th*CP, respectively) and characterized them for their biosurfactant properties.

2. Results

2.1. Fungal Growth in Oil as a Carbon Source and Protein Secretion

The marine strains *A. terreus* and *T. harzianum*, isolated from spill-oil polluted site, were grown in the presence of oil as the sole carbon source to induce the production of biosurfactants. Culture broths were depleted of high molecular weight proteins (>30 kDa), by simple ultrafiltration, and then concentrated and dialyzed in 10 mM sodium phosphate buffer pH 7.0. When the proteins secreted by the cultures grown in oil were analyzed by SDS PAGE, only one band was observed in both fungal samples (Figure 1). Otherwise, when the same procedure was applied to the cultural broths of the two fungi grown in rich medium, several protein bands were detected in both cases (Figure S1). Hence, analyses herein reported were performed on the homogeneous samples obtained from the oil supplemented cultures with the abovementioned procedures. The amount of proteins secreted as function of the salt concentration in the cultural broth was evaluated (Table S1 of Supplementary Materials), and the maximum protein yields (2.7 ± 0.3 and 1.7 ± 0.5 mg/L of cultural broth of *A. terreus* and *T. harzianum*, respectively) were obtained at 30 g/L of NaCl. At least three biological replicated were analyzed in each condition.

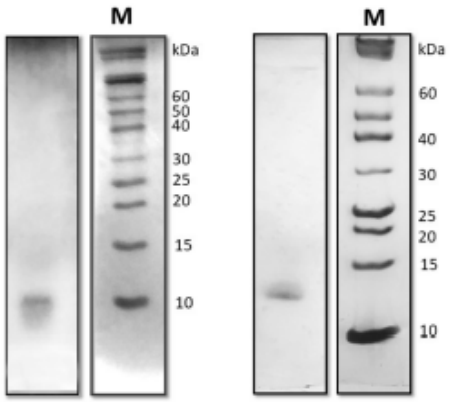

Figure 1. Silver stained SDS PAGE of proteins secreted by *T. harzianum* (left) and *A. terreus* (right) grown in the presence of 1% lampant oil as carbon source and 30 g/L NaCl (M: molecular weight markers).

The proteins obtained in these conditions from the marine strains of *T. harzianum* and *A. terreus* were named *Th*CP and *At*CP, respectively.

2.2. Emulsification Tests

To investigate the performances of these proteins as emulsifying agents, emulsification tests were performed using Dectol (a mix of Decane-Toluene 65:35, *v/v*), according the protocol of Blesic et al. [19]. The tests were carried out at two protein concentrations, 0.05 and 0.1 mg/mL. As negative control, a sample containing only phosphate buffer was used.

*At*CP showed an emulsification index E_{24} value slightly higher than *Th*CP (Figure 2) at the tested concentrations.

The protein nature of these BS was confirmed by incubation of the samples with proteinase K, since emulsification activity was quite lost after this treatment (Figure S2).

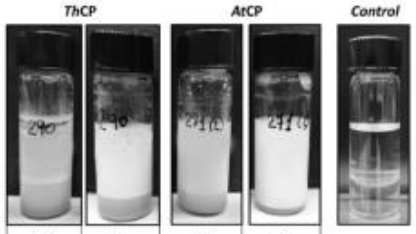

Protein Concentration (mg/ml)	0.05	0.1	0.05	0.1
E_{24}	44%	70%	56%	83%

Figure 2. Dectol emulsions at two different protein concentrations. *Th*CP and *At*CP solutions were mixed with Dectol (2:1 *v/v*) and analyzed after 24 h. Dectol emulsion with 10 mM Phosphate buffer, pH 7, is reported as control.

2.3. Protein Identification and Characterization

A proteomic approach was adopted to identify the isolated proteins. Only one protein band was visible in each of the SDS PAGE, and those bands were excised and submitted to a classical proteomic approach to identify the proteins. Only a single protein from *T. harzianum* and one from *A. terreus* could be confidently identified in the respective protein bands; therefore, these samples can be considered homogeneous, at least according to the commonly accepted criteria of protein purification assessment. The identified proteins are ascribed to the *Cerato Platanins* family (Table 1), classified as a group of extra-cellular, small cysteine-rich fungal proteins. This family is characterized by high hydrophobicity like HFBs. In addition, cysteines and tryptophans are reported to be essential for their functions, with the four conserved cysteines involved in the formation of two disulphide bridges and the tryptophan important for their eliciting ability [20].

Table 1. Proteins were identified by searching NCBI database with MSMS Ion search Mascot software (Matrix Science) with Fungi as the taxonomy restriction, with carboxyamidomethylation of Cys as fixed modifications, and oxidation on Met, pyro-Glu formation at Gln at the N-terminus of peptides as variable modifications.

Sample	Protein name[a,b] (Entry Code)	Family	Peptides (Ion Score)	Sequence Coverage (Number of Peptides)
T. harzianum	*Th*CP[a] SnodProt1[b] (gi|818166392)	Cerato-platanins	R.YHWSTQGQIPR.F (25)	45% (4)
			R.SLNVVSCSDGPNGLETR.Y (70)	
			R.FPYIGGVQAVAGWNSASCGTCWK.L (28)	
			R.VSATASQVAVK.N (57)	
A. terreus	*At*CP[a] allergen Asp f 15[b] (gi|115384120)	Cerato-platanins	K.LTYGGK.S (29)	31% (4)
			K.WPTPGSVPK.F (26)	
			R.VQATYQEVAK.S (54)	
			K.FPHIGGSPTIPGWNSPNCGK.C (35)	

Only proteins presenting two or more peptides, with at least one above the ion score threshold of 40 were considered as positively identified. Ion score was −10 log(P), where P is the probability that the observed match is a random event. Individual ion scores >40 indicated identity or extensive homology ($p < 0.05$). Peptides are reported with the flanking residues with dots to indicate tryptic cleavage sites. [a]name of the protein, herein attributed; [b]name of the identified protein.

Analysis of the circular dichroism (CD) spectra (Figure 3) showed that the two proteins exhibit different conformations. While the α-helix was the preponderant secondary structure in *At*CP (38% α-helix, 16% β-strands, 18% turns, 28% random coil), a higher percentage of β-structure (17% α-helix, 30% β-strands, 20% turns, 33% random coil) was observed in the case of *Th*CP. It is worth to note that the protein samples stored at 4 °C retained these conformations for at least one month.

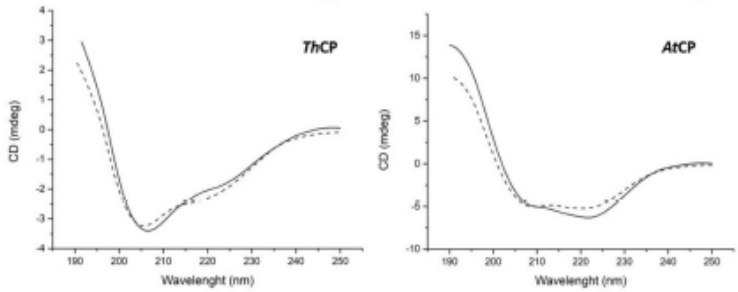

Figure 3. Circular dichroism (CD) spectra of CPs (0.05 mg/mL) from *T. harzianum* (*Th*CP) and from *A. terreus* (*At*CP) dissolved in 10 mM phosphate buffer pH 7. Dotted lines indicate CD spectra of the same samples acquired after 1 month of storage.

2.4. Surface Tension Measurements

The protein samples were diluted with 10 mM phosphate buffer, pH 7, at different concentrations, starting from the maximum concentration achievable, up to the γ value of the buffer used as reference. Indeed, at protein concentrations of *Th*CP higher than 0.10 mg/mL (7×10^{-6} M) and of *At*CP higher than 0.17 mg/mL (1×10^{-5} M), aggregation phenomena occur. In Figure 4, the surface tension trends as function of protein concentration (M) are shown.

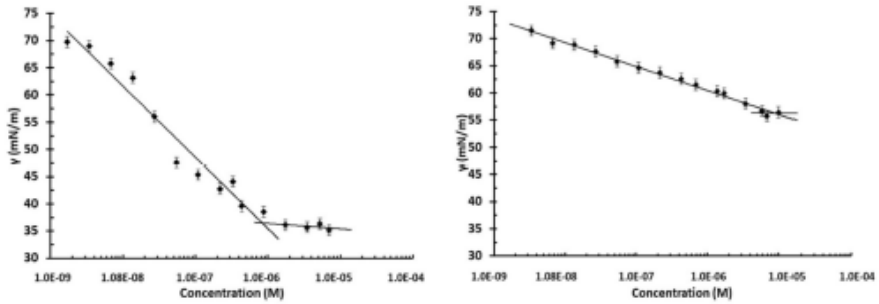

Figure 4. Surface tension of *Th*CP (left) and *At*CP (right) in 10 mM phosphate buffer pH 7, as a function of protein concentration.

A very low value of γ (36.4 mN/m) was observed in the case of *Th*CP with respect to that of *At*CP (56.3 mN/m). The critical micelle concentration (CMC), which indicates the minimum concentration of biosurfactant necessary to achieve the lowest stable surface tension, was 8×10^{-7} M (0.01 mg/mL) in the case of *Th*CP, significantly lower than the CMC of *At*CP (9×10^{-6} M, 0.12 mg/mL).

2.5. Cellulose Loosening

We tested the ability of both proteins to weaken cellulose, according to the protocol set up by Baccelli et al. [16]. The action of CPs on cellulose was clearly observable as turbidity increases because paper fragments are released from filter paper discs. In order to quantify solution turbidity, the absorbance at 500 nm of each sample was measured after three days of incubation at 37 °C. A solution containing bovine serum albumin (BSA) was used as control. Hence, *At*CP and *Th*CP were both able to weaken cellulose (Figure 5).

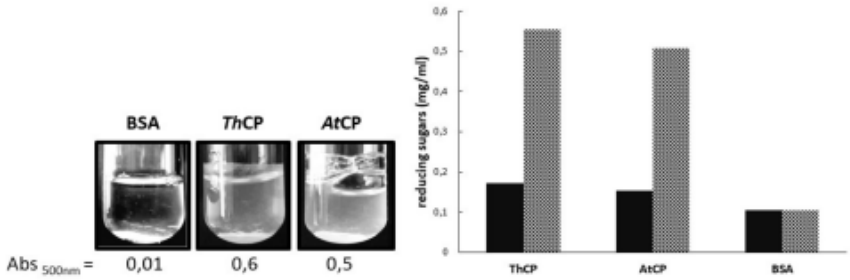

Figure 5. Left panel: protein samples (0.05 mg/mL), after incubation for three days at 37 °C in the presence of a paper disc, and the corresponding absorbance values at 500 nm. Right panel: concentration of reducing sugars (RS) measured for each sample. Continuous black columns: RS determined on the supernatants of the samples described above. Dashed columns: RS determined on the samples described above, further incubated with cellulase (1 U tot). 0.05 mg/mL. Bovine serum albumin (BSA) was used as reference.

To verify if the action of CPs on paper improved the availability of cellulose in solution, the amount of reducing sugars was measured in the supernatants of the CP samples incubated with paper. The increase of cellulose availability was measured using the DNS method. Figure 5 shows the amount of reducing sugars detected before and after cellulase treatment for both proteins. Both CPs were capable to triple the quantity of reducing sugars in solution, compared to the control.

2.6. Water Contact Angle (WCA) Measurement

CPs were deposited on hydrophobic surfaces (Teflon) and hydrophilic surfaces (glass) and WCA was analyzed after drying and phosphate buffer washing. The deposition on glass surface did not reveal significant changes of surface wettability. On the opposite, interesting results were obtained using the hydrophobic surface. When deposited on Teflon, both *Th*CP and *At*CP layers increased the wettability of the surface, as shown by the alteration of the water droplet shapes (Figure 6). The treatment of the plastic material was also resistant to extensive phosphate buffer washing.

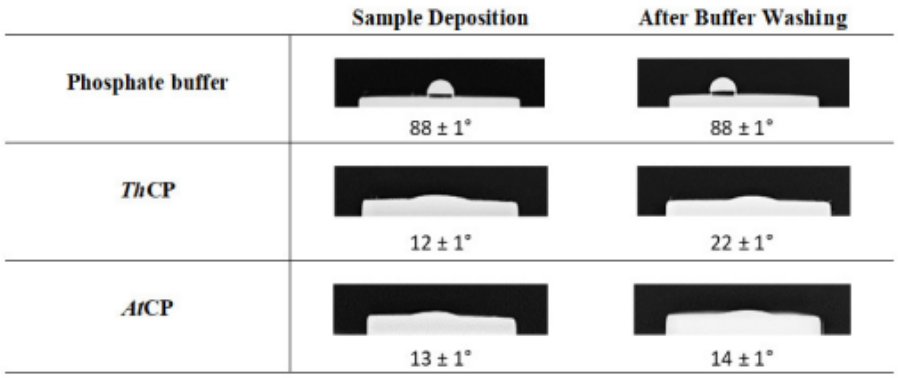

Figure 6. Water Contact Angle (WCA) analysis of hydrophobic surface (PTFE) upon deposition of CPs, before and after washing with 10 mM Phosphate buffer.

3. Discussion

In the search for new protein biosurfactants with improved performances with respect to the already known ones, the proteins secreted by marine fungi isolated in polluted sea by oil spills were analyzed. In particular, the strains *T. harzianum* MUT 290 and *A. terreus* MUT 271 [4], able to grow in the presence of crude oil as their sole carbon source were examined for protein biosurfactant production since this condition should induce the production of biosurfactants to solubilize organic molecules, as a necessary step in the metabolizing process of lipophilic molecules [6].

Previously, protocols were set up to isolate the most surface-active known proteins, the HFBs, from fungal culture broth [21]. When these protocols were herein used with culture broths of *T. harzianum* and *A. terreus*, only one secreted protein band could be detected by SDS PAGE in both cases, in which only one protein could be confidently identified. Then, a very simple protocol was adopted to obtain homogeneous samples of these proteins.

Generally speaking, high molecular weight BS, such as proteins, can be better defined as BE, being able to stabilize emulsions more than to reduce the surface tension of water [7,22]. Therefore, as a first approach, the ability of both proteins to stabilize emulsions was verified. Indeed, the obtained E_{24} values were comparable to those of other proteins and to commercially available surfactants analyzed in the same way [19,23].

Both these proteins were identified and ascribed to the family of cerato-platanins (CP): small, conserved, hydrophobic proteins, whose function is still a matter of debate. Even if CPs have been included among the fungal surface-active and surfactant proteins [10], to the best of our knowledge, no clear evidence of these activities has been reported thus far. As a matter of fact, Frischmann et al. [12] reported that the cultural broth of *T. atroviride* containing CP proteins produced a lot of stable foam, but no other analytical study on this CP characteristic was performed. We also analyzed the surface tension reduction of these CPs and unexpectedly observed that *Th*CP behaves as a good BS, beyond being a good BE. Indeed, the surface tension value reached in the presence of *Th*CP was much lower than those of *At*CP and of Sap-*Pc*, another BE protein recently purified from a marine strain of *Penicillium chrysogenum*, measured in comparable conditions [23].

Another issue concerned the ability of CPs to change the wettability of surfaces and the comparison of their behavior to that of HFBs. At first, CPs were described as a class of proteins like that of HFBs [24]; afterwards, Frishmann et al. [12] reported that CPs increased the polarity of surfaces rather than decreased it, differently from HFBs, whose layers inverted the wettability of surfaces. We analyzed the behavior of the two CPs using the same procedure adopted for HFBs [21] and observed that both CPs were able to make hydrophilic a hydrophobic surface, like the HFBs. They also formed a stable layer, which was not removed even after washing of the surface. The similar properties of the two classes of proteins, CPs and HFBs, are related to their common BS abilities, which should be the result of the presence of an exposed hydrophobic patch on the surface of the molecules, rendering them amphiphilic. However, while this characteristic was observed in the known three-dimensional structures of HFBs, it was not an evident feature of the structure of CP from *Ceratocystis platani* [15], and in the deposited structure of Sm1 (3M3G in Protein Data Bank) from *Trichoderma virens* [13], a protein whose sequence is 92.5% identical to SnodProt1, the protein we identified in *T. harzianum*, herein named *Th*CP. However, the exposure of a flexible and hydrophobic moiety of the protein molecule could also occur in the presence of hydrophobic/hydrophilic interfaces, and this could eventually be an alternative and plausible mechanism to interact with hydrophobic surfaces. It is also worth noting that the CD spectrum of *Th*CP is different from those reported for other CPs [25,26], thus suggesting that the *Th*CP structure is indeed consistently different from the other cases reported, at least in the conditions we tested.

As far as the comparison of CPs with HFBs is concerned, it was reported that some CPs form amyloid-like aggregates, but only under stress conditions [26,27]. In fact, *Th*CP and *At*CP do not show the same propensity to form amyloid-like fibrils as Class I HFBs, since the CD spectra of *Th*CP and

*At*CP were unchanged even after one month, differently from what occurs to Class I HFBs, which change their conformation after some days in mild conditions [28,29].

An extremely interesting feature of CPs is their ability to weaken cellulose, similar to another class of fungal proteins, the expansins [16]. We observed a remarkable cellulose loosening activity of both CPs, which allowed a much more effective attack of cellulase on its substrate, disrupting the ordered chains of cellulose and increasing its surface area. This feature allows to envisage other potential biotechnology applications of CPs, in addition to those related to their BS activity, such as, for example, in the pre-treatment of lignocellulose waste materials in bioconversion processes to biofuels.

In conclusion, we identified two CPs, secreted by marine fungi grown on oil as sole carbon source, and characterized them for their BE property. Notably, *Th*CP showed very good performance in reducing surface tension, thus possessing both surfactant and emulsifying activities, which can suggest, as with other BS and BE, its exploitation in a broad range of industrial application fields, such as medical, pharmaceuticals, food and beverages, cosmetics, agriculture, agrochemical, paint, detergent, textiles and petrochemical production.

4. Materials and Methods

4.1. Fungal Growth

MF strains were maintained through periodic transfer on agar plate at 20 °C, using XNST30 agar medium (malt extract 3 g/L; agar 15 g/L; yeast extract 3 g/L; NaCl 30 g/L; 10 g/L glucose and 5 g/L peptone) [21].

Mycelium disks (10 mm diameter) were taken from the margin of the actively growing colonies, and pre-inoculated in 100 mL flasks containing 50 mL of ONR7 mineral medium [30] supplemented with 10 g/L glucose, 2 g/L peptone, in triplicates and incubated at 28 °C for 5 days. Then, 50 mL of these pre-inoculum were inoculated in 1 L flasks containing ONR7 (500 mL) added with 1% *v/v* lampant oil and 0.1% *v/v* Tween 80. Lampant oil is a clear oil used to prevent corrosion to protect mechanical compounds of industrial and laboratory machines. It contains a rich hydrocarbon fraction that may be a suitable substrate for biosurfactant production. Flasks were inoculated in triplicates and incubated in the dark at 28 °C for 14 days.

4.2. Purification of the Proteins

Mycelia were separated from the culture broth using a Whatman 3MM paper filters (Termo Fischer Scientific, Rodano (MI), Italy). Culture broth was filtered using Stericup GP vacuum filtration system (0.22 µm pore size, Merck KGaA, Darmstadt, Germany), and biosurfactants were concentrated by air bubbling, using a Waring blender. The formed foam was separated and collected until further foam was not formed. The collected foam was loaded in an Amicon Ultrafiltration cell equipped with a 30 kDa cut-off PES Millipore Ultrafiltration Disc (Merck KGaA, Darmstadt, Germany). The ultrafiltrate, depleted of high molecular weight proteins (>30 kDa), was concentrated using the same cell equipped with a 3 kDa cut-off disc and dialyzed in 10 mM sodium phosphate buffer pH 7.0. Protein concentration was evaluated using the Pierce 660 nm Protein Assay kit (Termo Fischer Scientific, Rodano (MI), Italy) using bovine serum albumin as standard.

4.3. Emulsification Activity

The emulsification capability of samples was investigated at different protein concentrations. In the experiment, 2 mL of Dectol (a mix of Decane-Toluene 65:35, *v/v*) was added as emulsifying agent to 1 mL of each surfactant protein in 10 mM phosphate buffer (pH 7.0) in 5 mL glass vials [19]. This mixture was homogenized using the IKA T-10 Basic Ultra Turrax Homogenizer IKA-Werke GmbH, Staufen, Germany) for 2 min; then, the stability of the emulsions after 24 h was evaluated. The stability is reported in terms of emulsification index E_{24}:

$$E_{24} = \frac{height\ emulsion}{total\ height} \times 100$$

Proteins samples, 0.05 mg/mL, were incubated with Proteinase K (from *Tritirachium album*, Sigma-Aldrich, St. Louis, MO, USA) 1 mg/mL at 37 °C for 10 min. Then, an emulsification test was performed as described above.

4.4. Protein Identification by Mass Spectrometry

Protein identification was performed on Coomassie Blue stained bands excised from mono-dimensional SDS PAGE (15%). For each sample, 3 µg of proteins were treated with sample buffer containing 0.1 M DTT, and then, were further denatured, boiling them at 100 °C for 10 min.

Because these proteins are poorly stained with Coomassie Brilliant Blue, the samples were loaded in duplicates on the same gel and a set of samples was Coomassie stained, whereas the other set was analyzed by silver staining. By superimposing the Coomassie-stained and silver-stained protein bands, we localized the protein bands corresponding to the proteins of interest (apparent molecular mass between 12 and 17 kDa), which were excised from gel and processed as reported in Cicatiello et al. [23] on a 6520 Accurate-Mass Q-TOF LC/MS system (Agilent Technologies, Palo Alto, CA, USA) equipped with a 1200 HPLC system and a chip cube. The acquired MS/MS spectra were transformed in Mascot Generic Format (.mgf) and used to query the NCBI nonredundant (NR) database (http://www.ncbi.nlm.nih.gov), version 20160114, 79 354 501 sequences and 28 992 349 963 residues for "Fungi" as taxonomy restriction, for protein identification with a licensed version of MASCOT software (www.matrixscience.com) version 2.4.0, which was performed as previously described [25]. Only proteins presenting two or more peptides, with at least one above the ion score threshold of 40, were considered as positively identified. the ion score was −10 log(P), where P is the probability that the observed match is a random event. Individual ion scores >40 indicated the identity or extensive homology ($p < 0.05$).

4.5. Circular Dichroism (CD) Spectroscopy

CD spectra were recorded on a Jasco J715 spectropolarimeter (Jasco Corporation, Cremella (LC), Italy) equipped with a Peltier thermostatic cell holder in a quartz cell (0.1 cm light path) from 190 to 250 nm. The temperature was kept at 20 °C, and the sample compartment was continuously flushed with nitrogen gas. The final spectra were obtained by averaging three scans, using a bandwidth of 1 nm, a step width of 0.5 nm and a 4 s averaging per point. Secondary structure analysis of the collected CD data were processed by DichroWeb [31], using Selcon3 and ContiLL algorithms.

4.6. Surface Tension Measurement

The surface tension, γ, of the extracted proteins was measured with a Sigma 70 tensiometer (KSV, Stockholm, Sweden) using the Du Noüy ring method as described elsewhere [32]. The ring is submerged into the solution and then slowly pulled through the liquid–air interface to detach it from the interface, γ was correlated with the force required to raise the ring from the surface of the liquid–air interface. Aliquots of the proteins suspended in phosphate buffer pH 7.0 were prepared at different concentrations; each sample was filtered with a 0.22 µm filter before testing. In total, 7 mL of sample was added to the vessel, mixed using a magnetic stirrer and allowed to equilibrate 5 min prior to measuring the surface tension. Phosphate buffer 10 mM with surface tension of 72 mN/m was used to calibrate the tensiometer.

4.7. Cellulose Loosening and Cellulolytic Activity Assay

Whatman filter paper (3MM) was used as substrate to assay the CPs effect on cellulosic materials [16]. Five mm diameter paper disks were incubated in 1 mL of 10 mM phosphate buffer, pH 7.0, containing 0.05 mg/mL of CPs from *T. harzianum* and *A. terreus*. Bovine serum albumin (BSA) was used as negative control. The experiments were performed in Pyrex 20 mL glass culture tubes and

samples incubated at 37 °C, for 72 h, onto an orbital shaker at 320 rpm. At the end of the incubation period, disks were removed and the absorbance at 500 nm was measured, in order to quantify the turbidity of the obtained dispersion.

The presence of reducing sugars (RS) was verified using the dinitrosalicylic acid (DNS) method. The obtained dispersions were centrifuged (5 min at 5000 rpm). In total, 300 µL were directly tested with DNS; 300 µL was further incubated for 3 h at 37 °C, under agitation, 320 rpm, in the presence of 1 U of cellulase (≥0.3 units/mg solid, Sigma-Aldrich, St. Louis, MO, USA). After the addition of 300 µL of 1% DNS solution, all samples were incubated at 90 °C for 15 min, cooled at room temperature and the absorbance at 575 nm was then measured. The absorbance values were interpolated into a glucose calibration curve made in 10 mM sodium phosphate buffer (pH 7.0) to determine the concentration of reducing sugars. The reducing sugars released were then measured by the DNS method as previously described.

4.8. Water Contact Angle Determination

To test the ability of the proteins to self-assemble into a stable amphiphilic layer and to functionalize a solid surface, protein samples (50 µL of 0.05 mg/mL protein solution) were deposited on politetrafluoroetilene (PTFE) or glass, dried at 60 °C and washed with phosphate buffer. Drop shapes were modeled with the software program Image J (Rasband, W.S., ImageJ, U. S. National Institutes of Health, Bethesda, Maryland, USA, https://imagej.nih.gov/ij/, 1997-2018).

Supplementary Materials: Supplementary materials can be found at http://www.mdpi.com/1422-0067/21/8/2913/s1.

Author Contributions: Conceptualization P.G., G.C.V.; Data curation R.P. and P.C.; Investigation R.P., P.C., E.B. and L.B.; Writing—Original Draft Preparation, P.G.; Validation, A.P., L.B. and G.C.V.; Writing—Review and Editing, A.P., L.B., G.C.V. and P.G. All authors have read and agreed to the published version of the manuscript.

Funding: This research received no external funding.

Acknowledgments: These surface tension analyses were performed in collaboration with Gerardino D'Errico from the Department of Chemical Sciences, University of Naples Federico II, we gratefully acknowledge.

Conflicts of Interest: The authors declare no conflict of interest.

References

1. Raghukumar, C. Marine fungal biotechnology: An ecological perspective. *Fungal Divers.* **2008**, *31*, 19–36.
2. Amend, A.; Heitman, J.; Hom, E.F.Y.; Ianiri, G.; Jones, A.C.; Kagami, M.; Picard, K.T.; Quandt, C.A.; Raghukumar, S.; Riquelme, M.; et al. Fungi in the Marine Environment: Open Questions and Unsolved Problems. *Ecol. Evol. Sci.* **2019**, *10*, 1–15.
3. Mcgenity, T.J.; Folwell, B.D.; Mckew, B.A.; Sanni, G.O. Marine crude-oil biodegradation: A central role for interspecies interactions. *Aquat. Biosyst.* **2012**, *8*, 1–19. [CrossRef]
4. Bovio, E.; Gnavi, G.; Prigione, V.; Spina, F.; Denaro, R.; Yakimov, M.; Calogero, R.; Crisa, F.; Cristina, G. The culturable mycobiota of a Mediterranean marine site after an oil spill: Isolation, identification and potential application in bioremediation. *Sci. Total Environ.* **2017**, *576*, 310–318. [CrossRef]
5. Perfumo, A.; Smyth, T.J.P.; Marchant, R.; Banat, I.M. Production and Roles of Biosurfactants and Bioemulsifiers in Accessing Hydrophobic Substrates. In *Handbook of Hydrocarbon and Lipid Microbiology*; Timmis, K.N., Ed.; Springer-Verlag: Heidelberg, Germany, 2010; pp. 1501–1512.
6. Kubicki, S.; Bollinger, A.; Katzke, N.; Jaeger, K.; Loeschcke, A.; Thies, S. Marine Biosurfactants: Biosynthesis, Structural Diversity and Biotechnological Applications. *Mar. Drugs* **2019**, *17*, 408. [CrossRef]
7. Uzoigwe, C.; Burgess, J.G.; Ennis, C.J.; Rahman, P.K.S.M. Bioemulsifiers are not biosurfactants and require different screening approaches. *Front. Microbiol.* **2015**, *6*, 1–6. [CrossRef]
8. Lo, V.; Lai, J.I.; Sunde, M. Fungal Hydrophobins and Their Self-Assembly into Functional Nanomaterials. *Adv. Exp. Med. Biol.* **2019**, *1174*, 161–185.
9. Cicatiello, P.; Sorrentino, I.; Piscitelli, A.; Giardina, P. Spotlight on Class I hydrophobins: Their intriguing biochemical properties and industrial prospects. In *Grand Challenges In Funga IBiotechnology*; Nevalainen, H., Ed.; Springer Nature: Cham, Switzerland, 2020; pp. 333–348.

10. Sunde, M.; Pham, C.L.L.; Kwan, A.H. Molecular Characteristics and Biological Functions of Surface-Active and Surfactant Proteins. *Annu. Rev. Biochem.* **2017**, *86*, 585–608. [CrossRef] [PubMed]
11. Baccelli, I. Cerato-platanin family proteins: One function for multiple biological roles? *Front. Plant Sci.* **2015**, *5*, 2013–2016. [CrossRef] [PubMed]
12. Frischmann, A.; Neudl, S.; Gaderer, R.; Bonazza, K.; Zach, S.; Gruber, S.; Spadiut, O.; Friedbacher, G.; Grothe, H.; Seidl-seiboth, V. Self-assembly at Air/Water Interfaces and Carbohydrate Binding Properties of the Small Secreted Protein EPL1 from the fungus *Trichoderma atroviride*. *J. Biol. Chem.* **2013**, *288*, 4278–4287. [CrossRef] [PubMed]
13. Gaderer, R.; Bonazza, K. Cerato-platanins: A fungal protein family with intriguing properties and application potential. *Appl. Microbiol. Biotechnol.* **2014**, *98*, 4795–4803. [CrossRef]
14. Bonazza, K.; Gaderer, R.; Neudl, S.; Przylucka, A.; Allmaier, G.; Druzhinina, I.S. The fungal cerato-platanin protein EPL1 forms highly ordered layers at hydrophobic/hydrophilic interfaces. *Soft Matter* **2015**, *11*, 1723–1732. [CrossRef] [PubMed]
15. De Oliveira, A.L.; Gallo, M.; Pazzagli, L.; Benedetti, C.E.; Cappugi, G.; Scala, A.; Pantera, B.; Spisni, A.; Pertinhez, T.A.; Cicero, D.O. The Structure of the Elicitor Cerato-platanin (CP), the First Member of the CP Fungal Protein Family, Reveals a Double ψβ-Barrel Fold and Carbohydrate Binding. *J. Biol. Chem.* **2011**, *286*, 17560–17568. [CrossRef] [PubMed]
16. Baccelli, I.; Luti, S.; Bernardi, R. Cerato-platanin shows expansin-like activity on cellulosic materials. *Appl. Microbiol. Biotechnol.* **2014**, *98*, 175–184. [CrossRef] [PubMed]
17. Arantes, V.; Saddler, J.N. Access to cellulose limits the efficiency of enzymatic hydrolysis: The role of amorphogenesis. *Biotechnol. Biofuels* **2010**, *3*, 1–11. [CrossRef]
18. Djonovic, S.; Vargas, W.A.; Kolomiets, M.V.; Horndeski, M. A Proteinaceous Elicitor Sm1 from the Beneficial Fungus *Trichoderma virens* Is Required for Induced Systemic Resistance in Maize. *Plant Physiol.* **2007**, *145*, 875–889. [CrossRef]
19. Blesic, M.; Dichiarante, V.; Milani, R.; Linder, M. Evaluating the potential of natural surfactants in the petroleum industry: The case of hydrophobins. *Pure Appl. Chem.* **2017**, *90*, 305–314. [CrossRef]
20. Chen, H.; Kovalchuk, A.; Keriö, S.; Asiegbu, F.O.; Chen, H.; Kovalchuk, A.; Keriö, S.; Asiegbu, F.O. Distribution and bioinformatic analysis of the cerato-platanin protein family in Dikarya. *Mycologia* **2017**, *5514*, 1479–1488. [CrossRef]
21. Cicatiello, P.; Gravagnuolo, A.M.; Gnavi, G.; Varese, G.C.; Giardina, P. Marine fungi as source of new hydrophobins. *Int. J. Biol. Macromol.* **2016**, *92*, 1229–1233. [CrossRef]
22. Mujumdar, S.; Joshi, P.; Karve, N. Production, characterization, and applications of bioemulsifiers (BE) and biosurfactants (BS) produced by Acinetobacter spp.: A review. *J. Basic. Microbiol.* **2019**, *59*, 277–287. [CrossRef]
23. Cicatiello, P.; Stanzione, I.; Dardano, P.; De Stefano, L.; Birolo, L.; De Chiaro, A.; Monti, D.M.; Petruk, G.; D'Errico, G.; Giardina, P. Characterization of a Surface-Active Protein Extracted from a Marine Strain of *Penicillium chrysogenum*. *Int. J. Biol. Macromol.* **2019**, *20*, 3242. [CrossRef] [PubMed]
24. Pazzagli, L.; Cappugi, G.; Manao, G.; Camici, G.; Santini, A.; Scala, A. Purification, Characterization, and Amino Acid Sequence of Cerato-platanin, a New Phytotoxic Protein from *Ceratocystis fimbriata* f. sp. platani. *J. Biol. Chem.* **1999**, *274*, 24959–24964. [CrossRef] [PubMed]
25. Martellini, F.; Faoro, F.; Carresi, L.; Pantera, B. Cerato-Populin and Cerato-Platanin, Two Non-Catalytic Proteins from Phytopathogenic Fungi, Interact with Hydrophobic Inanimate Surfaces and Leaves. *Mol. Biotechnol.* **2013**, *55*, 27–42. [CrossRef] [PubMed]
26. Pazzagli, L.; Zoppi, C.; Carresi, L.; Tiribilli, B.; Sbrana, F.; Schiff, S.; Pertinhez, T.A.; Scala, A.; Cappugi, G. Characterization of ordered aggregates of cerato-platanin and their involvement in fungus–host interactions. *BBA-Gen. Subj.* **2009**, *1790*, 1334–1344. [CrossRef]
27. Barsottini, M.R.D.O.; Oliveira, J.F.; De Adamoski, D.; Teixeira, P.J.P.L.; Prado, P.F.V.; Tiezzi, H.O.; Sforça, M.L.; Cassago, A.; Oliveira, P.S.L.; De Zeri, A.C.D.M.; et al. Functional Diversification of Cerato-Platanins in Moniliophthora perniciosa as Seen by Differential Expression and Protein Function Specialization. *MPMI* **2013**, *26*, 1281–1293. [CrossRef]
28. Gravagnuolo, A.M.; Longobardi, S.; Luchini, A.; Appavou, M.; Stefano, L.; De Notomista, E.; Paduano, L.; Giardina, P. Class I Hydrophobin Vmh2 Adopts Atypical Mechanisms to Self-Assemble into Functional Amyloid Fibrils. *Biomacromolecules* **2016**, *17*, 954–964. [CrossRef]

29. Cicatiello, P.; Dardano, P.; Pirozzi, M.; Gravagnuolo, A.M.; Stefano, L.; De Giardina, P. Self-Assembly of Two Hydrophobins from Marine Fungi Affected by Interaction With Surfaces. *Biotechnol. Bioeng.* **2017**, *114*, 2173–2186. [CrossRef]
30. Dyksterhouse, S.E.; Gray, J.P.; Herwig, R.P.; Lara, J.C.; Staley, J.T. Hydrocarbon-Degrading Bacterium from Marine Sediments. *Int. J. Syst. Bacteriol.* **1995**, *45*, 116–123. [CrossRef]
31. Whitmore, L.; Wallace, B.A. Protein secondary structure analyses from circular dichroism spectroscopy: Methods and reference databases. *Biopolymers* **2007**, *89*, 392–400. [CrossRef]
32. Russo, L.; Imperatore, R.; Santis, A.; De Luchini, A.; Paduano, L.; Errico, G.D. Structure and dynamics of cetyltrimethylammonium chloride-sodium dodecylsulfate (CTAC-SDS) catanionic vesicles: High-value nano-vehicles from low-cost surfactants. *J. Colloid Interface Sci.* **2017**, *501*, 112–122. [CrossRef]

Journal of proteome research

pubs.acs.org/jpr

Article

Proteomic Characterization of Collagen-Based Animal Glues for Restoration

Georgia Ntasi, Sara Sbriglia, Rossana Pitocchi, Roberto Vinciguerra, Chiara Melchiorre, Laura Dello Ioio, Giancarlo Fatigati, Emanuele Crisci, Ilaria Bonaduce, Andrea Carpentieri, Gennaro Marino, and Leila Birolo*

Cite This: J. Proteome Res. 2022, 21, 2173–2184

Read Online

ACCESS | Metrics & More | Article Recommendations | Supporting Information

ABSTRACT: Animal glues are widely used in restoration as adhesives, binders, and consolidants for organic and inorganic materials. Their variable performances are intrinsically linked to the adhesive properties of collagen, which determine the chemical, physical, and mechanical properties of the glue. We have molecularly characterized the protein components of a range of homemade and commercial glues using mass spectrometry techniques. A shotgun proteomic analysis provided animal origin, even when blended, and allowed us to distinguish between hide and bone glue on the basis of the presence of collagen type III, which is abundant in connective skin/leather tissues and poorly synthetized in bones. Furthermore, chemical modifications, a consequence of the preparation protocols from the original animal tissue, were thoroughly evaluated. Deamidation, methionine oxidation, and backbone cleavage have been analyzed as major collagen modifications, demonstrating their variability among different glues and showing that, on average, bone glues are less deamidated than hide glues, but more fragmented, and mixed-collagen glues are overall less deamidated than pure glues. We believe that these data may be of general analytical interest in the characterization of collagen-based materials and may help restorers in the selection of the most appropriate materials to be used in conservation treatments.

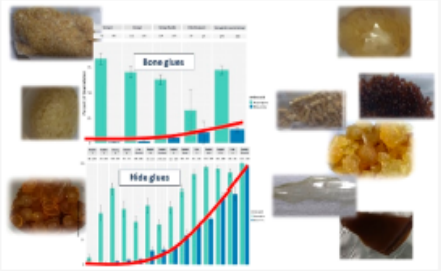

KEYWORDS: *animal glue, collagen, LC-MSMS, GC-MS, protein degradation, protein aging, deamidation, protein modification, proteomics*

INTRODUCTION

Animal glues are widely used in restoration, serving as adhesives, binders, coatings, and consolidants for organic and inorganic materials.[1,2] The term animal glue usually refers to an adhesive prepared from vertebrate connective tissues, namely, bones, skin/hide, or sinew. Upon treatment with acids or alkalis in hot water, the otherwise insoluble collagen, the main constituent protein of all these tissues, becomes soluble. The first archeological evidence of collagen-based coatings was identified in baskets from the Nahal Hemal cave (Israel, ca. 8200–7300 BC).[3] The earliest finding of animal-based adhesives in Europe dates back to the fourth millennium BC, when farmers in the Zurich area performed rudimentary chemical extractions to produce hide glue, most likely from the skins and other collagen-rich connective tissues of domestic cattle and ovicaprids.[4]

A simple procedure for making animal glue was reported in 2000 BC, while the first commercial glue factory was started in the 1700s in Holland, where animal glue was made from hides, and the first patent was issued for a fish glue in Britain about 50 years later.[2] Later on, there was a flourish of patents for glue recipes made from bones and skins of slaughtered animals, fish, starch, and milk.[5] Leather glues come from tannery waste, while bone glues are obviously made from animal bones. Fish glues are nonedible byproducts from fisheries such as skins, bones, cartilages, and swim bladders.

All animal glues are made from collagen. Collagen in its natural state is a triple helix protein and has the distinctive Gly–X–Y repetitive sequence and a unique high content of Pro and Hyp, making it easily recognizable in the protein universe. It is naturally insoluble in water, and it must be processed into soluble gelatin to be used as animal glue.

The performance of the glue depends on the original source of collagen but is also strongly influenced by the extraction and

Received: April 20, 2022
Published: August 15, 2022

https://doi.org/10.1021/acs.jproteome.2c00232
J. Proteome Res. 2022, 21, 2173–2184

preparation procedures, since both the specific sequence and the processing of the starting material affect the resistance of the polypeptide chains to hydrolysis and the (partial) denaturation of the triple helix that occurs upon heating in the gelatinization process.[5]

These factors have a significant influence on glue properties, in terms of viscosity, strength, and overall mechanical behavior.[6] The conservators' choice of commercial glue to use is primarily based on their empirical experience and often lacks a scientific characterization that could help them in making a properly informed decision.

In this regard, this paper aims to provide a diagnostic protocol that can be used to molecularly characterize commercial animal glues from different sources. With a variety of different animal glues on the market, such as hide and bone glues, fish glues, isinglass, and gelatin, their individual molecular properties must be well understood to link them to specific products. However, while the identification of collagen-based glues in artworks and their discrimination from other types of protein binders, such as milk and egg, for instance, can be easily performed based on the Gly, Pro, and Hyp peculiar high content,[7] unambiguous species determination is made difficult by the repetitiveness of the collagen sequence pattern and, more importantly, by the extreme sequence conservation. In addition, species identification becomes extremely challenging with samples containing multiple glues derived from different animals. It is also well-known that some suppliers provide rabbit glue mixed with bovine glue to alter its properties.[6] In this regard, proteomic analysis is the method of choice.

Proteomics is gaining momentum in the field of diagnostic tools for cultural heritage. Besides being of interest to art historians and archeologists in the characterization of materials and the state of conservation of artworks or archeological remains, it can also be useful to conservators during the selection of the most suitable materials to be used. Due to the high accuracy and sensitivity of mass spectrometry, proteomics has already been widely used for collagen analysis to discriminate bone fragments of different animal species[8−10] and to identify protein binders in paintings[11,12] and gilt samples.[13]

Moreover, proteomic analysis is extremely powerful in addressing the problem of characterizing the changes that occur during collagen degradation in animal glue because, as clearly stated by Schellmann,[6] during the extraction and preparation procedure, collagen chemistry can be significantly altered. Molecular weight distribution is certainly affected by preparation protocols, as is pI, which can be altered by extensive deamidation, one of the most common chemical modifications in damaged proteins.[14,15] What happens to collagen during glue preparation can therefore significantly affect the glue properties. Manufacturers tend to keep their recipes secret, and collagen-derived performance is therefore not easily predictable based on the label alone. Using a combination of mass spectrometric techniques (GC-MS, LC-MS/MS, and Py-GC-MS) and denaturing electrophoresis, we have provided extensive molecular characterization of a set of glue samples to give a broad picture in terms of constituent proteins and their modifications.

EXPERIMENTAL SECTION

Animal Glue Samples

A set of 19 animal glues provided by the restoration workshop of the University Suor Orsola Benincasa in Naples, and by Museo Nacional del Prado in Madrid, have been analyzed and characterized. The label of the samples along with a picture, their reported source, and new classification in **H**ide and **B**one, **P**ure and **M**ixed, and **F**ish **M**ixed on the basis of proteomic analysis herein carried out are reported in Table S1.

Gel Electrophoresis under Denaturing Conditions (SDS-PAGE)

Acid-soluble collagen (ASC) was extracted as reported in Hong et al 2017,[16] with slight modifications. Each animal glue sample (10 mg) was dissolved in a solution of acetic acid 0.5 M (1:10 w/v) under continuous stirring for 24 h. The solution was centrifuged at 10000*g* for 15 min at 4 °C. The supernatant, which consists of acid-soluble collagen (ASC), was collected and extensively dialyzed (10 kDa cut off) in a solution of ammonium bicarbonate 1.26 M at 4 °C for 24 h. pH was measured, verifying neutralization. Subsequently, 10 μL of each acid soluble collagen (ACS) fraction were diluted with 8 μL of sample buffer (65.8 mM Tris-HCl, pH 6.8, 2.1% SDS, 26.3% (w/v) glycerol, 0.01% bromophenol blue) containing 0.1 M DTT and heat denatured at 100 °C for 10 min. The samples were loaded onto a monodimensional SDS-PAGE (7%). To visualize the protein bands, gel was stained with Coomassie brilliant blue. Gel was then scanned with ChemiDoc MP imaging system (Bio-Rad).

Protein Extraction and Digestion

Samples were prepared as reported in ref 17. Briefly, 1−2 mg of each pellet was resuspended in 10 μL of 6 M urea. Samples were incubated for 20 min at room temperature and then for 30 min in the sonicator. Samples were then 6-fold diluted with 10 mM ammonium bicarbonate at pH 7.5, and enzymatic digestion was carried out by the addition of 1 μg of trypsin at 37 °C for 16 h. The supernatants were then recovered by centrifugation and filtered on 0.22 μm PVDF membrane (Millipore), and peptides were desalted and concentrated on in-house made C18 extraction stage tips as described by Cappellini et al.[18] Peptides were eluted with 20 μL of 50% acetonitrile and 0.1% formic acid in Milli-Q water and analyzed by LC-MS/MS.

LC-MS/MS

Samples were analyzed on a 6520 Accurate-Mass Q-Tof LC/MS System (Agilent Technologies, Palo Alto, CA, U.S.A.) equipped with a 1200 HPLC System and a chip cube (Agilent Technologies) as reported in ref 17. Samples were fractionated on a C18 reverse-phase capillary column (Agilent Technologies) at a flow rate of 400 nL/min, with a linear gradient of eluent B (0.1% formic acid in 95% acetonitrile) in A (0.1% formic acid in 2% aceto-nitrile) from 3% to 80% in 50 min. Peptide analysis was performed using data-dependent acquisition (DDA) of one MS scan (mass range from 300 to 2000 m/z) followed by MS/MS scans of the three most abundant ions in each MS scan. MS/MS spectra were measured automatically when the MS signal surpassed the thresh-old of 50 000 counts. Double and triple charged ions were preferably isolated and fragmented.

Alternatively, peptide fractionation was performed on LTQ Orbitrap XL Hybrid Ion Trap-Orbitrap MS System (Thermo Scientific, Bremen, Germany) on a C18 capillary reverse-phase

https://doi.org/10.1021/acs.jproteome.2c00232
J. Proteome Res. 2022, 21, 2173−2184

column (200 mm, 75 μm, 5 μm) at 250 nl min^{-1} flow rate, using a step gradient of eluent B (0.2% formic acid, 95% acetonitrile LC-MS grade) in eluent A (0.2% formic acid in 2% acetonitrile) from 5 to 50% over 80 min and to 80% over 5 min. Mass spectrometric analyses were performed using data-dependent acquisition (DDA) mode over the 400 to 1800 mz^{-1} range, at a resolution of 60 000, and the automatic gain control (AGC) target was set to 1×10^6, followed by acquisition in MS/MS of the five most abundant ions. For the MS/MS scans, the resolution was set to 15 000, the AGC target was set to 1×10^5, the precursor isolation width was 2 Da, and the maximum injection time was set to 500 ms. The CID normalized collision energy was 35%; AGC target was set to 1×10^5. Data were acquired by Xcalibur software (Thermo Fisher Scientific).

Protein Identification and Semiquantitative Evaluation of Chemical Modifications

MS/MS spectra were transformed in Mascot Generic files (.mgf) format and routinely used to query the SwissProt database 2015_04 (548 208 sequences; 195 282 524 residues), with Chordata as the taxonomy restriction for protein identification. A licensed version of MASCOT software (www.matrixscience.com) version 2.4.0 was used. Standard parameters in the searches were trypsin as the enzyme (semitrypsin when searching for backbone cleavages); 3, as the allowed number of missed cleavages; 10 ppm MS tolerance and 0.6 Da MS/MS tolerance; and peptide charge from 2+ to 3+. In all the database searches, no fixed chemical modification was inserted, but possible oxidation of methionine residues, deamidation at asparagines and glutamines, and hydroxylation on lysine and proline were considered as variable modifications. To reduce the search space and recover more focused results, ultimate searches were carried out using a homemade database, which we named COLLE (60 sequences; 88 859 residues), that collects the sequences of collagen type I and III for all the common domesticates generally used for animal glues). Mass spectrometry data and the COLLE database have been deposited to Mendeley Data (https://data.mendeley.com/datasets/hbmc8yhf7y/2).

Semiquantitative evaluation of deamidation was carried out by MaxQuant software.[19] Parameters common among all runs are as follows: tryptic search with up to two missed cleavages; minimum peptide length was set to 7; and no fixed modification was set, while oxidation of methionine, hydroxylation of proline and hydroxylation of lysine were set as variable modifications, with up to a maximum of 5 modifications per peptide. Protein identifications were supported by a false discovery rate (FDR) of 0.01 applied (same FDR for dependent peptides when applied) and manually filtered by at least 2 different nonoverlapping peptides above the 40 ion score threshold. Contaminant proteins were assessed using the contamination.fasta provided by MQ, which includes common laboratory contaminants (see MaxQuant Downloads -contaminants.fasta, can be found under http://www.coxdocs.org/doku.php?id=maxquant:start_downloads.htm, n.d). These protein hits were excluded from further analysis. After each run, the evidence file.txt of each animal glue was first cross validated for its peptides and proteins according to the protein identification that had already been performed with the use of Mascot. Afterward, the "evidence" files were used for the evaluation of deamidation (N, Q) level both in the total sample (global deamidation) and for the single polypeptide chain identified in each animal glue, with the public available software (https://github.com/dblyon/deamidation). The visualization of all deamidation plots was performed with the use of R studio.

Backbone cleavage evaluation was carried out by setting the same parameters as for standard protein identification as described above but "semitrypsin" as enzyme and an ion score cut off $\geq$ 25 for unmodified and modified peptides. The assessment of the occurrence of backbone cleavage was carried out by counting the PSMs (Peptide Spectrum Matches) in the single samples, focusing on Type I and Type III collagen chains only.

A site-specific evaluation of the deamidation (Asn, Gln) and oxidation (M) occurrence along the amino acidic sequence was performed by manually inspection of MS/MS data. The positions of Asn and Gln that were detected as unmodified were characterized as X; the positions that were found only deamidated as D; the position that were detected both as deamidated and unmodified as DX; and finally, the positions that were not detected at all, neither unmodified nor deamidated, as NF. Similarly, for the evaluation of oxidation, the detected oxidized positions were characterized as OX; those that have been detected as unmodified as X; and the nondetected as NF.

GC-MS Analysis of Proteins

Samples (1−5 mg) were subjected to acidic hydrolysis in the vapor phase assisted by microwaves, at 160 °C with 6 M hydrochloric acid, power of 350W, for 35 min. At the end of the hydrolysis, samples were reconstituted with 300 μL of double-distilled water. Then 2 μL of the water solution of amino acids was then added with 5 μL of a standard solution of norleucine (internal standard, 73.77 ppm), dried under nitrogen flow, and subjected to silylation with *N*-methyl-*N*-(tert-butyldimethylsilyl)trifluoroacetamide (MTBSTFA). Analyses were carried out with a 6890N GC System Gas Chromatograph (Agilent Technologies, Palo Alto, CA, U.S.A.), coupled with a 5975 Mass Selective Detector (Agilent Technologies, Palo Alto, CA, U.S.A.) a single quadrupole mass spectrometer, equipped with a PTV injector. Samples were analyzed in duplicates. Quantitation was performed though calibration curves working in the SIM mode. Details of the operating conditions are reported in the literature.[20]

Analytical Pyrolysis Coupled to GC-MS (Py-GC-MS)

Samples (ca. 100−200 μm) were subjected to flash pyrolysis at 550 °C for 0.2 min, and the interface temperature was 280 °C. The split/splitless injector was used at a 1:50 split ratio. The Pyrolyser was a Multi-Shot Pyrolyzer EGA/Py-3030D (Frontier Lab) coupled to a gas chromatograph 6890 coupled with a 5973 Mass Selective Detector Agilent Technologies (U.S.A.). Chromatographic and mass spectrometric conditions are reported in detail in the literature.[21] To assess the simultaneous presence of other organic components, analytical pyrolysis was also carried out with *in situ* silylation. Samples (ca. 100−200 μm) were admixed to 2 μL of hexamethyldisilazane in the cup before the pyrolysis, carried out at 550 °C, Py-GC interface set at 280 °C, pyrolysis time of 0.2 min.

■ RESULTS AND DISCUSSION

Protein Identification

Amino Acid Composition. The amino acid composition of the samples was determined by gas chromatography mass

https://doi.org/10.1021/acs.jproteome.2c00232
J. Proteome Res. 2022, 21, 2173−2184

spectrometry. The samples were first hydrolyzed, then silylated, and finally analyzed by GC-MS. The quantitative determination of amino acids was performed by building calibration curves using standard solutions and evaluating daily recoveries. SIM mode was used for the quantitation. The quantified amino acids were: Ala, Gly, Val, Leu, Ile, Met, Ser, Pro, Phe, Asp, Glu, Hyp and Tyr. The results are listed in Table S2 where, for the sake of homogeneity, samples are named following classification upon proteomic analysis results

Data clearly show that the amino acid composition of the different samples is extremely similar to one another, as expected from samples based on collagen. The average amino acidic profile, obtained averaging the amino acidic profiles of all the samples analyzed, is shown in Table 1, with the confidence interval ($\alpha = 0.05$).

Table 1. Average Amino Acidic Profile of All the Samples Analyzed and Relative Confidence Interval ($\alpha = 0.05$).

amino acid	relative content (%)	confidence interval
Ala	9.8	±0.4
Gly	27.6	±1.0
Val	2.4	±0.2
Leu	3.1	±0.2
Ile	1.5	±0.2
Met	0.6	±0.1
Ser	4.8	±0.5
Pro	16.2	±0.6
Phe	2.0	±0.1
Asp	7.5	±0.5
Glu	11.2	±0.7
Hyp	12.5	±1.2
Tyr	0.7	±0.4

As expected, Gly is the most abundant amino acid, followed by Pro and Hyp, and in general, very little variability is observed.

The amino acid profile of fish glue (FM) compared with all other glues, which are obtained from mammals, is interesting. Amino acids responsible for the formation of stabilizing H-bridges in the triple helix are more abundant in mammalian collagen than in that of marine species.[6] The FM sample has the lowest relative amount of polar amino acids (Pro, Hyp, Asp, Glu, Ser), whose total is around 45%, while all other glues have values between 50% and 55%.

Proteomics. Proteins were identified in the set of 19 animal glue samples by a shotgun proteomics approach by LC-MS/MS, allowing to molecularly establish the glue source as well as distinguishing between hide and bone glues (details in Tables S3−S21). Identification of collagen alpha-1(III) is indicative that the adhesive was produced from soft connective tissues and skin, as this molecule, together with collagen alpha-1 and −2(I) that are ubiquitous in all the collagen-bearing tissues, is abundant in these tissues, while it is poorly synthetized in bones.[22] While hide glues are primarily derived from bovine skins and smaller mammals, and sometimes connective tissue, bone glues are predominantly prepared with fresh or extracted bones (degreased and demineralized) from cattle and pigs.[6]

In a preliminary search in the SwissProt database with Chordata as taxonomic restriction, collagen type I was identified in all the samples and collagen type III in some of them, allowing therefore the classification of the samples in hide and bone proteins. It is worth noting that in the BM2 sample, bovine alpha S1 casein was confidently identified (Table S9), indicating the copresence of some milk glue. However, the overall amino acidic profile of this sample, together with the detection of only 3 peptides of alpha S1 casein, while all other milk proteins remained undetected, clearly suggests that the animal glue in BM2 is mainly collagen based.

A straightforward species determination of collagen is however hampered by several factors: the intrinsic simplicity of collagenic protein sequence (which is a hallmark of collagen); the extremely high sequence similarity among the species because of the high degree of evolutionarily conservation; protein sequences of some species of interest to conservation science are either missing in common databases or covered only partly. As a result, although assessing the presence of collagen is relatively easy, in some cases, the discrimination between two animal species (even i.e., between bovine and porcine collagen, for instance) could be quite challenging, since it relies only on the detection of a very few unique peptides.

To simplify species assignment, the search space was reduced to sequences of collagen type I and III of the common domesticates generally used for animal glues, and ultimate searches were carried out using a homemade database, which we named COLLE (60 sequences; 88 859 residues).

Identified collagen chains are summarized in table 2, and the details of protein identifications are provided in Tables S3−S21. Moreover, glues were classified as pure and mixed, when more than a single organism origin was clearly identified. As a result, 13 samples are hide glues (8 pure, HP, and 5 mixed, HM), and 5 are bone glues (all mixed, BM). No pure glue made from bone was identified, and, in our set, fish collagen was confidently identified only in a single sample (FM).

Although the label "rabbit glue", would suggest that rabbit skin glues should be produced purely from rabbit skins, we identified the collagen from *Oryctolagus cuniculus* only in five samples (HP1, HM2, HM3, HM4, and HM5), and actually only the sample originally labeled as *Rabbit glue* (SOB1), namely HP1, appears to be a truly pure rabbit glue. As reported by Schellmann,[6] suppliers might mix rabbit skin glue with bovine hide glue to alter its properties. All the claimed rabbit glues but HP1 contain some bovine and/or sheep collagen, and the sample HM5 contains mainly porcine glue. All the rabbit glues are hide glues since collagen type III was identified.

The samples tagged as bone glues were consistent with their labels since no collagen of type III was detected. Specifically, all of them are mixtures of bovine with porcine collagen, although in some cases, donkey collagen was also identified. Protein identification details of the single samples are reported in the Supplementary Information (Tables S3−S21).

Rather surprisingly, among the samples labeled as fish glues, only in *Sturgeon glue* did we identify some fish collagen, although not from a member of the Acipenseridae family (to which sturgeon species belong) but from the Scyliorhinidae family, as the confident identification of collagen type I *of Scyliorhinus canicula* suggests.

Following the identifications, samples were clustered and relabeled on the basis of the proteins content as Bone glues (B), Hide glues (H), and subdivided in Pure (P) and Mixed (M), as reported in Table 2.

https://doi.org/10.1021/acs.jproteome.2c00232
J. Proteome Res. 2022, 21, 2173−2184

Table 2. Collagen Chains Identified in the Animal Glue Samples by LC-MSMS[a]

sample	label on the basis of protein content[b]	taxonomy	collagen α1(I)	collagen α2(I)	collagen α1(III)
rabbit glue SOB1	HP1	*Oryctolagus cuniculus*	yes	yes	yes
rabbit glue SOB2	HP2	*Bos taurus*	yes	yes	yes
rabbit glue SOB3	HP3	*Bos taurus*	yes	yes	yes
rabbit glue SOB4	HP4	*Bos taurus*	yes	yes	yes
rabbit glue SOB5	HM1	*Bos taurus*	yes	yes	yes
		Sus scrofa	yes	yes	yes
rabbit glue 10	HP8	*Bos taurus*	yes	yes	yes
rabbit glue 2	HM2	*Oryctolagus cuniculus*	yes	yes	
		Ovis aries		yes	yes
		Capra hircus	yes		
rabbit glue 3	HM3	*Bos taurus*	yes	yes	yes
		Oryctolagus cuniculus	yes	yes	yes
		Ovis aries		yes	
rabbit glue 7	HM5	*Oryctolagus cuniculus*	yes		
		Sus scrofa	yes	yes	yes
rabbit glue 6	HM4	*Bos taurus*	yes	yes	yes
		Oryctolagus cuniculus	yes	yes	
fish glue SOB6	HP5	*Sus scrofa*	yes	yes	yes
fish glue 4	HP6	*Bos taurus*	yes	yes	yes
fish glue 5	HP7	*Bos taurus*	yes	yes	yes
sturgeon fish glue SOB7	FM	*Scyliorhinus canicula*	yes	yes	
strong glue SOB8	BM1	*Sus scrofa*	yes	yes	
		Bos taurus	yes	yes	
		Sus scrofa	yes	yes	
strong glue SOB9	BM2	*Bos taurus*	yes	yes	
		Sus scrofa	yes	yes	
		Equus asinus	yes	yes	
strong glue 8	BM4	*Bos taurus*	yes	yes	
		Sus scrofa	yes	yes	
		Equus asinus		yes	
strong glue 9	BM5	*Bos taurus*	yes	yes	
		Sus scrofa	yes		
		Ovis aries	yes	yes	
		Equus asinus	yes	yes	
strong glue 1	BM3	*Bos taurus*	yes	yes	
		Sus scrofa		yes	
		Equus asinus	yes	yes	

[a]Raw data were searched by Mascot MS/MS Ion search using the homemade COLLE database. Details of the identifications are reported in the Supporting Information. [b]Protein identification was used to classify glue samples as bone glues (B) and hide glues (H) and further subdivide them into pure (P) and mixed (M).

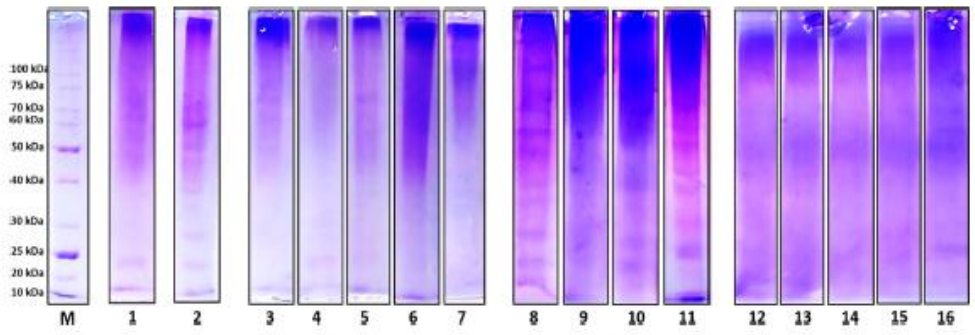

Figure 1. Image of SDS-PAGE of the acid soluble collagen (ASC) fractions prepared from the animal glue samples. Proteins were stained with Coomassie Brilliant Blue (CBB). M: molecular weight markers; Pure rabbit glue: 1: HP1.Pure porcine glue: 2: HP5. Pure bovine glues: 3: HP8; 4: HP2; 5: HP6; 6: HP3; 7: HP4. Mixed animal hide glues: 8: HM1; 9: HM3; 10: HM4; 11: HM5. Mixed animal bone glues: 12: BM3; 13: BM5; 14:BM4; 15: BM1; 16: BM2.

https://doi.org/10.1021/acs.jproteome.2c00232
J. Proteome Res. 2022, 21, 2173−2184

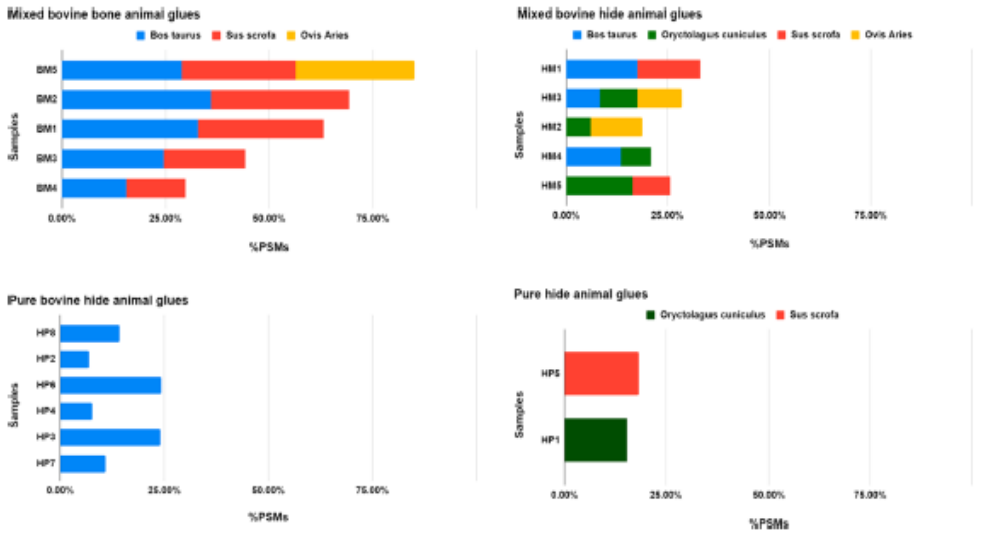

Figure 2. Occurrence of backbone cleavage in animal glue samples. The occurrence of cleavages was semiquantitatively evaluated by calculating the PSMs of semitryptic peptides normalized by the total number of PSMs for the chain (tryptic plus semitryptic). Mixed bovine bone animal glues: BM5, BM2, BM1, BM3, BM4. Mixed bovine hide animal glues: HM1, HM3, HM2, HM4, HM5. Pure bovine hide animal glues: HP8, HP2, HP6, HP4, HP3, HP7. Pure hide animal glues: HP5, HP1.

Collagen Modification: Backbone Cleavage

Animal glue properties, namely, gel strength and viscosity, are influenced by the molecular weight of the constituent protein fragments generated during the material treatment.[6] A preliminary picture of the molecular weight distribution was obtained by running the acid-soluble collagen fractions on denaturing gel electrophoresis, while some molecular details on the occurrence of polypeptide backbone cleavages was provided by the analysis of the incidence of nonenzymatic hydrolysis sites.

Collagen is a quite challenging material for SDS−PAGE because of its gelling properties, its high molecular weight, and the high occurrence of interchain cross-links impairing protein migration and separation. In the perspective of looking at the occurrence of relatively low-molecular-weight bands (below 100 kDa), we focused on readily soluble species and extracted acid soluble collagen (ASC) fractions following the protocol reported in Hong et al. 2017.[16] Figure 1 shows the ASC different patterns of the samples that were grouped as pure and mixed collagen hide and bone glues, according to the protein identifications reported above. In particular, mixed-collagen hide glues exhibit a higher number of discrete bands with respect to pure hide and mixed-collagen bone glues, or to the pure rabbit glue sample, an artisanal animal glue. This might suggest a less random backbone cleavage (discrete bands rather than a continuous smear), with a residual structural effect behind that deserves further analysis in the future.

Backbone cleavage of the polypeptide chain is an expected degradation feature in proteins[23−26] and is expected in animal glues: collagen is insoluble in cold water and is transformed into soluble gelatin by denaturation and partial hydrolysis, which is achieved by hot water extraction (hydrolytic breakdown).[6] Such damage at the backbone can be evaluated as semitryptic peptides that will be generated upon trypsin hydrolysis, with a trypsin cleavage site only at one end.[17,27] The occurrence of semitryptic peptides was semiquantitatively evaluated by counting peptide to spectrum matches (PSMs) and dividing the PSMs of semitryptic peptides with the total PSMs of identified peptides, including both tryptic and semitryptic peptides. We evaluated the backbone cleavage occurrence in the single collagen chains in all the bone and hide samples. As shown in Figure 2, bone glues appear broadly more fragmented in comparison to hide glues. Furthermore, interestingly, more semitryptic peptides were identified in mixed-collagen glues than in pure animal glues.

The data presented so far relate to the portion of the proteins that become soluble after the treatment necessary for the proteomics analyses. To further investigate the degree of backbone cleavage, gaining information on the totality of the samples, analytical (flash) pyrolysis coupled with gas chromatography−mass spectrometry was carried out on all samples.

Pyrolysis products were identified with the help of the NIST20 mass spectral library and by comparison with mass spectra reported in the literature,[28] and are listed in Table S22. Figure S1 shows the pyrogram of HP6, as an example.

The most characteristic pyrolysis products of proteins are cyclic dipeptides, 2,5-diketopiperazines (DKPs).[21] Their formation is hypothesized to be a depolymerization involving the cyclization of neighboring amino acids in a polypeptide chain.

In all chromatograms the most intense peak is ascribable to DKP Cyclo (Pro-Gly) (#10, Figure S1). This in fact originates from the cyclization of proline and glycine which are two of the most abundant amino acids present in the collagen chain. Another DKP detected with a high abundance is Cyclo (Pro-Hyp) (#12, Figure S1) and is an identifying marker of collagen.

https://doi.org/10.1021/acs.jproteome.2c00232
J. Proteome Res. 2022, 21, 2173−2184

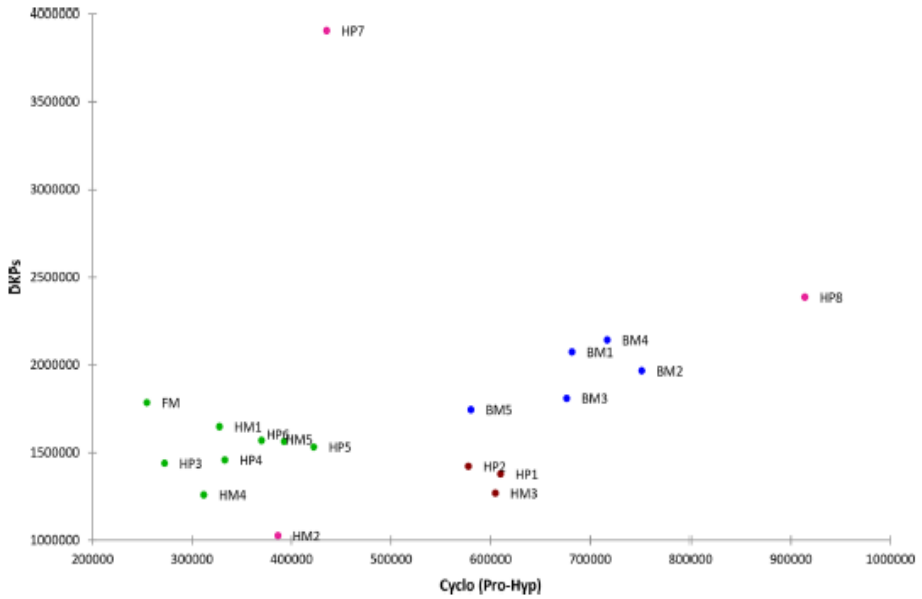

Figure 3. Plot of sum of the areas of all the DPKs versus the area of DPKs Cyclo (Pro-Hyp)

In addition to DKPs, aromatic compounds are also detected, as expected in the pyrolytic profile of animal glue.[21]

All samples were also analyzed by pyrolysis with *in situ* sialylation in order to detect the presence of fatty acids, lipids, and saccharide additives. The data clearly show that fatty acids are present in significant amounts only in samples HP2, HM3, HP1, and HM2. With the exception of rabbit skin animal glue, which has comparatively high fat levels of around 5%,[6] other glues are at times added with fatty acids to reduce the surface tension and thus to improve wetting and prevent foaming.[6] HM3, HP1, and HM2 contain animal glue extracted from rabbit, while HP2 is pure bovine glue, indicating that at least in this sample, fatty acids were actually added to the glue and not present as natural components. No other lipid material nor saccharides were detected in the rest of the samples.

To compare the pyrolytic profiles of the different samples, a semiquantitative analyses of DKPs' was carried out. In particular, the areas of all DKPs detected were normalized for the sample weight (average values of three replicate measurements, RSD < 15%), and the sum of the resulting values are shown in Figure S2.

As DKPs are produced by depolymerization of the polypeptide chain, a relatively high yield of DKPs might be ascribed to a high degree of hydrolysis of the protein. In general, all the bone glue samples present a relatively higher yield of DKPs. This is in agreement with the proteomics data on the soluble fraction and the fact that bone glues have generally a lower molecular weight when compared with hide glues.[1] Furthermore, the electrophoresis carried out on these samples shows a wider molecular weight distribution for the bone glues, resulting in a smear of bands, thus suggesting a general more randomized degree of hydrolysis. Similarly, the hide glues generally present a lower yield of DKPs, and in fact they exhibit a lower molecular weight distribution in the electrophoresis analysis. Sample HP7, HP8, and FM also present a relatively high yield of DKPs. The position of fish glue in the group with the higher yield of DKPs is not surprising, as glues derived from fish cleave more easily on extensive heating which is needed during the glue preparation procedure.[6]

The sum of the areas of all the DPKs was also plotted versus the area of the DPKs Cyclo (Pro-Hyp), and the graph obtained is shown in Figure 3.

The plot shows two main regions. Samples located on the right side of the graph present a relatively higher yield of cyclo (Pro-Hyp) during pyrolysis. All bone glue samples are located on the right of the graph. Samples HP2, HM3, and HP1 are tightly grouped together on the right side of the graph. Their position could be influenced though by the presence of fatty acids in the sample, which might affect the mechanism of formation of diketopiperazines. Samples HP7 and HP8 are quite separated from the rest of the graph, both presenting a high reaction yield of DKPs, and sample HP8 shows also a high yield of Cyclo (Pro-Hyp). The relatively high yield of cyclo (Pro-Hyp) could be due to a relatively high concentration of hydroxyproline in the polypeptide chain. Although, generally, samples presenting a higher yield of cyclo (Pro-Hyp) also present a relatively higher content of Hyp, as determined by the GC-MS analyses, this is not strictly true for all the samples (BM2 for example has a low Hyp content, while sample HP3 has a high Hyp content). Another factor that could affect the yield of cyclo (Pro-Hyp) could be the structural arrangement of the polypeptide chain: hydrogen bonds might favor other pyrolytic processes with respect to depolymerisation, as already shown for ovalbumin.[29] If this is the case, data would suggest that in the bone glue samples hydroxyproline is less involved in hydrogen bonds and, thus, that polypeptide chains are less tightly organized with respect

https://doi.org/10.1021/acs.jproteome.2c00232
J. Proteome Res. 2022, 21, 2173−2184

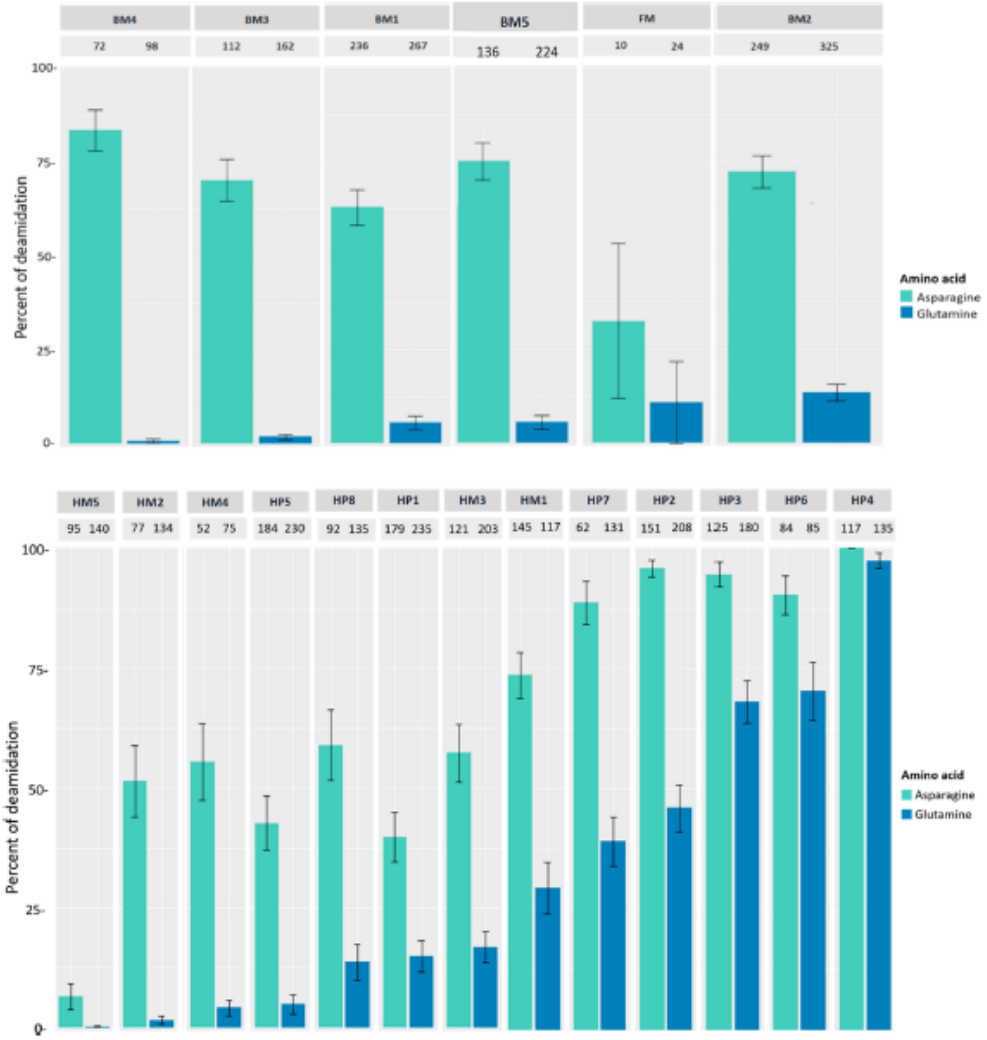

Figure 4. Overall percentage of deamidation for asparagines (N) and glutamines (Q) residues for the collagen chains identified in the bone (upper panel) and hide (lower panel) glue samples. Error bars represent standard deviation and numbers above each bar represent the number of peptides the data is based on.

to the hide glue samples. More research is necessary to clarify this point.

Collagen Modification: Deamidation of Glutamine and Asparagine

Charge distribution in collagen chains is reported to affect animal glue properties, like dependence of viscosity on pH.[6] During glue processing, the acidic or alkaline treatments favor hydrolysis of the amide groups in collagen to a greater or lesser extent, by deamidating the lateral chain of glutamine and asparagine, thus affecting the isoelectric point by unlocking charged functions[2,6] and by hydrolyzing the peptide bond. Bones and tissues are both subject to alkaline and acidic treatments, to remove unwanted material and to initiate the protein denaturation, making the protein available for extraction in hot water in the following stages.[30,31] Deamidation of glutamine and asparagine residues is a nonenzymatic modification that can be followed by mass spectrometry. It results in a +0.98402 mass shift as a consequence of the conversion of the polar, noncharged side-chain amide group to the carboxylate moiety.

We evaluated deamidation occurrence in the set of samples keeping in mind that deamidation is routinely searched for in aged proteins[32,18] and viewed as a global indicator of sample preservational quality,[33] since rates and levels of deamidation

https://doi.org/10.1021/acs.jproteome.2c00232
J. Proteome Res. 2022, 21, 2173−2184

are affected by several chemical and environmental factors. Harsher conditions of collagen extraction in the preparation of glues might have been imprinted also in the profile and level of collagen deamidation.

Deamidation was evaluated from raw LC-MS/MS data by MaxQuant software with an in-house script based on peptide spectrum matches intensities for semiquantitative evaluation, as reported in.[32] Asparagine (Asn) deamidation is faster than glutamine (Gln) deamidation and therefore usually less informative,[33] and consequently, although we always report deamidation at both, our considerations mainly refer to glutamine deamidation.

The deamidation levels of the glue samples are reported in figure 4. Deamidation levels are extremely variable, with deamidation of hide glues being extremely variable, ranging between 2 and 98%. It is possible to observe that, on average, bone glues are less deamidated, with values ranging between 2 and 12%.

It is interesting to observe that, among the hide glues, the most deamidated are those that contain only bovine collagen (HP2, HP3, HP4, HP6). To further investigate this feature, we evaluated the deamidation level in the single collagen chains of glues that contain collagen from a single animal species. Figures S3 and S4 show the deamidation levels in the collagen chains in the pure bovine glues, pure rabbit, and pure porcine glues, respectively. All the collagen chains of the pure bovine glues are extensively deamidated in comparison to the porcine (Figure S4A) and rabbit (Figure S4B) ones. The deamidation level of the bovine collagen chains in the mixed glues is then reported in Figure S5. The comparison of the values in Figures S3 and S5 suggests that bovine chains are most prone to deamidation, or that the procedures used to extract the glue from bovine hides promote a more extensive deamidation. It has been reported that acid-processed glue brings to little amide group modification, while alkaline-processed glue is characterized by extensive hydrolysis of the amide groups. Harsh alkaline treatments at relatively high temperatures[2] are carried out on chromium tanned leather wastes, to remove chromium and separate the collagen to be used for the glue production.[34] A possible explanation of the higher degree of deamidation observed in pure bovine glues could be the fact that bovine skins used in their production derive from leather wastes. More research is necessary to understand this point.

As a further investigation, we manually combined the peptides on the basis of the protein family regardless of the animal species in mixed animal glue samples. Figures S6–S8 report the deamidation of the three more abundant protein families: collagen-type I chain 1, collagen-type I chain 2, and collagen-type III chain 1. From the comparison of the S3A and S6 we can observe that collagen-type I chain 1 in the mixed glues are less deamidated than in the pure bovine glues. This observation is confirmed also from the comparison of the other protein families of mixed glues with the same protein families of the pure glues: Figure S7 versus Figure S3B and Figure S8 versus Figure S3C. Mixed-collagen glues are overall less deamidated than pure glues (see also Figure 4).

Furthermore, we examined site-specific deamidation distribution (i.e., whether deamidation preferentially occurs in specific positions in the protein chain) in the animal glue samples. Attention was primarily focused to the pure bovine animal glues only, to avoid the ambiguity of homologous peptides of collagen from different species. A site-specific evaluation of deamidation (NQ) patterns was performed manually by checking the fragmentation spectra of the peptides containing Asn and Gln.

We classified the single positions of asparagines and glutamines along the collagen sequences as those detected only as unmodified (X), those detected only as deamidated (D), those that were identified both as deamidated and unmodified (DX) and, finally, those that were not detected at all, nor unmodified nor deamidated (NF) (see Tables S23 and S24). This preliminary first and simple approach provides a glance on deamidation occurrence in the main chains of collagen α1(I) and collagen α2(I).

As shown in Tables S23 and S24, almost all of the glutamines and asparagines positions that have been identified underwent some deamidation, that means that were detected either only as deamidated or both deamidated and unmodified. It is worth mentioning that some glutamines and asparagines are in regions that have not been covered in the identification. Interestingly, our experiments, at least at this level, where only detection of deamidated/unmodified was considered, do not point out any marked difference among the samples, and deamidation seems to be spread along the sequences, without any hot spot, suggesting the absence of any three-dimensional effect. This might not come as a surprise, if we consider that, in the glues, collagen is denatured, as a consequence of the extraction procedure, and, actually, the acidic and alkaline treatments are specifically used to break intermolecular and intramolecular bonds, thus exposing the whole polypeptide chain to the aqueous environment. This could eventually make a marked difference in respect to the situation observed with ancient collagen from bone, where three-dimensional structural effects seem to play a significant role on deamidation.[35]

Furthermore, it is interesting to note that almost all the methionine detected were found as oxidized (see Tables S23 and S24). For instance, in the collagen I chain a1 the methionine in positions 300, 579, 728 and M were detected always and only oxidized. Similarly, in collagen type I chain 2 the M in position 445 was detected always as oxidized, with all the other positions belonging to regions that were not covered at all in the identification. Site-specific methionine oxidation trend is the same regardless the sample preparation of the single animal glue.

■ CONCLUSIONS

This work focused on the molecular characterization of a series of collagen-based animal glues produced for restoration purposes. Molecular weight distribution, stabilization of the protein matrix by hydrogen bonding, charge distribution, all have an impact on the performances of the glue and are determined by amino acid composition, but also and most importantly by chemical modifications occurring during preparation procedures. Although much attention has been devoted to physical properties of collagen based animal glues,[2,6,36,37] a systematic characterization of molecular properties of glues is still lacking.

The most striking feature we found was the fairly common discrepancy in commercial glues between label and actual animal origin. A few samples were made of tissues from a single organism, and a classification in pure and mixed, hide and bone glues was made on the basis of proteomic results. Collagen type III was actually identified in all the hide glues, confirming the use of skin and cartilaginous tissue, and thus its identification can be safely proposed as an effective analytical molecular marker to discriminate between hide and bone glues.

https://doi.org/10.1021/acs.jproteome.2c00232
J. Proteome Res. 2022, 21, 2173−2184

This important quality parameter can be unequivocally assessed by the described proteomic analysis.

MS/MS data were used to investigate collagen degradation in animal glue. Modifications of amino acids, such as oxidation of methionine, deamidation of asparagine and glutamine, as well as backbone cleavage, were evaluated since they affect charge and molecular weight distributions.[6] This is the first detailed analysis on the occurrence of deamidations in a large and diversified set of collagen-based animal glues, and this modification is expected to strongly influence the rheological properties of the adhesive material since it changes collagen pI. Bone glues are on average less deamidated than hide glues. Exhaustive evaluation of deamidation levels is made difficult by the presence of multiple collagens in mixture in the mixed glues. We therefore collectively calculated deamidation for each family of collagen proteins in single samples (i.e., all type I, chain alpha 1 collagen sequences) and, interestingly, mixed-collagen animal glues were collectively found less deamidated than pure animal glues. Furthermore, the collagen chains of *Bos taurus* in hide-mixed glues are significantly less deamidated than the same chains in pure bovine glues. A possible explanation can be found in the origin of the hides used for the glue preparation, which might derive from tannery wastes.

Backbone cleavage, causing a partial depolymerization of collagen chains, is also a degradation feature that is expected to occur upon extreme pH treatments and extended heating during glue preparation. It is a fact that the resulting molecular weight distribution is considered among the most critical parameters determining glue properties.[6] Assessing the molecular weight distribution of fragmented collagen is not an easy task due to the intrinsic fibrous properties of collagen, and further complicated by the extensive network of intermolecular cross-links that are essential in providing the connective tissues with their stability, cohesiveness, and physicochemical properties.[38] The number of semitryptic peptides is connected to backbone cleavages and was higher in the bone glues than in the hide ones. This result agrees with the pyrolysis data, showing a higher yield of DKPs upon thermal degradation in the bone glues, and with the known generally harsher conditions used to extract collagen from bones.

Data herein presented confirm the heterogeneity of collagen-based animal glues at the molecular level, heterogeneity strongly increased by the preparation and manufacturing procedures, affecting the properties of the glue, possibly more than the collagen origin itself. These data, showing that, on average, bone glues are less deamidated than hide glues, but more fragmented, and mixed-collagen glues are overall less deamidated than pure glues, pave the way to a correlation between molecular modifications and material performances in animal glues. Moreover, this original analytical characterization will be useful in a wider, comparative perspective aimed at the characterization of the variety of collagen-based materials.

■ ASSOCIATED CONTENT

Supporting Information

The Supporting Information is available free of charge at https://pubs.acs.org/doi/10.1021/acs.jproteome.2c00232.

Animal glues' information, provenience, and classification upon proteomic analysis results (Table S1); relative content of amino acids obtained by GC-MS (Table S2); proteomic identification details (Tables S3–S21); backbone cleavage by (flash) pyrolysis GC-MS (Figures S1–S2, Table S22); deamidation of collagen (Figures S3–S8, Tables S23–S24); accession entries in COLLe database (Table S25) (PDF)

■ AUTHOR INFORMATION

Corresponding Author

Leila Birolo – *Department of Chemical Sciences, University of Naples Federico II, Complesso Universitario di Monte S. Angelo, 80126 Naples, Italy; Task Force "Metodologie Analitiche per la Salvaguardia dei Beni Culturali", University of Naples Federico II, 80138 Naples, Italy;* orcid.org/0000-0002-0915-7501; Phone: +39-081-679939; Email: birolo@unina.it

Authors

Georgia Ntasi – *Department of Chemical Sciences, University of Naples Federico II, Complesso Universitario di Monte S. Angelo, 80126 Naples, Italy*

Sara Sbriglia – *Department of Chemical Sciences, University of Naples Federico II, Complesso Universitario di Monte S. Angelo, 80126 Naples, Italy*

Rossana Pitocchi – *Department of Chemical Sciences, University of Naples Federico II, Complesso Universitario di Monte S. Angelo, 80126 Naples, Italy;* orcid.org/0000-0001-8327-1380

Roberto Vinciguerra – *Department of Chemical Sciences, University of Naples Federico II, Complesso Universitario di Monte S. Angelo, 80126 Naples, Italy*

Chiara Melchiorre – *Department of Chemical Sciences, University of Naples Federico II, Complesso Universitario di Monte S. Angelo, 80126 Naples, Italy*

Laura Dello Ioio – *Dello Ioio Restauri, 80069 Naples, Italy*

Giancarlo Fatigati – *Department of Humanities, University Suor Orsola Benincasa, 80132 Naples, Italy*

Emanuele Crisci – *Department of Chemistry and Industrial Chemistry, University of Pisa, 56126 Pisa, Italy*

Ilaria Bonaduce – *Department of Chemistry and Industrial Chemistry, University of Pisa, 56126 Pisa, Italy;* orcid.org/0000-0003-0346-8373

Andrea Carpentieri – *Department of Chemical Sciences, University of Naples Federico II, Complesso Universitario di Monte S. Angelo, 80126 Naples, Italy; Department of Humanities, University Suor Orsola Benincasa, 80132 Naples, Italy; Task Force "Metodologie Analitiche per la Salvaguardia dei Beni Culturali", University of Naples Federico II, 80138 Naples, Italy;* orcid.org/0000-0002-1944-5355

Gennaro Marino – *Department of Chemical Sciences, University of Naples Federico II, Complesso Universitario di Monte S. Angelo, 80126 Naples, Italy; Department of Humanities, University Suor Orsola Benincasa, 80132 Naples, Italy*

Complete contact information is available at: https://pubs.acs.org/10.1021/acs.jproteome.2c00232

Author Contributions

L.B. conceived the project and L.B, G.N., I.B and G.M. outlined the experiments. G.N., S.S., R.V. carried out the proteomic analyses; G.N., S.S., L.B., R.V., A.C. and C.M. interpreted experimental data; R.P. carried out electrophoretic analysis, I.B., E.C. carried out Py-GC-MS and GC-MS analyses.

I.B. and E.C. interpreted Py-GC-MS and GC-MS data; L.D.I. and G.F. provided the samples and the restorers' point of view. All authors contributed to write the paper.

Notes

The authors declare no competing financial interest.

■ ACKNOWLEDGMENTS

This project has received funding (to L.B. and G.N.) from the European Union's Horizon 2020 Research and Innovation Program under the Marie Sklodowska-Curie Grant Agreement No. 722606, TEMPERA (Teaching Emerging Methods in Palaeoproteomics for the European Research Area). The authors gratefully acknowledge the Museo Nacional del Prado for providing the animal glue samples, and are indebted to Mr. Luigi Coletta, dean of restorers, who turned the attention of GM to the poor quality of today's glues compared to those available in the prewar period and generously provided us with some samples manufactured in those times.

■ REFERENCES

(1) Adhesives. In *Building Decorative Materials (Woodhead Publishing Series in Civil and Structural Engineering)*; Li, Y.; Ren, S., Eds.; Woodhead Publishing, 2011; pp 325−341.
(2) Pearson, C. Animal Glues and Adhesives. In *Handbook of Adhesive Technology, Revised and Expanded*; CRC Press, 2003; pp 476−491.
(3) Solazzo, C.; Courel, B.; Connan, J.; Van Dongen, B. E.; Barden, H.; Penkman, K.; Taylor, S.; Demarchi, B.; Adam, P.; Schaeffer, P.; Nissenbaum, A.; Bar-Yosef, O.; Buckley, M. Identification of the Earliest Collagen- and Plant-Based Coatings from Neolithic Artefacts (Nahal Hemar Cave, Israel). *Sci. Rep.* **2016**, *6*, 31053.
(4) Bleicher, N.; Kelstrup, C.; Olsen, J. V.; Cappellini, E. Molecular Evidence of Use of Hide Glue in 4th Millennium BC Europe. *J. Archaeol. Sci.* **2015**, *63*, 65−71.
(5) Ebnesajjad, S. Chapter 8. Characteristics of Adhesive Materials. In *Plastics Design Library, Handbook of Adhesives and Surface Preparation*; William Andrew Publishing, 2011, 137−183.
(6) Schellmann, N. C. Animal Glues: A Review of Their Key Properties Relevant to Conservation. *Stud Conserv* **2007**, *52* (sup1), 55−66.
(7) Přikryl, P.; Havlíčkova, L.; Pacáková, V.; Hradilová, J.; Štulík, K.; Hofta, P. An Evaluation of GC-MS and HPLC-FD Methods for Analysis of Protein Binders in Paintings. *J. Sep. Sci.* **2006**, *29*, 2653−2663.
(8) Buckley, M.; Collins, M.; Thomas-Oates, J.; Wilson, J. C. Species Identification by Analysis of Bone Collagen Using Matrix-Assisted Laser Desorption/Ionisation Time-of-Flight Mass Spectrometry. *Rapid Commun. Mass Spectrom.* **2009**, *23*, 3843−3854.
(9) Welker, F.; Soressi, M.; Rendu, W.; Hublin, J.-J.; Collins, M. Using ZooMS to Identify Fragmentary Bone from the Late Middle/Early Upper Palaeolithic Sequence of Les Cottes, France. *J. Archaeol. Sci.* **2015**, *54*, 279−286.
(10) Welker, F.; Collins, M. J.; Thomas, J. A.; Wadsley, M.; Brace, S.; Cappellini, E.; Turvey, S. T.; Reguero, M.; Gelfo, J. N.; Kramarz, A.; Burger, J.; Thomas-Oates, J.; Ashford, D. A.; Ashton, P. D.; Rowsell, K.; Porter, D. M.; Kessler, B.; Fischer, R.; Baessmann, C.; Kaspar, S.; Olsen, J. V; Kiley, P.; Elliott, J. A.; Kelstrup, C. D.; Mullin, V.; Hofreiter, M.; Willerslev, E.; Hublin, J.-J.; Orlando, L.; Barnes, I.; MacPhee, R. D. E. Ancient Proteins Resolve the Evolutionary History of Darwin/'s South American Ungulates. *Nature* **2015**, *522*, 81−84.
(11) Leo, G.; Cartechini, L.; Pucci, P.; Sgamellotti, A.; Marino, G.; Birolo, L. Proteomic Strategies for the Identification of Proteinaceous Binders in Paintings. *Anal. Bioanal. Chem.* **2009**, *395*, 2269−2280.
(12) Fremout, W.; Dhaenens, M.; Saverwyns, S.; Sanyova, J.; Vandenabeele, P.; Deforce, D.; Moens, L. Tryptic Peptide Analysis of Protein Binders in Works of Art by Liquid Chromatography−Tandem Mass Spectrometry. *Anal. Chim. Acta* **2010**, *658*, 156−162.
(13) Dallongeville, S.; Koperska, M.; Garnier, N.; Reille-Taillefert, G.; Rolando, C.; Tokarski, C. Identification of Animal Glue Species in Artworks Using Proteomics: Application to a 18th Century Gilt Sample. *Anal. Chem.* **2011**, *83*, 9431−9437.
(14) Pal Chowdhury, M.; Buckley, M. Trends in Deamidation across Archaeological Bones, Ceramics and Dental Calculus. *Methods* **2022**, *200*, 67−79.
(15) Dallongeville, S.; Garnier, N.; Rolando, C.; Tokarski, C. Proteins in Art, Archaeology, and Paleontology: From Detection to Identification. *Chem. Rev.* **2016**, *116*, 2−79.
(16) Hong, H.; Chaplot, S.; Chalamaiah, M.; Roy, B. C.; Bruce, H. L.; Wu, J. Removing Cross-Linked Telopeptides Enhances the Production of Low-Molecular-Weight Collagen Peptides from Spent Hens. *J. Agric. Food Chem.* **2017**, *65*, 7491−7499.
(17) Vinciguerra, R.; De Chiaro, A.; Pucci, P.; Marino, G.; Birolo, L. Proteomic Strategies for Cultural Heritage: Form Bones to Paintings. *Microchem. J.* **2016**, *126*, 341−348.
(18) Cappellini, E.; Jensen, L. J.; Szklarczyk, D.; Ginolhac, A.; Da Fonseca, R. A. R.; Stafford, T. W.; Holen, S. R.; Collins, M. J.; Orlando, L.; Willerslev, E.; Gilbert, M. T. P.; Olsen, J. V. Proteomic Analysis of a Pleistocene Mammoth Femur Reveals More than One Hundred Ancient Bone Proteins. *J. Proteome Res.* **2012**, *11*, 917−926.
(19) Cox, J.; Mann, M. MaxQuant Enables High Peptide Identification Rates, Individualized p.p.b.-Range Mass Accuracies and Proteome-Wide Protein Quantification. *Nat. Biotechnol.* **2008**, *26*, 1367−1372.
(20) Bonaduce, I.; Cito, M.; Colombini, M. P. The Development of a Gas Chromatographic-Mass Spectrometric Analytical Procedure for the Determination of Lipids, Proteins and Resins in the Same Paint Micro-Sample Avoiding Interferences from Inorganic Media. *J. Chromatogr. A* **2009**, *1216*, 5931−5939.
(21) Orsini, S.; Parlanti, F.; Bonaduce, I. Analytical Pyrolysis of Proteins in Samples from Artistic and Archaeological Objects. *J. Anal. Appl. Pyrolysis* **2017**, *124*, 643−657.
(22) Kuivaniemi, H.; Tromp, G. Type III Collagen (COL3A1): Gene and Protein Structure, Tissue Distribution, and Associated Diseases. *Gene* **2019**, *707*, 151−171.
(23) Cleland, T. P.; Schroeter, E. R.; Schweitzer, M. H. Biologically and Diagenetically Derived Peptide Modifications in Moa Collagens. *Proc. R. Soc. B Biol. Sci.* **2015**, *282*, 20150015.
(24) Orsini, S.; Yadav, A.; Dilillo, M.; McDonnell, L. A.; Bonaduce, I. Characterization of Degraded Proteins in Paintings Using Bottom-Up Proteomic Approaches: New Strategies for Protein Digestion and Analysis of Data. *Anal. Chem.* **2018**, *90*, 6403−6408.
(25) Davies, M. J. The Oxidative Environment and Protein Damage. *Biochim. Biophys. Acta - Proteins Proteomics* **2005**, *1703*, 93−109.
(26) Hendy, J. Ancient Protein Analysis in Archaeology. *Sci. Adv.* **2021**, *7*, eabb9314.
(27) Welker, F.; Hajdinjak, M.; Talamo, S.; Jaouen, K.; Dannemann, M.; David, F.; Julien, M.; Meyer, M.; Kelso, J.; Barnes, I.; Brace, S.; Kamminga, P.; Fischer, R.; Kessler, B. M.; Stewart, J. R.; Pääbo, S.; Collins, M. J.; Hublin, J.-J. Palaeoproteomic Evidence Identifies Archaic Hominins Associated with the Châtelperronian at the Grotte Du Renne. *Proc. Natl. Acad. Sci.* **2016**, *113*, 11162−11167.
(28) Adamiano Alessio. *Pyrolysis of Peptides and Proteins. Analytical Study and Environmental Applications*, Alma Mater Studiorum Università di Bologna, 2012. DOI: 10.6092/unibo/amsdottorato/4671.
(29) Orsini, S.; Duce, C.; Bonaduce, I. Analytical Pyrolysis of Ovalbumin. *J. Anal. Appl. Pyrolysis* **2018**, *130*, 62−71.
(30) Idris, A.; Saed, K.; Hung, Y. Animal Glue Production from Skin Wastes. In *Environmental Bioengineering. Handbook of Environmental Engineering*, vol *11*; Wang, L., Tay, J. H., Tay, S., Hung, Y. T. (eds); Humana Press, Totowa, NJ, 2010; pp 685−697.
(31) Negash, G. T.; Emiru, A.; Amare, D.; Reda, M. Production and Characterization of Glue from Tannery Hide Trimming Waste. In *Advances of Science and Technology. ICAST 2019. Lecture Notes of the*

Institute for Computer Sciences, Social Informatics and Telecommunications Engineering; Habtu, N., Ayele, D., Fanta, S., Admasu, B., Bitew, M. (eds); Springer, Cham., 2020; Vol. *308*, pp 59-70.

(32) Mackie, M.; Rüther, P.; Samodova, D.; Di Gianvincenzo, F.; Granzotto, C.; Lyon, D.; Peggie, D. A.; Howard, H.; Harrison, L.; Jensen, L. J.; Olsen, J. V.; Cappellini, E. Palaeoproteomic Profiling of Conservation Layers on a 14th Century Italian Wall Painting. *Angew. Chem - Int. Ed.* **2018**, *57*, 7369−7374.

(33) Schroeter, E. R.; Cleland, T. P. Glutamine Deamidation: An Indicator of Antiquity, or Preservational Quality? *Rapid Commun. Mass Spectrom.* **2016**, *30*, 251−255.

(34) Pati, A.; Chaudhary, R.; Subramani, S. A Review on Management of Chrome-Tanned Leather Shavings: A Holistic Paradigm to Combat the Environmental Issues. *Environ. Sci. Pollut. Res.* **2014**, *21*, 11266−11282.

(35) Van Doorn, N. L.; Wilson, J.; Hollund, H.; Soressi, M.; Collins, M. J. Site-Specific Deamidation of Glutamine: A New Marker of Bone Collagen Deterioration. *Rapid Commun. Mass Spectrom.* **2012**, *26*, 2319−2327.

(36) Román, J. K.; Wilker, J. J. Cooking Chemistry Transforms Proteins into High-Strength Adhesives. *J. Am. Chem. Soc.* **2019**, *141*, 1359−1365.

(37) Gunorubon, A. J.; Misel, U. Production of Glues from Animal Bones. *ARPN J. Eng. Appl. Sci.* **2014**, *9*, 1592−1597.

(38) Depalle, B.; Qin, Z.; Shefelbine, S. J.; Buehler, M. J. Influence of Cross-Link Structure, Density and Mechanical Properties in the Mesoscale Deformation Mechanisms of Collagen Fibrils. *J. Mech. Behav. Biomed. Mater.* **2015**, *52*, 1−13.

https://doi.org/10.1021/acs.jproteome.2c00232
J. Proteome Res. 2022, 21, 2173−2184